New Catalysts for Stereoselective Living Radical Polymerization of Functional α-Olefins

Shifeng Nian
Bengbu, Anhui, China

B.S. Chemistry, University of Science and Technology of China, 2013

A Thesis presented to the Graduate Faculty
of the University of Virginia in Candidacy for the Degree of
Master of Science

Department of Chemistry

University of Virginia
May, 2016 Degree **will be Conferred**

Abstract

New Catalysts for Stereoselective Living Radical Polymerization of Functional α-Olefin

The stereostructure of polymeric chains can greatly influence their physical and chemical properties. Therefore, controlling the stereostructures (tacticity) of polymers is very important in materials chemistry. There have been numerous studies on how to control the tacticity of polymer during a radical polymerization process. However, only a few monomers can be applied to stereospecific living radical polymerization.

A Lewis acid–mediated stereocontrolled atom transfer radical polymerization (ATRP) of various acrylamide monomers was successfully achieved by using the newly designed catalysts. Schiff base-based macrocylclic compounds were synthesized from the condensation of an aryl dialdehyde with achiral and chiral diamines. These macrocyclic Schiff bases and their corresponding reduced macrocyclic amines were used as the ligands for the ATRP. The polymerization was conducted in methanol by using the copper(I)-macrocyclic ligand complex as the catalyst and ethyl 2-bromoisobutyrate as the initiator in the presence of 5 mol % $Yb(OTf)_3$ at room temperature (20℃). Polymers with high isotacticty and narrow polyisodispersity index (PDI) were obtained along with high conversion of the monomers. The resulting poly (*N*,*N*-dimethylacrylamide) had an isotacticity as high as 90% and a PDI of 1.05. The resulting poly (*N*-isopropylacrylamide) had an isotacticity as high as 89% and a PDI of 1.12. It is the first time that the copper-mediated stereocontrolled ATRP of *N*-isopropylacrylamide was successfully achieved.

Acknowledgement

I would like to give my deepest appreciation to my graduate advisor, Prof. Lin Pu, for his continuous guidance and help during my studies.

I would also like to thank Prof. Gunnoe and Prof. McGarvey for giving me advice on my research.

I wish to express my gratitude to all my groupmates who helped me a lot on my research project.

Last but not least, I would like to thank my parents for always believing in me and encouraging me to finish my Master Degree.

Table of content

List of Figures

List of Schemes

List of Tables

Chapter 1. Living Radical Polymerization and Tacticity Control of Polymers

1. Living Radical Polymerization

1.1. Introduction

Free radical polymerization is one of the most common and useful methods for making polymers. This kind of polymerization is initiated by reactive species termed initiator, which can generate radicals and add to monomer molecules by activating its π-bond to form a new radical. This process is repeated as more and more monomers are added to the propagating chain continuously and finally a polymer chain is formed[1]. Free radical polymerization consists of four elementary reactions: initiation, propagation, transfer and termination. **Scheme 1.1** shows a general radical polymerization process. In conventional radical polymerization (RP), the average life time of the propagating polymer chain is about 1 second, which is too short for any synthetic manipulation, chain end group functionalization and molecular weight (MW) control. Although about 50% of all commercially polymers are made by conventional RP, no polymers with controlled architecture can be synthesized by using this method[2].

Scheme 1.1. Free radical polymerization process

Initiation

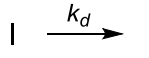

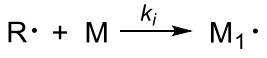

Propagation

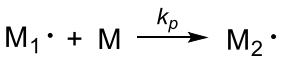

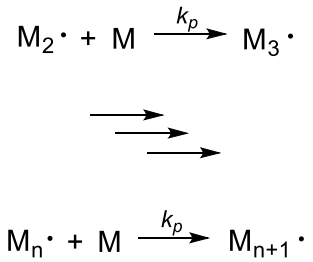

Termination

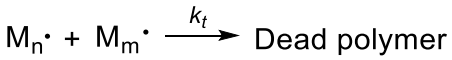

In order to control the structural parameters of polymer, a new kind of RP, termed controlled/living radical polymerization (CRP), has been developed magnificently within the recent two decades[3]. CRP has the properties of fast initiation and absence of termination, which means that simultaneous propagation of all polymer chains can be realized and narrow polydispersity index (PDI, equals to M_w / M_n) can be achieved. Also, because of the absence of termination step, the MW can be easily controlled and numerous block copolymers can be synthesized. In general, the development of CRP greatly expands the synthesis of new polymeric materials and application of polymers.

1.2. Controlled/Living Radical Polymerization

The central principle of the CRP is that a dynamic equilibrium between radical of propagating chains and dormant species has to be established in a polymerization system. There are basically two major approaches of CRP. The first approach involves an activation/deactivation process of radicals, which is based on the persistent radical effect (PRE). PRE refers to a phenomenon that transient radicals can be rapidly trapped and deactivated by persistent (long lived) radicals to form a dormant species in a reaction system, and the dormant species can be activated by heat, light or a catalyst to reform

transient radicals[4]. The CRP systems which obey the PRE principle include stable free radical polymerization (SFRP) and atom transfer radical polymerization (ATRP). The second approach is not based on PRE principle. It follows the conventional RP kinetics, which has a slow initiation and fast termination process. The reaction system employs degenerative transfer (DT) process. In the system, the concentration of transfer agent is much higher than the concentration of initiator. Therefore, the transfer agent performs as part of the dormant species and only a very small concentration of radicals exists in the system, which involves in the chain propagation, termination and undergoes DT with dormant species in a controlled manner.

1.2.1. Stable Free Radical Polymerization (SFRP)

In SFRP, the sources of stable free radicals are generally the nitroxide and some organometallic compound, and nitroxides are the most widely used ones. Therefore, nitroxide mediated polymerization (NMP) is the most popular SFRP[5]. **Scheme 1.2** shows the mechanism of NMP. In NMP system, the dormant species are the alkoxyamines, which can establish an equilibrium with the propagating chain radicals. Under activation, one alkoxyamine can generate one nitroxide stable radical and one propagating radical, which can be trapped and deactivated by stable radical again. (2,2,6,6-tetramethylpiperidin-1-yl)oxyl (TEMPO) and its derivatives are the most widely used nitroxide. For example, polystyrene was synthesized successfully by using TEMPO as a stable free radical source, and the polymerization showed a living property[6]. Acrylates[7] and acrylamides[8] were also polymerized successfully by the NMP process.

Scheme 1.2. Mechanism of NMP

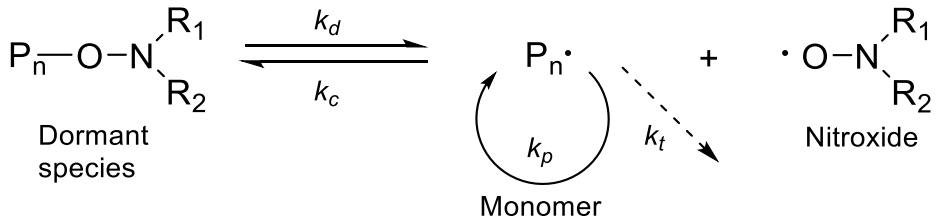

1.2.2. Degenerative Transfer (DT) Process

Polymerization process based on DT doesn't obey PRE principle but is very similar with conventional RP. In conventional RP, the rate of initiation and termination are the same, according to steady state theory, and the concentration of radical remains stable. In order to make the polymerization process living, the concentration of chain transfer agent should be much higher than the concentration of initiator. Also, the rate of transfer must be much higher than the rate of propagation. The purpose of these conditions is to make sure the concentration of the propagating radical stays in the very low level and the polymerization is controllable. The chain transfer agents can be atoms, functional groups, unsaturated polymethacrylates and dithioesters[3]. The most successfully polymerization under DT process is achieved by using dithioesters and its derivatives, and the method is called reversible addition-fragmentation chain transfer (RAFT)[9]. **Scheme 1.3** shows the mechanism of the RAFT process. The propagating radical can add to the reactive carbon sulfur double bond and form an intermediate. The intermediate can either undergo the reversible addition process, or it can release another growing radical to initiate more monomers. In this process, an equilibrium is established between dormant and active species. There are many examples of RAFT process in the polymerization of styrene, acrylates and methacrylates, acrylamides and methacrylamide[10].

Scheme 1.3. Mechanism of RAFT polymerization

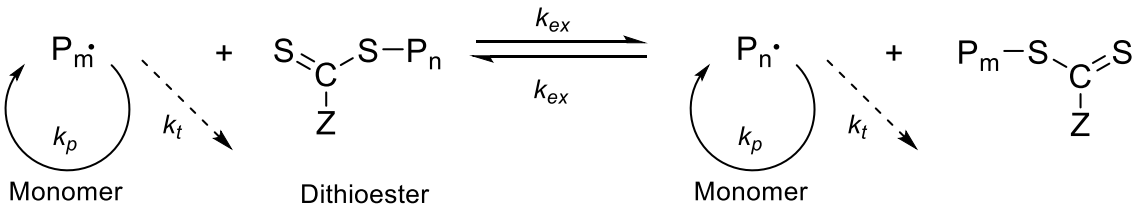

1.3. Atom Transfer Radical Polymerization (ATRP)

ATRP is one of the most widely used CRP and is employed in this project. Compare to other CRP process, ATRP has its own advantages. One advantage is that all ATRP reagents (initiators, ligands and transition metals) are commercially available. In addition, the equilibrium between active radicals and dormant species can be properly adjusted in a polymerization system simply by modifying the structure of the complexing ligand.

1.3.1. Mechanism of ATRP

ATRP also obeys the PRE principle. **Scheme 1.4** shows the mechanism of ATRP process. The equilibrium is established between propagating radicals and dormant species, usually a polymer chain with a halogen or pseudohalogen atom at the end of the chain. The propagating radicals are generated by a reversible redox process, which is catalyzed by a transition metal complex. The metal complex can abstract a halogen or pseudohalogen atom from the dormant species and undergo a one electron oxidation process. A homocleavage of carbon halogen bond of the dormant species occurs and the propagating radicals are generated to initiate more monomers and form polymer chains. The transition metal species need to have the ability to expand its coordination site and change its oxidation number in order to achieve the redox process.

Scheme 1.4. Mechanism of ATRP

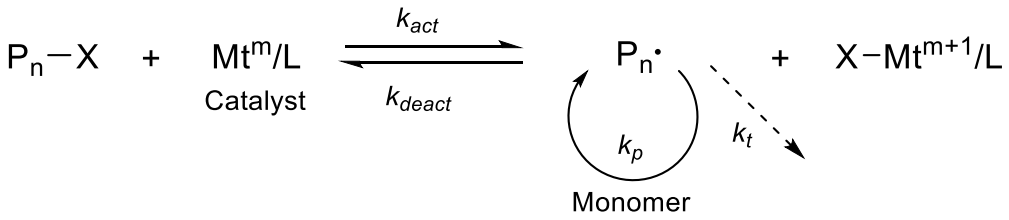

In ATRP, the rate constant of activation, k_{act}, is much smaller than the rate constant of deactivation, k_{deact}. In general, the equilibrium constant K_{ATRP}, which equals to k_{act} /k_{deact}, is in the range of 10^{-9} to 10^{-4}. The very small equilibrium constant ensures that most of the polymer chains are in the dormant state and the propagating radicals are in very low concentration, which greatly reduce the probability of termination between polymer chains[3]. Typically, less than 5% of the polymer chains undergo termination in ATRP process, and the absence of termination makes the propagating radical controllable and the polymerization exhibits a living property.

1.3.2. Components of ATRP

In general, the ATRP system consists of monomer, initiator with a halogen or pseudohalogen atom and a catalyst, which is a metal complex composed of metal species and ligand. Some ATRP systems require solvent as well.

1.3.2.1. Initiators

The major role of an initiator is to determine the number of propagating polymer chains in the ATRP system. In ATRP, the initiation is fast and the termination and chain transfer are negligible. In this case, the number of the growing chains is constant and is

proportional to the concentration of the initiator. And the theoretical degree of polymerization (DP) can be calculated simply from the concentration of the monomer and initiator.

$$DP = [M]_0/[Initiator]_0 \times conversion \quad (\mathbf{1.1})$$

The initiators are typically alkyl halides (RX) in ATRP. To obtain polymers with good MW control and narrow PDI, the halide atom, X, must migrate between the propagating chain and metal complex rapidly, which requires fast initiation. The MW control works best when X is chlorine or bromine. Fluorine is not used because of the difficulty in the homocleavage of a carbon fluorine bond. Some pseudohalogen molecules, such as thiocyanates, have been successfully used in the ATRP of styrenes[11].

A variety of initiators have been used in ATRP. Most of them are alkyl halides. They are classified on the basis of their structures. Halogenated alkanes, such as $CHCl_3$ and CCl_4, are one of the first studied ATRP initiators. They have been successfully used in the Ruthenium-catalyzed ATRP of methyl methacrylate (MMA)[12] and the Cu-based ATRP of styrene[13]. Benzylic halides are structurally similar to styrene and its derivatives. As a result, they are good initiators for this kind of monomers. For example, ATRP of styrene was successfully achieved in the presence of benzylic chloride and lithium molybdate complex[14]. α-Haloesters and α-haloketones are also widely used initiator in ATRP system. Various monomers can undergo ATRP in the presence of these initiators, such as MMA[11], acrylates and acrylamides. α-Halonitriles and sulfonyl halides are fast radical generators which have much faster initiation rate than propagation. They have been employed in the ATRP of acrylonitrile[15], styrene[16] and acrylates[17]. **Figure 1.1** shows the structure of some commonly used initiators.

Figure 1.1. Structures of some common initiators

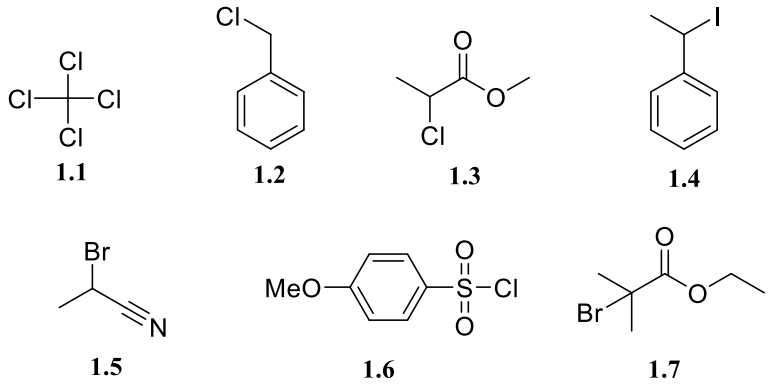

1.3.2.2. Transition Metal Complexes

A metal complex is the most important component in ATRP since it determines the equilibrium between the active and dormant species. As mentioned previously, the transition metal center must have two adjacent oxidation states and is able to expand its coordination sphere. In addition, the metal center should have proper affinity to halogen or pseudohalogen atoms in order to establish an appropriate ATRP equilibrium. The metal centers can vary from group 6 to group 11, and will be introduced in the following paragraph.

The group 6 molybdenum was used in the ATRP process. However, the process is less successful in comparison with other metal centers. The lithium molybdate (V) complexes are applied in the ATRP of styrene with benzylic halides as the initiator. The PDI of polystyrene was relatively high (about 1.5) and the efficiency of the initiator was poor. In addition, a side reaction could happen between the metal complex and the initiators[14].

The group 7 rhenium (V) complex is highly effective for the polymerization of styrene[18]. $ReO_2I(PPh_3)_2$ proved a good complex for the ATRP of styrene with an alkyl

iodide as the initiator. Polystyrene with high MW (up to 40000) and narrow PDI (1.19) was obtained even at 30℃. **Figure 1.2** shows the structure of some Mo and Re complexes.

Figure 1.2. Mo and Re complexes

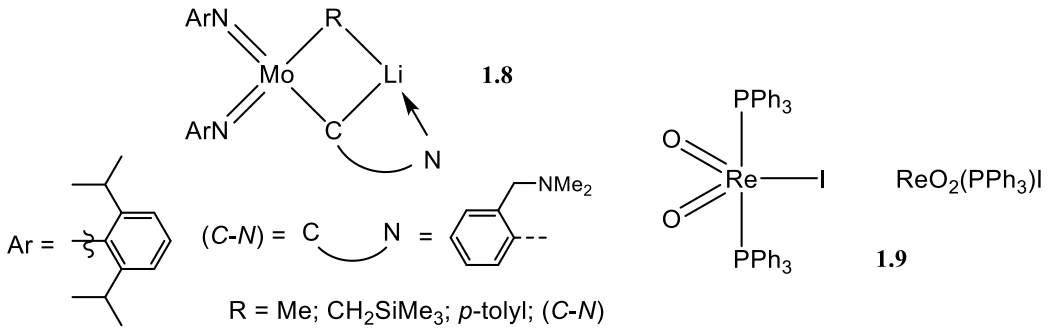

Group 8 ruthenium and iron were also studied. In 1995, Sawamoto et al. first reported the ruthenium-catalyzed ATRP of MMA[19]. $RuCl_2(PPh_3)_3$ was used as metal complex and CCl_4 as the initiator, and a Lewis acid was also required as the activator. The polymerization showed living properties with relatively low PDI (1.3). The ATRP of a ruthenium catalyst without the addition of a Lewis acid was also studied. $RuCl_2$(*p*-cymene)(PR_3) was reported to successfully catalyze the ATRP of MMA using bromoester as the initiator and in the absence of Lewis acid[20]. High MW (up to 60000) and narrow PDI (less than 1.25) were obtained. Iron-based catalysts were also applied for the ATRP of variuos monomers. In 1997, Sawamoto et al. reported the ATRP of MMA using $FeCl_2(PPh_3)_2$ as catalyst and various alkyl halides as the initiator[21]. When $CH_3CBr(CO_2C_2H_5)_2$ was the initiator, the polymerization showed a living property and the PDI was narrow (1.1-1.3). Matyjaszewski et al. also reported the ATRP of MMA and styrene using various iron complexes[22]. An iron complex with $N(nBu)_3$ as ligand proved an effective catalyst for the ATRP of styrene. And a complex with 4,4'-Bis(5-nonyl)-2,2'-

bipyridine (dNbipy) as the ligand showed good ATRP control of MMA. **Figure 1.3** shows the structure of some Fe and Ru complexes.

Figure 1.3. Fe and Ru complexes

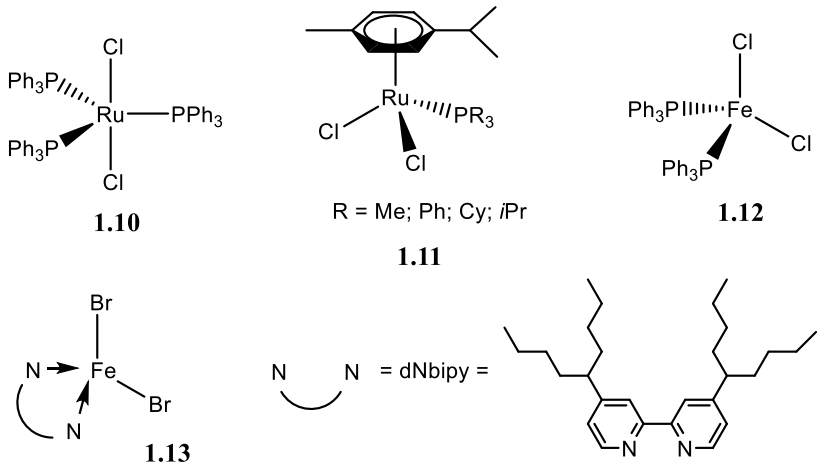

The group 9 rhodium complex $RhCl(PPh_3)_3$, known as Wilkinson catalyst, is a widely used hydrogenation catalyst. Jerome et al. also tried to apply it to the ATRP system and the result was promising[23]. By using 2,2'-dichloroacetophenone as the initiator and in the presence of 7 mol% PPh_3, the ATRP of MMA was successfully achieved. The MW of PMMA reached 58400 g/mol and the PDI is less than 1.4. And the polymerization was even tolerant to water.

Figure 1.4. Rh, Ni and Pd complex

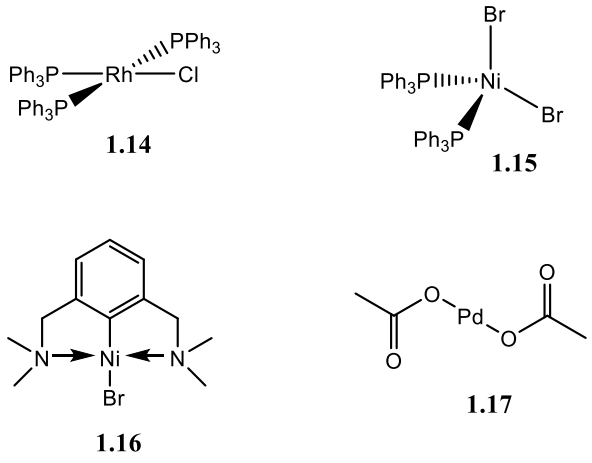

Group 10 nickel and palladium have been widely used in the processes of carbon-carbon bond formation. Their complexes can also be employed in the ATRP process. Teyssie et al. reported the ATRP of MMA and n-butyl methacrylate using Ni{*o*,*o*'$(CH_2NMe_2)_2C_6H_3$}Br as the catalyst and α-halocarbonyl compound as the initiator[24]. The polymers had narrow PDI (less than 1.3), representing a living polymerization. Sawamoto et al. studied the use of nickel(II) bis(triphenylphosphine)halides [$NiX_2(PPh_3)_2$; X=Cl, Br] as the metal complex in ATRP system[25]. MMA was successfully polymerized by using the nickel complex and CCl_4 or CCl_3Br as the initiator. The polymerization showed a living property and the PDI of PMMA is relatively low, about 1.2. Palladium acetate ($Pd(OAc)_2$), can be used for the ATRP of MMA with CCl_4 as the initiator and PPh_3 as the ligand[26]. The polymerization showed a living property and the PDI of PMMA was narrow (1.3). **Figure 1.4** shows some Rh, Ni and Pd complexes.

Group 11 copper complexes have a dominant position among metal catalysts. A large proportion of ATRP is achieved by copper catalysts because of their high versatility and relatively low cost. A variety of monomers have been successfully polymerized under the copper catalyzed ATRP. The copper based ATRP was first reported in 1995. Matyjaszewski et al. reported the first ATRP of styrene using CuCl and 2,2'-bipyridine as the catalyst and 1-phenylethyl chloride as the initiator[27]. The polymerization had a controlled manner and the PDI is less than 1.5. In the same year, Percec et al also published the ATRP of styrene using the same catalytic system, and the initiator was changed to arylsulfonyl chloride[16]. ATRP of MMA was achieved by using the 2-pyridinecarbaldehyde imine copper(I) complexes and an alkyl bromide as the initiator[28]. Methyl acrylate was also

reported to undergo ATRP process using CuBr/ tris[2-(dimethylamino)ethyl]amine (Me_6TREN) as the catalyst and ethyl 2-bromopropionate as initiator[29]. ATRP of *N*-isopropylacrylamide was also accomplished in the presence of the CuCl/Me_6TREN catalyst and the methyl 2-chloropropionate initiator[30].

1.3.2.3. Ligands

The major role of a ligand is to make the metal salts soluble in organic solutions to ensure the homogeneity of the ATRP system. In addition, a ligand can be used to adjust the redox potential of a metal center to obtain proper reactivity and equilibrium for certain ATRP system[31]. There are several classes of ligands. The most common one is nitrogen ligands. Nitrogen ligands have been widely used in the copper catalyzed ATRP system. Monodentate and bidentate ligands have been successfully applied in the iron based ATRP. However, they didn't perform well in the copper based systems. In contrast, multidentate nitrogen ligands gave good performance in the copper catalyzed system and have been extensively developed. Ligands can have a significant electric and steric effects on the activity of catalysts. Too much steric hinderance will decrease the efficiency of a catalyst, so does strong electron-withdrawing groups on the ligand. The activity of a catalyst is usually higher for bridged and cyclic ligands than for linear ones. For example, copper complexes with Me_6TREN or 4,11-dimethyl-1,4,8,11-tetraazabicyclo[6.6.2]hexadecane (Cyclam-B) as ligand have the highest activity rate constant due to the cyclic or bridged structure[32]. **Figure 1.5** shows the structure of some nitrogen ligands.

Figure 1.5. Nitrogen ligands used for copper-mediated ATRP

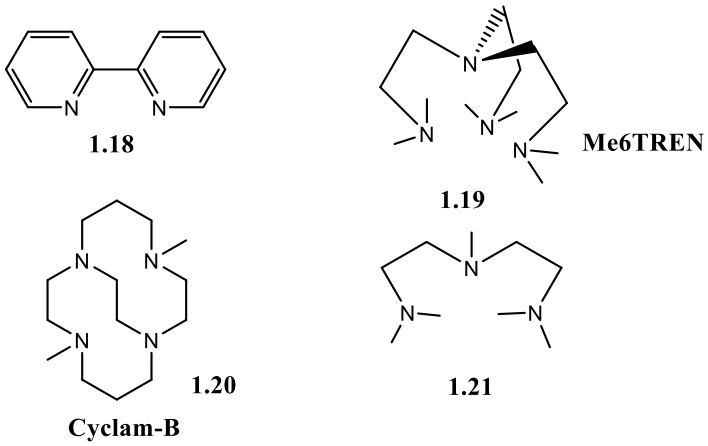

Phosphorus-based ligands have been applied to transition metals other than copper. Various metal catalytic systems, including rhenium, ruthenium, iron, rhodium, nickel and palladium, have utilized phosphorus ligands in ATRP process as decribed in section 1.3.3.2.

1.3.2.4. Monomers

Various monomers have been successfully polymerized by using the ATRP systems. The common monomers are styrenes, (meth)acrylates, acrylamides and acrylonitriles. The polymerization of MMA has been successfully achieved using multiple catalytic systems, which have been introduced previously. Others are functional α-olefins and will be introduced in the next paragraph.

1.4. ATRP of Functional α-Olefins

Functional α-olefins are derived from ethylene, when one of the hydrogen atom is substituted by other functional groups such as ester or amide. Extensive research has been

focused on the ATRP of functional α-olefins because their functional side groups may influence the chemical and physical properties of polymers.

1.4.1. Styrenes

The polymerization of styrene has been reported using various metal catalytic systems such as copper, iron, rhodium and ruthenium, which have been introduced in the previous section. The ATRP of substituted styrenes were also studied. Matyjaszewski et al. reported the ATRP of 3 and 4 position substituted styrenes using CuBr in combination with 4,4'-Di-(5-nonyl)-2,2'-bipyridine (dNbipy) as the catalyst and 1-phenylethyl bromide as initiator[15]. The monomers included 4-F, 4-Cl, 4-Br, 4-CH_3, 4-CF_3, 4-CMe_3, 4-OMe, 3-CH_3 and 3-CF_3 substituted styrenes (**Figure 1.6**). All monomers except 4-OMe styrene polymerized by the ATRP process. It showed that styrenes with electron-withdrawing groups had higher polymerization rate than styrenes with electron-donating groups. And all the polymers had relatively low PDI. Interestingly, 4-OMe styrene did not polymerize and its dimer or trimer was the dominate product. This might be due to the heterolysis of Cu-Br bond to generate cations rather than radicals.

Figure 1.6. Structure of styrene monomers

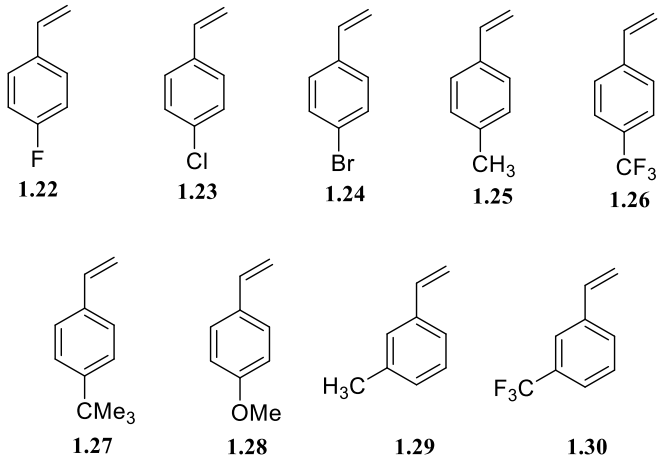

1.4.2. Acrylates

The ATRP of methyl acrylate was successfully conducted by using CuBr/Me_6TREN as the catalyst and ethyl 2-bromopropionate as the initiator[29]. The polymer with relatively high MW (about 18000) and narrow PDI (1.1) was obtained. The ATRP of acrylate derivatives were also studied[33]. Glycidyl acrylate was polymerized with CuBr/dNbipy as the catalyst and methyl 2-bromopropionate as the initiator[34]. The polymerization showed a controlled manner and the PDI was narrow (less than 1.25). The monomer glycidyl acrylate has a pendant oxirane ring, which can be opened for the introduction of other functional groups into the polymer, further increasing the functionality of the polymer. In addition, the ATRP of 2-hydroxyethyl acrylate was also successfully conducted[35] by using CuBr/bpy as the catalyst and methyl 2-bromopropionate as the initiator. The polymer had a high MW of 78000 and narrow PDI of 1.3. The monomer has a hydroxyl group, which enables the polymer to be soluble in water and may have some biomaterial applications. **Figure 1.7** shows the structure of some acrylate monomers.

Figure 1.7. Structure of acrylate monomers

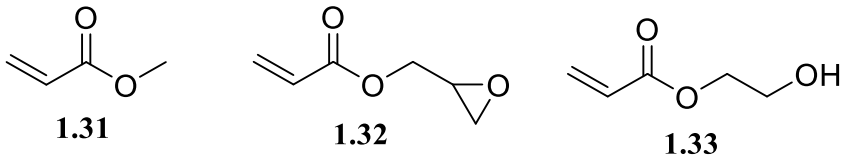

1.4.3. Acrylamides

Various acrylamides have been polymerized by the ATRP methods. *N*,*N*-dimethylacrylamide (DMAA) and *N*,*N*-diethylacrylamide (DEAA) were successfully polymerized by using the ruthenium-based catalytic system. By using $RuCl_2(PPh_3)_3$ as the catalyst and CCl_3Br as the initiator, DMAA with controlled MW and relatively narrow PDI

(1.55) was obtained[36]. The ATRP of DEAA was also achieved by using the same catalytic system. The polymer had a relatively narrow PDI of 1.59. ATRP of *N*-*tert*-butylacrylamide was also studied[37] by using CuCl/Me_6TREN as the catalyst and methyl 2-chloropropionate as the initiator. The MW of the resulting polymer was well controlled and the PDI was quiet narrow (1.15). ATRP of *N*-isopropylacrylamide (NIPAM) was also studied. Stover et al. reported the ATRP of NIPAM with CuCl/Me_6TREN as the catalyst and methyl 2-chloropropionate as the initiator[30]. The controlled MW of PNIPAM was obtained and the PDI was narrow (less than 1.2). **Figure 1.8** shows the structure of some acrylamide monomers.

Figure 1.8. Structure of acrylamide monomers

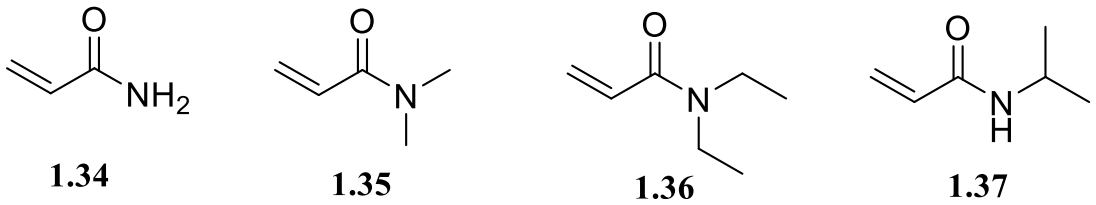

1.34 **1.35** **1.36** **1.37**

1.4.4. Acrylonitrile

Polyacrylonitrile has attractive properties such as hardness and rigidity, which lead to many applications[38]. The ATRP of acrylonitrile has been successfully accomplished by using CuBr/bpy as the catalyst and 2-bromopropionitrile as the initiator[15]. The polymer had a MW up to 10000 and a narrow PDI (less than 1.1). **Figure 1.9** shows the structure of acrylonitrile.

Figure 1.9. Structure of acrylonitrile

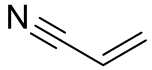

1.38

1.5. Summary

ATRP has been successfully to polymerize various monomers including styrenes, (meth)acrylates, (meth)acrylamides and acrylonitriles. It provides a new method for controlling the radical polymerization process, which considered impossible previously. The precise MW control and architecture manipulation greatly expand the design and application of new materials.

However, ATRP has its limitation in the polymerization of certain monomers. The acidic monomers fail to undergo ATRP process because the proton on the monomer can protonate nitrogen ligand and disable the catalytic system. Other monomers, such as alkyl-substituted olefins and halogenated alkenes, have low reactivity in ATRP system. The design of new ligands and catalytic systems may solve these problems and further improve ATRP method.

2. Tacticity Control of Polymers

2.1. Concept of Tacticity

Tacticity, in definition, represents the relative stereochemistry of adjacent chiral centers in the polymer chain. For α-olefins (CH_2=CHR), there is one side group (R group) for each monomer, and the structure of the whole polymer chain is determined by the arrangement of these R groups. In general, there are three kinds of tacticities for a polymer chain, termed isotactic, syndiotactic and atactic. In the polymer chain, each repeating unit should have a stereocenter, which is the carbon attached with the R group. For isotactic polymers, the stereocenter for each repeating unit in a polymer chain has the same configuration, which means all the R groups align on the same side of the plane of the polymer chain. For syndiotactic polymers, the configuration alternates from one unit to the adjacent repeating unit, which means the R groups are on the opposite side of the plane of polymer chain alternatively. For atactic polymers, the two configurations are placed in the polymer chain randomly. **Figure 1.10** shows the α-olefin based polymers structure with different tacticities.

Figure 1.10. α-olefin based polymers structure with different tacticities

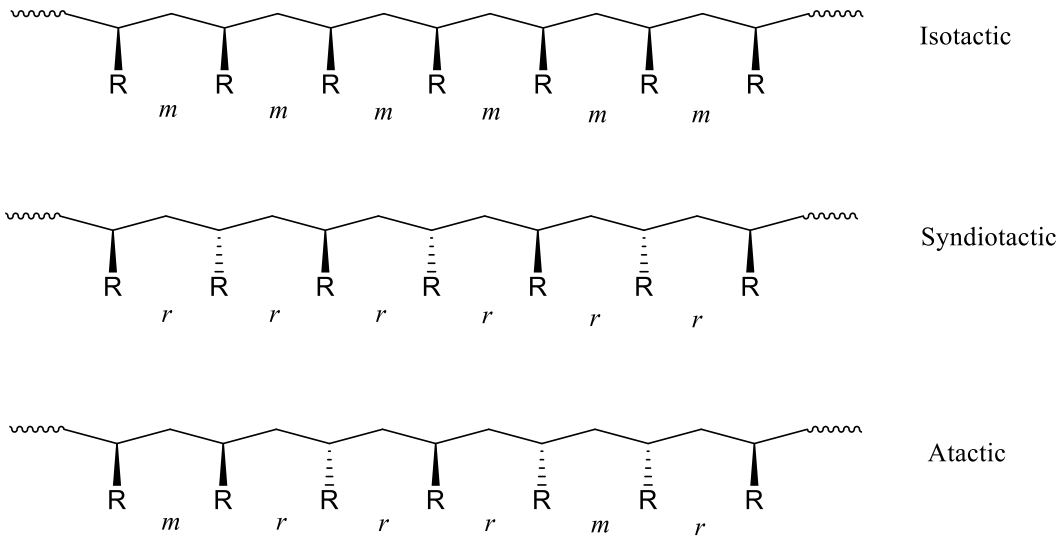

The isotactic and syndiotactic polymers have highly regular structure. However, atactic polymer lacks regularity in its polymer chain. The regularity of the polymer chain will greatly influence the property of the polymer, and the difference is mainly on their ability to crystallize[1]. The ordered structures of the isotactic and syndiotactic polymers are able to pack into a crystal lattice. Therefore, these two kinds of polymers are usually highly crystalline materials. In contrast, atatic polymers are generally amorphous and noncrytalline due to its irregular structure. Crystallinity leads to high melting point, high mechanical strength of polymeric materials as well as increasing their solvent and chemical resistance. This is why isotactic polypropylene has high melting point (165℃) and strong physical strength and is used as plastic and fiber. Atactic polymers are usually soft or oily due to the lack of crystallization and have low melting point and weak mechanical strength.

2.2. Determination of Tacticity

There are several methods to determine the tacticity of a polymer sample. The analysis of tacticity using X-ray diffraction[39,40] or IR spectroscopy[41,42] methods is limited. And the measurement of solubility or melting point can only give a relatively qualitative conclusion on the tacticity of a sample. The most powerful method is nuclear magnetic resonance (NMR). The chemical shift of polymer nuclei such as hydrogen and carbon are sensitive to adjacent stereocenters, which can provide quantitative information about the stereochemistry of the polymer sample.

If two adjacent stereocenters in a polymer chain have the same configuration, the dyad is considered isotactic and represented as *meso* dyad (*m*). If two adjacent stereocenters have opposite configuration, the dyad is considered syndiotactic and represented as

racemic dyad (*r*) (**Figure 1.10**). The total ratio of *meso* and *racemic* dyad is 100%, and the percentage of *m* and *r* demonstrates the tacticity of the polymer. If the percentage of the *meso* dyads is large than 50%, the polymer is isotactic rich. The higher the ratio, the more isotactic of the polymer. The situation is the same for the *racemic* dyad.

Proton NMR can be used to calculate the tacticity of a polymer very easily. The chemical shifts of the two hydrogens on the methylene group are influenced by the two adjacent stereocenters. If the dyad is isotactic, which means the two stereocenters have the same configuration, the two hydrogens are under different chemical environment and show two distinct peaks on the spectrum. If the dyad is syndiotactic, the two hydrogens are under the same chemical environment and only one peak appears on the spectrum. By integrating the area of the two kinds of peaks, the isotacticity and syndiotacticity can be calculated based on the area of the peaks.

Carbon NMR is able to discover the more detailed microstructure of the polymer chain compared with proton NMR, which can usually provide the information of dyad and triad distributions. It can provide the sequence distributions of stereocenters in the polymer chain. For high resolution carbon NMR, the distribution of configurations of five, six or even seven repeating units can be revealed in a spectrum, and the chemical shift differences are large enough to be distinguished from one to another. Therefore, carbon NMR is one of the most powerful tools in the determination of polymer structure.

2.3. Tacticity Control Method in Radical Polymerization

Although the development of CRP has reached a high level, the development of stereocontrol of polymers using radical polymerization is still not satisfying. The most

possible reason is that there is no efficient method for the stereospecific propagation of the sp^2-planar radical species. The radicals can attack the two sides of the carbon-carbon double bond with almost the same probability and generate a stereocenter with opposite configuration in the same chance, leading to the generation of atactic polymer. However, there have been some methods to solve this problem and polymers with moderate or highly stereocontrolled structure can be obtained.

2.3.1. Polymerization in Confined Media

Stereocontrolled polymers have been obtained in confined media, such as porous materials and templates. The structure of these polymers can be controlled because the monomers and propagating radicals are confined in a pre-designed space and cannot rotate or move freely. The well-organized confined media can induce a highly stereospecific chain propagation and lead to isotactic or syndiotactic polymers. In addition, as the media constrains the movement of the propagating radicals, the termination between radicals becomes more difficult, which means the life of the radicals is much long than usual. The long-lived radicals make chain length control possible although the PDI is still broader than the CRP method.

Porous materials have channel-like cavities in their structures. These channels are suitable for certain polymer chain growth, which depends on both the size of the channel and the size of the monomer. Early studies focused on the radical polymerization in zeolites, which are porous inorganic materials and can absorb monomers onto the surface. For example, Chachaty et al. studied the polymerization of acrylonitrile (AN) and methyl methacrylate (MMA) absorbed on zeolite and the tacticity of the obtained polymers[43]. The

polymerization was induced by γ-ray. And the poly (AN) and poly (MMA) had higher isotacticity than polymers synthesized in solution, which was probably because the monomers performed an isotactic placement on the zeolite surface. More recently, the polymerization in porous coordination polymers (PCPs) is under great attention. PCPs are porous materials consisting of metal ions and organic ligands[44]. The channel structure and pore size can be easily tuned by using variuos metal ions and ligands. Therefore, a fine-tuned polymerization of variuos monomers in PCPs became possible and stereocontrol of the polymer chains was also achieved. In 2008, Kitagawa et al. reported the polymerization of MMA, styrene and vinyl acetate in PCPs, which consists of Cu or Zn metal ions and aromatic dicarboxylic acid ligand[45]. The resulting polymers were more isotactic rich than the polymers obtained in solution and the PDI were narrower, which reflected the capability of PCPs to control the stereochemistry and chain propagation of polymers. In 2010, Kitagawa et al. published another paper on the polymerization of MMA by PCPs[46]. The PCPs were made of Cu ions and substituted aromatic carboxylic acid ligand, and the isotaciticity increased significantly in comparison with the previous paper (*mm* from 10 to 28) by employing these new PCPs.

Template polymerization is another widely used method to control the tacticity of polymers. In template polymerization, the propagation of polymer chains occurs predominantly along a template macromolecule chain. This process can be achieved due to specific interactions between the monomer and the template, such as hydrogen bonding and Van der Waals interactions[47]. Template polymerization of MMA has been well studied. It has been known that an isotactic and a syndiotactic PMMA can form a stereocomplex via Van der Waals interaction, in which the isotactic PMMA is surrounded by a helix of

syndiotactic PMMA[48]. According to this property, a syndiotactic PMMA can be obtained by using an isotactic PMMA template and *vice versa*. Akashi et al. reported the stereospecific template polymerization of MMA in the presence of iso- or syndiotactic PMMA porous films as template[49]. The daughter PMMA can be synthesized within the porous film and highly iso- or syndiotactic daughter PMMAs were obtained. The daughter PMMA with a template (*mm*: *mr*: *rr* = 1: 6: 93) had high syndiotacticity (*mm*: *mr*: *rr* = 97: 3: 0). And the daughter PMMA with a template (*mm*: *mr*: *rr* = 97: 3: 0) had high isotacticity (*mm*: *mr*: *rr* = 0: 2: 98). Even though the PIDs were relatively large (around 2) for daughter PMMAs, the template polymerization proved to be a very effective way to control the stereochemistry of polymers.

2.3.2. Stereocontrol by Monomer Structure

In solution radical polymerization, the reaction environment cannot provide sufficient stereocontrol on the propagating polymer chain because unlike the confined media, the monomers and polymer chain radicals can move freely in solution. Therefore, the tacticity of the polymers is mainly determined by the chemical structure of the monomer, which can greatly influence the stereochemistry of the polymer.

In general, vinyl monomers have pendant side groups attached to the carbon-carbon double bond, and the size of the side group has significant effect on the tacticity of the polymer. The stereocontrolled radical polymerization of methacrylate and methacrylamide derivatives has been well studied and highly iso- and syndiotactic polymers have been obtained. Generally, PMMA and other common poly-methacrylates have syndiotactic rich structure, probably because of the steric repulsion among α-methyl group, ester group of

the incoming monomer and one or two chain end repeating units[50]. The syndiotacticity usually increases at lower polymerization temperature. For example, Bovey reported the polymerization of MMA at -78℃[51]. The PMMA obtained was more syndiotactic than PMMA synthesized at higher temperature (*mm*: *mr*: *rr* = 5: 17: 78). More importantly, the tacticity of the polymer is significantly influenced by the bulkiness of the side group. The syndiotacticity of poly methacrylates decreases as the bulkiness of the side ester group increases. For instance, the radical polymerization of triarylmethyl methacrylate, which has an extremely bulky side group, gives polymer with high isotacticity (*mm*: *mr*: *rr* = 98.2: 1.7: 0.1)[52]. This is mostly because the bulky side groups inhibit the generation of the planar zig-zag conformation of the polymer chain. Instead, the less hindered helical structure in a gauche-staggered conformation is formed. The results are similar for other bulky monomers. The polymerization of other bulky methacrylates, such as 1-phenyldibenzosuberyl methacrylate (PDBSMA)[53], 1-(3-Pyridyl)dibenzosuberyl methacrylate[54], and 10,10-dimethyl-9-phenyl-9,10-dihydro-9-anthracenyl methacrylate[52] (**Figure 1.11**), all yield polymers with isotacticity larger than 99%.

Figure 1.11. Structure of some methacrylate monomers

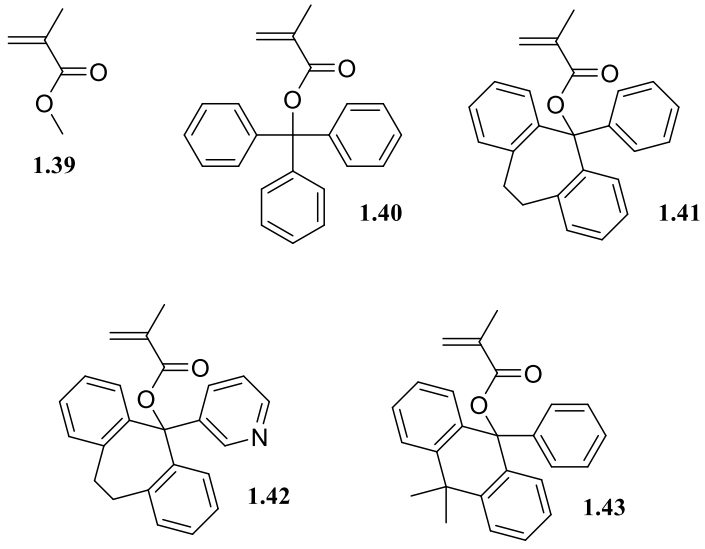

The effect of the monomer bulkiness of monomer is the same for methacrylamides. Polymerization of methacrylamides with the bulky side groups resulted in polymers with high isotacticity. For example, *N*-triphenylmethylmethacrylamide[55], *N*-(1-phenyldibenzosuberyl) methacrylamide[9], and their alkylated derivatives were all polymerized into highly isotactic polymers (**Figure 1.12**).

Figure 1.12. Structure of some bulky methacrylamide monomers

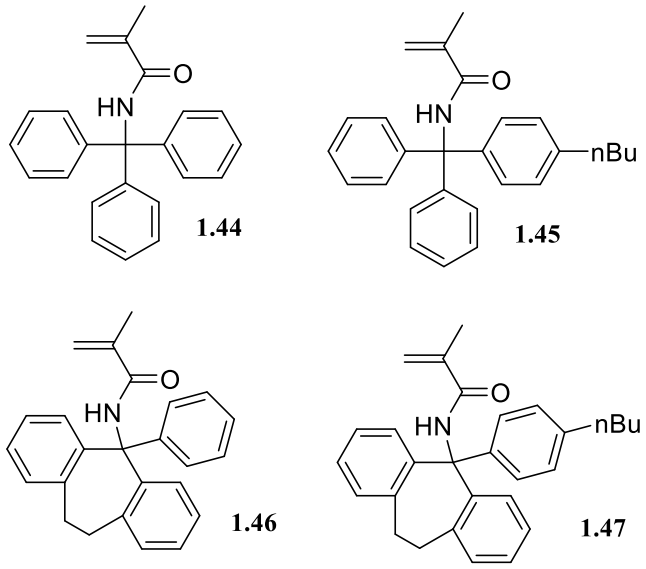

However, in contrast to the aforementioned two classes of monomers with α-methyl group, the polymerization of monosubstituted functional olefins gave almost atactic polymers, and the monomer structure and reaction temperature have less effect on the tacticity[56]. As the side group of monomers became bulkier, the polymers were more syndiotactic rich, probably due to the steric repulsion between adjacent pendant groups. For example, the polymerization of 1-phenyldibenzosuberyl acrylate yielded syndiotactic rich polymer (*m*: *r* = 44: 56)[57]. And the polymerization of *N*,*N*-diphenylacrylamide gave

polymer with high syndiotacticity (*m*: *r* = 12: 88)[54]. **Figure 1.13** shows the structure of some bulky acrylates.

Figure 1.13. Structure of bulky acrylate and acrylamide

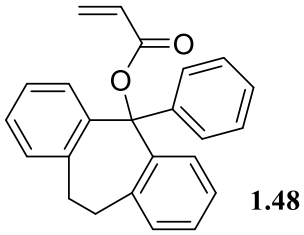

1.48

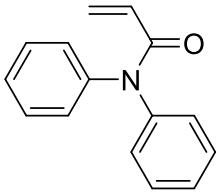

1.49

The chirality of monomer may also influence the tacticity of polymer chain. The stereocontrol of the polymer chain depends on the enantioselectivity between incoming monomer and propagating radical[58]. The monomer with chiral center on the pendant group might influence the enantioselectivity. As a result, one configuration of the stereocenter on the polymer chain will be more favored than the other, leading to the isotactic or syndiotactic rich polymers. However, it is difficult to obtain the desired tacticity using this method, probably because tacticity control needs diastereoselectivity, which is hard to achieve during radical polymerization. Still et al. reported the radical polymerization of a chiral lactone, which is an aliphatic cyclic monomer[59]. The polymerization gave highly isotactic polymer, in which almost all the triads were *mm*, showing the success of stereocontrol by chiral monomers. Porter et al. studied the polymerization of acrylamides with chiral pyrrolidine[60] or oxazolidine[61], and highly isotactic polymers (mm = 88-92%) were obtained. It was explained that the stereocontrol of the polymerization resulted from the steric hindrance contributed by the chiral auxiliary of the monomers. **Figure 1.14** shows the structure of some chiral monomers.

Figure 1.14. Structure of some chiral monomers

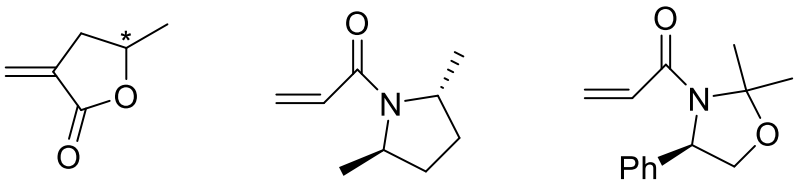

1.50 **1.51** **1.52**

2.3.3. Stereocontrol by Solvents or Additives

Stereocontrol by solvents or additives might be the most promising methods in radical polymerization, especially for CRP. Many specific solvents or additives could have various interactions with monomers to modify their structure, leading to the stereocontrolled radical polymerization[62].

Specific solvents are able to control the stereochemistry of the polymer chains. This is achieved by the interaction between solvents and side groups of monomers and polymer chains. The interaction, in most cases, is hydrogen bonding. **Scheme 1.5** shows the proposed mechanism of a solvent-mediated stereocontrolled polymerization process. The interaction increases the bulkiness of the side groups since solvents become part of the side groups. As a result, the steric repulsion between pendant groups of the chain terminal and incoming monomer becomes large, leading to the formation of syndiotactic polymers.

Scheme 1.5. Proposed mechanism of thesolvent-mediated stereocontrolled polymerization process

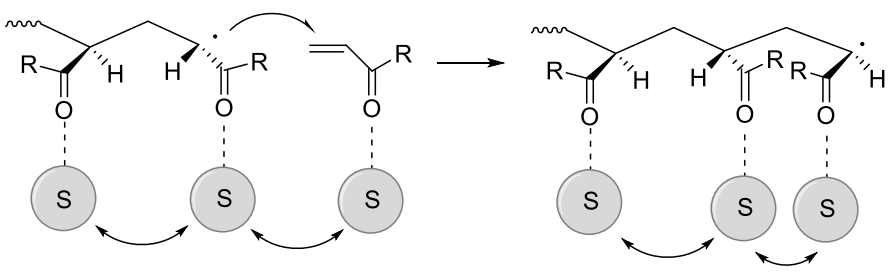

The method is extremely useful for monomers which can easily form hydrogen bonding with solvents. For example, Farmer et al. reported the radical polymerization of methacrylic acid (MAA) in variuos alcohols induced by cobalt 60 γ-radiation[63]. High syndiotactic polymers were obtained by using methanol, 1-propanol and 2-propanol as the solvent at -78℃, and polymerization with 2-propanol yielded the highest syndiotacticity (*mm*: *mr*: *rr* = 95: 5: 0). In more recent years, Okamoto et al. found that fluoroalcohols were the most efficient solvents for stereocontrol of polymers, especially for the formation of syndiotactic polymers[64]. Stereocontrol of the radical polymerization of vinyl acetated (VAc) cannot be achieved by using the common solvents. However, polymerization in fluoroalcohols such as nonafluoro-tert-butyl alcohol ($(CF_3)_3COH$) showed good syndiotacticity control[65]. Reaction at -78℃ yielded poly (VAc) with high syndiotacticity (*mm*: *mr*: *rr* = 5.4: 44.9: 49.8). Highly syndiotactic PMMA was also obtained using $(CF_3)_3COH$ as the solvent at -98℃[66]. The syndiotacticity was as high as 97% (*mm*: *mr*: *rr* = 0: 7: 93). In addition to the conventional radical polymerization, CRP using fluoroalcohol as the solvent was also achieved and polymers with both high syndiotacticity and narrow PDI were synthesized. The most successful examples of CRP with fluoroalcohols as he solvent were the CRP of methacrylates. Okamoto et al. reported the ATRP of MMA in fluoroalcohols using $RuCp^*Cl(PPh_3)_2$ as the metal complex and dimethyl 2-chloro-2,4,4-trimethylpentanedioate as the initiator[67]. The polymerization occurred at 0 ℃ in $(CF_3)_3COH$ gave PMMA with high syndiotacticity (*r* = 90%) and narrow PDI (1.07), showing a dual control on both stereochemistry and MW distribution of polymers. Kakuchi et al. also demonstrated the ATRP of MMA using fluoroalcohols as the solvent[68]. By using

Me_6TREN/CuBr as the metal complex and methyl 2-bromo-2-methylpropanoate as the initiator, a highly syndiotactic PMMA was obtained at -78 ℃ in $(CF_3)_2CHOH$ (*rr* = 84%) with narrow PDI (1.31).

Lewis acids of certain metal salts proved to be the most effective additives for the generation of isotactic polymers. **Scheme 1.6** shows the proposed mechanism of aLewis acid-mediated stereocontrolled polymerization process. These Lewis acids are able to coordinate with the carbonyl group of functional olefins to form complexes. This kind of coordination can force the side group of chain terminal and incoming monomer into a *meso* configuration, leading to the formation of isotactic polymers[69].

Scheme 1.6. Proposed mechanism of a Lewis acid-mediated stereocontrolled polymerization process

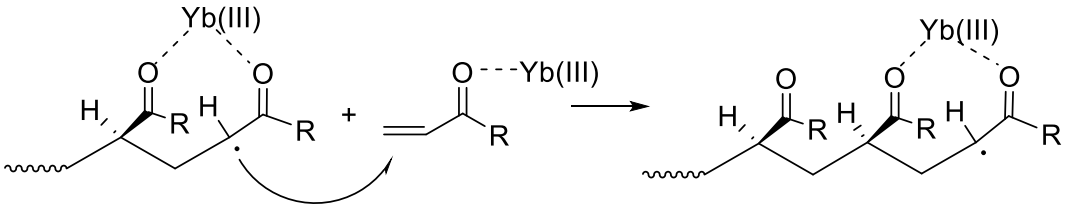

Early studies demonstrated the effect of $ZnCl_2$ on the stereochemistry of MMA polymerization[70]. Radical polymerization of MMA in the presence of a large amount of $ZnCl_2$ led to the PMMA with slightly increased isotacticity (*mm*: *mr*: *rr* = 15: 42: 43) than in the absence of a Lewis acid (*mm*: *mr*: *rr* = 5: 37: 58). More recently, rare earth metal triflates ($M(OTf)_3$, OTf = OSO_2CF_3) proved to be the most effective Lewis acids for tacticity control. Okamoto et al. first reported the stereocontrolled radical polymerization using metal triflates as additives[71]. Polymerization of α-(alkoxymethyl)acrylate in the

presence of 0.1 equivalent of $Sc(OTf)_3$ as additive resulted an isotactic rich polymer (m% = 70). An isotactic rich PMMA was also obtained by using $Sc(OTf)_3$ as an additive[72]. Polymerization of MMA in the presence of 0.08 equivalent of $Sc(OTf)_3$ yielded an isotactic rich PMMA (*mm*: *mr*: *rr* = 14: 46: 40) compared with the PMMA obtained in the absence of Lewis acid (*mm*: *mr*: *rr* = 3: 33: 64). The stereocontrolled RP of (meth)acrylamides in the presence of metal triflates was also studied. Okamoto et al. reported the polymerization of NIPAM, DMAA and acrylamide (AM) using variuos metal triflates as the additives[73]. Highly isotactic polymers were obtained. Polymerization of NIPAM in the presence of 0.2 equivalent of $Y(OTf)_3$ led to PNIPAM with isotacticity equals to 92%. Highly isotactic PDMAA (*m*: *r* = 88: 12) and PAM (*m*: *r* = 80: 20) were also synthesized in the presence of 0.1 equivalent of $Yb(OTf)_3$. The Lewis acid-mediated stereocontrolled CRP of various monomers, especially arylamides, was also achieved. Matyjaszewski et al. reported the ATRP and RAFT polymerization of DMAA using $Y(OTf)_3$ or $Yb(OTf)_3$ as additive and the results were quite promising[74]. The ATRP of DMAA used Me_6TREN/CuCl as the metal complex and methyl 2-chloropropionate as the initiator. In the presence of 0.05 equivalent of $Y(OTf)_3$ or $Yb(OTf)_3$ and methanol as the solvent, a PDMMA with isotacticity up to 86% was obtained, and the PDI was narrow (1.13). The RAFT polymerization of DMAA used 2,2'-azobisisobuytronitrile (AIBN) as the initiator and cumyl dithiobenzoate as the chain transfer agent. Similarly, in the presence of 0.1 equivalent of $Y(OTf)_3$ and methanol as the solvent, the resulting PDMAA showed highly isotactic property (*m* = 85%) and relatively narrow PDI (1.41). The stereocontrolled CRP of NIPAM was also reported by Sawamoto et al. The RAFT polymerization was conducted in methanol/toluene (1/1, v/v), with 1-phenylethyl phenyldithioacetate as the chain transfer agent and AIBN as the

initiator[75]. In the presence of 0.2 equivalent of $Y(OTf)_3$, a highly isotactic PNIPAM was obtained (m = 87%) with relatively narrow PDI (1.76). The ATRP of NIPAM used $[FeCp(CO)_2]_2$ as catalyst and alkyl iodide as initiator[67]. Polymerization in methanol/toluene (1/1, v/v) and in the presence of 0.05 equivalent of $Y(OTf)_3$ produced predominantly isotactic PNIPAM (m: r = 78: 22). However, the PDI of the PNIPAM was quite broad (2.56), reflecting the lack of MW distribution control of the system.

2.3.4. Stereocontrol by Chiral Ligands in ATRP

There has been significant reseaches on the stereocontrolled ATRP process, such as by using specific solvents and additives. In addition, the structure of ligands is also extensively studied. Ligands with chiral centers could control the stereochemistry of the propagating chain because the asymmetric centers might induce the chain radicals to attack one face of the incoming monomers more favorably than the other. However, no ligands reported had the effect to influence the tacticity of the polymers[76,77]. Haddleton et al. synthesized some chiral aryl/alkyl pyridylmethanimine ligands for copper-mediated ATRP of MMA[77]. Carbon NMR revealed that the tactcity of PMMA was almost the same as the PMMA synthesized with achiral ligands (m: r = 22: 78). Fraser et al. also reported the copper-mediated ATRP of MMA using chiral quadridentate ligands[78]. However, no stereoselectivity was observed during polymerization. Okamoto et al. studied the ruthenium-mediated ATRP of MA using chiral phosphane ligands[79]. **Figure 1.15** shows the structure of some chiral catalysts. The results showed that the stereocontrol of the polymerization by using the chiral metal complexes was not successful. The reason for the unsuccessful stereocontrol of ATRP can be attributed to the fact that radical addition to the

monomer might occur far away from the chiral metal center, which means the radical intermediate might have dissociated from the chiral metal site before its addition to the monomer.

Figure 1.15. Structure of some chiral catalysts

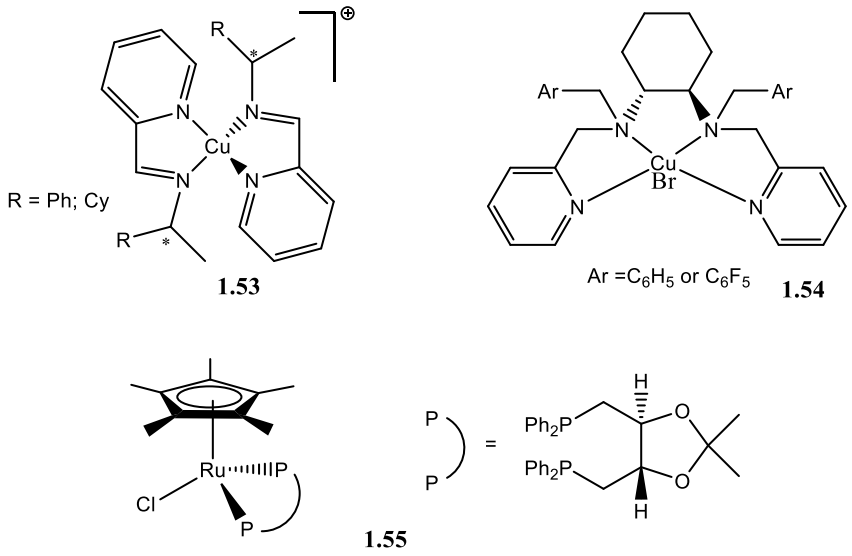

2.4. Summary

There have been various methods to control the tacticity of polymers, and some of them are very effective for producing polymers with high iso- or syndiotacticity. However, only a few methods such as solvent or Lewis acid mediated polymerization can be applied to the CRP process. In addition, the number of monomers that can be used for the stereocontrolled CRP is limited. Most functional α-olefins cannot undergo CRP to achieve high iso- or syndiotacticity by using the above-mentioned method. In order to further increase the tacticity of polymers and expand the substrates, new catalysts are required. In my project, the chiral macrocyclic compounds will be used as ligands and work together with metal triflates to further improve the isotacticity of different poly functional α-olefins in copper-mediated ATRP process.

Reference

(1) Odian, G. *Principles of Polymerization*, 4th ed.; Wiley, 2004.

(2) Coates, G. W. *Chem. Rev.* **2000**, *100* (M), 1223–1252.

(3) Braunecker, W. A.; Matyjaszewski, K. *Prog. Polym. Sci.* **2007**, *32* (1), 93–146.

(4) Studer, A. *Chem. - A Eur. J.* **2001**, *7* (6), 1159–1164.

(5) Hawker, C. J.; Bosman, A. W.; Harth, E. *Chem. Rev.* **2001**, *101* (12), 3661–3688.

(6) Georges, M.; Kazmaier, P. M.; Gordon, K. *Macromolecules* **1993**, *26*, 2987–2988.

(7) Benoit, D.; Chaplinski, V.; Braslau, R.; Hawker, C. J. *J. Am. Chem. Soc.* **1999**, *121* (16), 3904–3920.

(8) Grassl, B.; Clisson, G.; Khoukh, A.; Billon, L. *Eur. Polym. J.* **2008**, *44* (1), 50–58.

(9) Kali, G.; Georgiou, T. K.; Iván, B.; Patrickios, C. S. *J. Polym. Sci. Part a-Polymer Chem.* **2009**, *47*, 4289–4301.

(10) Perrier, S.; Takolpuckdee, P. *J. Polym. Sci. Part A Polym. Chem.* **2005**, *43* (22), 5347–5393.

(11) Singha, N. K.; Klumperman, B. *Macromol. Rapid Commun.* **2000**, *21* (16), 1116–1120.

(12) Kotani, Y.; Kato, M.; Kamigaito, M.; Sawamoto, M. *Macromolecules* **1996**, *29* (22), 6979–6982.

(13) Destarac, M.; Matyjaszewski, K.; Boutevin, B. *Macromol. Chem. Phys.* **2000**, *201* (2), 265–272.

(14) Brandts, J. a. M.; van de Geijn, P.; van Faassen, E. E.; Boersma, J.; van Koten, G. *J. Organomet. Chem.* **1999**, *584*, 246–253.

(15) Matyjaszewski, K.; Jo, S. M.; Paik, H.; Gaynor, S. G. *Macromolecules* **1997**, *30*

(97), 6398–6400.

(16) Percec, V.; Barboiu, B. *Macromolecules* **1995**, *28*, 7970–7972.

(17) Percec, V.; Barboiu, B.; Kim, H.-J. *J. Am. Chem. Soc.* **1998**, *120* (2), 305–316.

(18) Kotani, Y.; Kamigaito, M.; Sawamoto, M. *Macromolecules* **1999**, *32* (V), 2420–2424.

(19) Kato, M.; Kamigaito, M.; Sawamoto, M.; Higashimuras, T. *Macromolecules* **1995**, *28* (Ii), 1721–1723.

(20) Simal, F.; Demonceau, A.; Noels, A. F. *Angew. Chemie - Int. Ed.* **1999**, *38* (4), 538–540.

(21) Ando, T.; Kamigaito, M.; Sawamoto, M. *Macromolecules* **1997**, *30* (16), 4507–4510.

(22) Matyjaszewski, K.; Wei, M.; Xia, J.; Mcdermott, N. E. *Macromolecules* **1997**, *30* (1), 8161–8164.

(23) Moineau, G.; Granel, C.; Dubois, P. *Macromolecules* **1998**, *9297* (97), 542–544.

(24) Granel, C.; Dubois, P.; Jérôme, R.; Teyssié, P. *Macromolecules* **1996**, *29* (Ii), 8576–8582.

(25) Uegaki, H.; Kotani, Y.; Kamigaito, M.; Sawamoto, M. *Macromolecules* **1997**, *3* (Ii), 2249–2253.

(26) Lecomte, P.; Drapier, I.; Dubois, P.; Teyssie, P.; Jerome, R. *Macromolecules* **1997**, *30*, 7631–7633.

(27) Wang, J.; Matyjaszewski, K. *J. Am. Chem. Soc.* **1995**, *117* (6), 5614–5615.

(28) Haddleton, D. M.; Jasieczek, C. B.; Hannon, M. J.; Shooter, A. J. *Macromolecules* **1997**, *9297* (96), 2190–2193.

(29) Xia, J.; Gaynor, S. G.; Matyjaszewski, K. *Macromolecules* **1998**, *31*, 5958–5959.

(30) Xia, Y.; Yin, X.; Burke, N. a D.; Sto, H. D. H. *Macromolecules* **2005**, No. Scheme 1, 5937–5943.

(31) J Xia, X Zhang, K. M. *ACS Symp. Ser.* **2000**, *760*, 207.

(32) Tang, W.; Matyjaszewski, K. *Macromolecules* **2007**, *40* (6), 1858–1863.

(33) Matyjaszewski, K.; Nakagawa, Y.; Jasieczek, C. B. *Macromoleculars* **1998**, *9297* (Scheme 2), 1535–1541.

(34) Matyjaszewski, K.; Coca, S.; Jasieczek, C. B. *Macromol. Chem. Phys.* **1997**, *198* (12), 4011–4017.

(35) Coca, S.; Jasieczek, C. *J. Polym. Sci. Part A Polym. Chem.* **1998**, *36*, 1417–1424.

(36) Pph, R.; Systems, I.; Senoo, M.; Kotani, Y.; Kamigaito, M.; Sawamoto, M. *Macromolecules* **1999**, *32*, 8005–8009.

(37) Teodorescu, M.; Matyjaszewski, K. *Macromol. Rapid Commun.* **2000**, *21*, 190–194.

(38) Mark, H. F., Bikales, N. M., Overberger, C. G., Menges, G., Kroschwitz, J. I., E. *Encyclopedia of Polymer Science and Engineering*; Wiley: New York, 1995.

(39) Tsuji, H. *Polymer (Guildf).* **2002**, *43* (6), 1789–1796.

(40) Silvestre, C.; Cimmino, S.; Martuscelli, E.; Karasz, F. E.; MacKnight, W. J. *Polymer (Guildf).* **1987**, *28*, 1190–1199.

(41) Grohens, Y.; Brogly, M.; Labbe, C.; David, M.-O.; Jacques, S. *Langmuir* **2002**, *14* (11), 2929–2932.

(42) Kister, G.; Cassanas, G.; Vert, M. *Polymer (Guildf).* **1998**, *39* (2), 267–273.

(43) Natta, G. *J. Polym. Sci., Polym. Chem. Ed.* 1976, p 2703.

(44) Kitagawa, S.; Kitaura, R.; Noro, S. *Angew. Chemie - Int. Ed.* **2004**, *43*, 2334–2375.

(45) Uemura, T.; Ono, Y.; Kitagawa, K.; Kitagawa, S. *Macromolecules* **2008**, *41* (1), 87–94.

(46) Uemura, T.; Ono, Y.; Hijikata, Y.; Kitagawa, S. *J. Am. Chem. Soc.* **2010**, *132* (13), 4917–4924.

(47) Tan, Y. Y. *Prog. Polym. Sci.* **1994**, *19* (93), 561–588.

(48) Liu, H.; Liu, K. *Macromolecules* **1968**, *1199* (2), 157–162.

(49) Serizawa, T.; Hamada, K.; Akashi, M. *Nature* **2004**, *429* (May), 52–55.

(50) Moad, G.; Solomon, D. H.; Spurling, T. H.; Johns, S. R.; Willing, R. I. *Aust. J. Chem.* **1986**, *39* (1), 43–50.

(51) Bovey, F. A. *J. Polym. Sci.* **1960**, *46*, 59.

(52) Nakano, T.; Okamoto, Y. *Chem. Rev.* **2001**, *101* (12), 4013–4038.

(53) Nakano, T.; Matsuda, A.; Okamoto, Y. *Polymer Journal*. 1996, pp 556–558.

(54) Shiohara, K.; Habaue, S.; Okamoto, Y. *Polymer Journal*. 1998, pp 249–255.

(55) Hoshikawa, N.; Hotta, Y.; Okamoto, Y. *J. Am. Chem. Soc.* **2003**, *125* (41), 12380–12381.

(56) Pino, P.; Suter, U. W. *Polymer (Guildf).* **1976**, *17* (11), 977–995.

(57) Tanaka, T.; Okamoto, Y. *Polym. J.* **1995**, *27* (12), 1202–1207.

(58) Sibi, M. P.; Manyem, S.; Zimmerman, J. *Chem. Rev.* **2003**, *103* (8), 3263–3295.

(59) Suenaga, J.; Sutherlin, D. M.; Stille, J. K. *Macromolecules* **1984**, *17*, 2913–2916.

(60) Porter, N. A.; Breyer, R.; Swann, E.; Nally, J.; Pradhan, J.; Allen, T.; McPhail, A. T. *J. Am. Chem. Soc.* **1991**, *113*, 7002–7010.

(61) Porter, N.; Allen, T.; Breyer, R. *J. Am. Chem. Soc.* **1992**, *114* (HL 17921), 7676–

7683.

(62) Renaud, P.; Gerster, M. *Angew. Chem. Int. Ed.* **1998**, *37*, 2562–2579.

(63) Lando, J. B.; Farmer, B. *Macromolecules* **1970**, *145* (6), 524–527.

(64) Habaue, S.; Okamoto, Y. *Chem. Rec.* **2001**, *1* (1), 46–52.

(65) Yamada, K.; Nakano, T.; Okamoto, Y. *Macromolecules* **1998**, *31*, 7598–7605.

(66) Isobe, Y.; Yamada, K.; Nakano, T.; Okamoto, Y. *J. Polym. Sci. Part A Polym. Chem.* **2000**, 4693–4703.

(67) Sugiyama, Y.; Satoh, K.; Kamigaito, M.; Okamoto, Y. *J. Polym. Sci. Part A Polym. Chem.* **2006**, *44* (6), 2086–2098.

(68) Miura, Y.; Satoh, T.; Narumi, A.; Nishizawa, O.; Okamoto, Y.; Kakuchi, T. *Macromolecules* **2005**, *38*, 1041–1043.

(69) Okamoto, Y.; Habaue, S. *ACS Symp. Ser.* **2003**, *854*, 59.

(70) Okuzawa, S.; Makishima, S. *J. Polym. Sci. Part A Polym. Chem.* **1969**, *7*, 1039–1053.

(71) Liu, W.; Nakano, T.; Okamoto, Y. *Polymer journal*. 2000, pp 771–777.

(72) Isobe, Y.; Nakano, T.; Okamoto, Y. *J. Polym. Sci. Part A Polym. Chem.* **2001**, *39*, 1463–1471.

(73) Okamoto, Y.; Habaue, S. *Macromol. Symp.* **2003**, *195*, 75–80.

(74) Lutz, J. F.; Neugebauer, D.; Matyjaszewski, K. *J. Am. Chem. Soc.* **2003**, *125* (12), 6986–6993.

(75) Ray, B.; Isobe, Y.; Morioka, K. *Macromolecules* **2003**, *36*, 543–545.

(76) Stoffelbach, F.; Richard, P.; Poli, R.; Jenny, T.; Savary, C. *Inorganica Chim. Acta* **2006**, *359*, 4447–4453.

(77) Haddleton, D. M.; Duncalf, D. J.; Kukulj, D.; Heming, A. M.; Shooter, A. J.; Clark, A. J. *J. Mater. Chem.* **1998**, *8* (7), 1525–1532.

(78) Johnson, R. M.; Ng, C.; Samson, C. C. M.; Fraser, C. L. *Macromolecules* **2000**, *33*, 8618–8628.

(79) Iizuka, Y.; Li, Z.; Satoh, K.; Kamigaito, M.; Okamoto, Y.; Ito, J. I.; Nishiyama, H. *European J. Org. Chem.* **2007**, *4*, 782–791.

Chapter 2. Stereoselective Atom Transfer Radical Polymerization of Acrylamides using Achiral and Chiral Macrocyclic Catalysts

1. Introduction

So far, stereocontrolled ATRP can only be applied to limited numbers of α-olefins, and only a few monomers, such as DMAA and NIPAM, gave relatively good isotacticity under the Lewis acid-mediated ATRP. Expanding the substrates and further increasing the isotacticity of the polymers is highly-desired. Therefore, new catalysts are designed in order to achieve these goals. In this project, various chiral macrocyclic ligands are synthesized and incorporated with metal triflates to investigate their influence on the isotacticity of poly functional α-olefins in the copper-mediated ATRP system.

One of the reasons for the previous unsuccessful stereocontrol in ATRP using chiral metal catalysts may be that the radical addition to the monomer might occur far away from the chiral metal center. We propose that if we could bring the monomer closer to the chiral metal center to allow both the radical formation and the subsequent monomer addition to occur under the chiral environment, it would be possible to achieve stereoselectivity in ATRP. To achieve this goal, the Schiff base-based macrocyclic compounds that contain multiple chiral centers and two metal coordination sites and the corresponding hydrogenated ones are synthesized as ligands. As described in Chapter 1 section 2.2.3, metal triflates are very efficient additives for producing isotactic polymers. We hypothesize that if the metal triflates could coordinate with the newly designed chiral ligand, it could reinforce the stereoselectivity to generate highly isotactic polymers.

Scheme 2.1 shows the hypothesized stereocontrolled ATRP mechanism. The bimetallic catalyst **2.1** has two coordination sites, one site could coordinate with the

copper(I) salt and the other coordinate with metal triflate (for example, $Yb(OTf)_3$) to form two adjacent metal centers, a chiral bimetallic complex. When this kind of bimetallic complexes is used as catalyst for the ATRP of vinyl carbonyl monomer, the carbonyl group of monomer is able to coordinate with Yb(III), and the Br atom in the propagating chain end could interact with Cu(I) to generate **2.2**. Both the polymer chain end and the coordinated monomer are in the chiral environment. Therefore, it is possible for the chain end radical to attack one face of the carbon-carbon double bond more favorably than the other face. In addition, the proximity of the monomer to the Br-coordinated chain end should facilitate the addition of the transient radical, which is generated by the Cu-abstraction of the chain end Br, to the Yb(III) coordinated monomer. The newly generated chain end radical could rapidly associate with Br on the Cu(I) center. In this step, the radical carbon center in **2.3** should have two rapidly interconverting chiral configurations. Because the chiral environment around the copper center is designed to favor the interaction with only one of the two configurations, the stereochemistry of the α-carbon in the resulting **2.4** should be similar to that in **2.2** as depicted. By repeating this cycle, monomers are added to the polymer chain end one by one and the configuration of each stereocenter keeps the same, leading to the formation of isotactic polymers.

Scheme 2.1. A Proposed Mechanism for Stereoselective ATRP by Bimetallic Catalysis

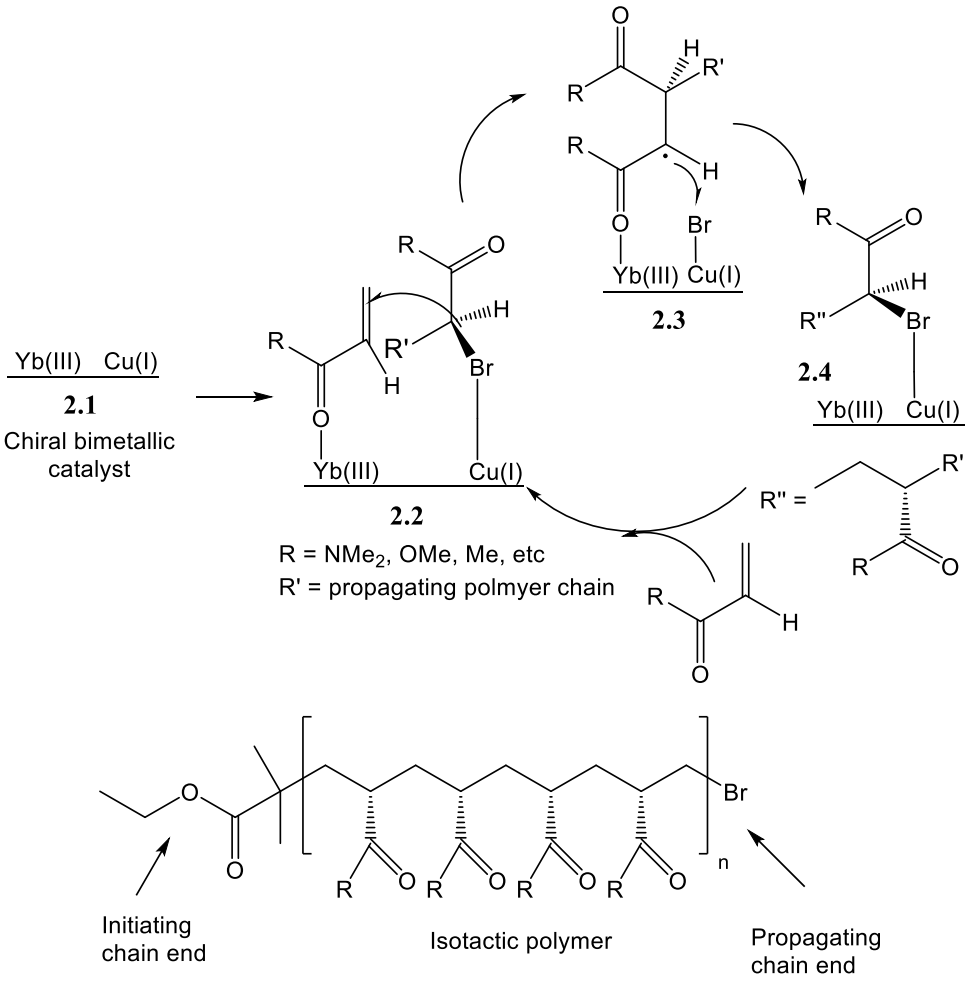

2. Synthesis of Achiral and Chiral Macrocyclic Ligands

The Schiff base-based macrocyclic compounds were synthesized by 1:1 equivalent of dialdehyde and diamine in ethanol[1]. The dialdehyde used was 2-hydroxy-5-methylisophthalaldehyde, which was oxidized from 2,6-bis(hydroxymethyl)-*p*-cresol by using manganese(IV) oxide (MnO_2) as the oxidant. The diamines were purchased or synthesized according to literature[2] (**Scheme 2.2**). Three Schiff base macrocycles **2.6**, **2.7** and **2.8** are derived from three commercially available diamines (ethylene diamine, (1S,2S)-1,2-diaminocyclohexane and (1S,2S)-1,2-diphenylethylenediamine), which were

synthesized first according to the literature[1,3] to compare the effectiveness among each other. Then, several substituted chiral diphenylethylenediamines were synthesized (**Scheme 2.3**). First, chiral *tert*-butanesulfinamide was reacted with various substituted benzaldehyde to generate chiral sulfinyl imines. Then, the imines underwent a coupling reaction by using SmI_2/HMPA in THF at -78 ^oC to generate the homocoupling products. After treating with HCl solution and then with sodium hydroxide, these chiral diamines were synthesized and used to produce new Schiff base macrocycles **2.18**, **2.19** and **2.20**, which are new compounds and have not been reported by previous literatures. Their catalytic effectiveness were also examined. **Figure 2.1** shows a ^1H NMR spectra of ligand **2.8**, which represents a typical structural feature of these Schiff base macrocyclic compounds. The intramolecular hydrogen bonding leads to the different chemical shifts of the two symmetric parts of the molecule, and all the peaks have been assigned on the spectrum.

Figure 2.1. ^1H NMR spectra of ligand **2.8** (DMSO – d_6, 25℃)

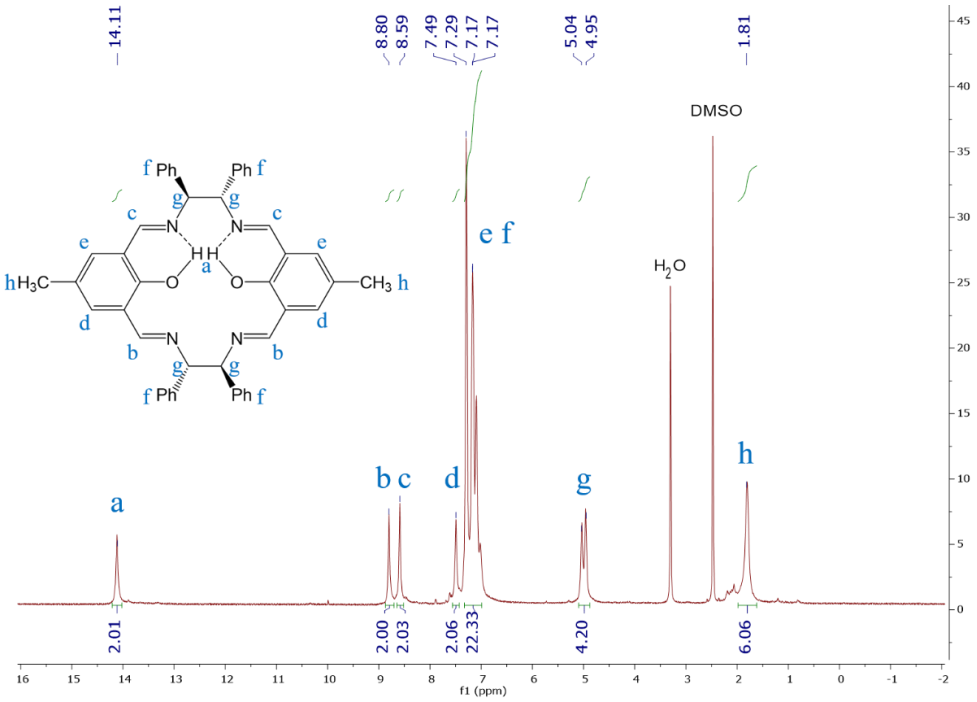

Scheme 2.2. Synthesis of Schiff base macrocycles from commercially available diamines

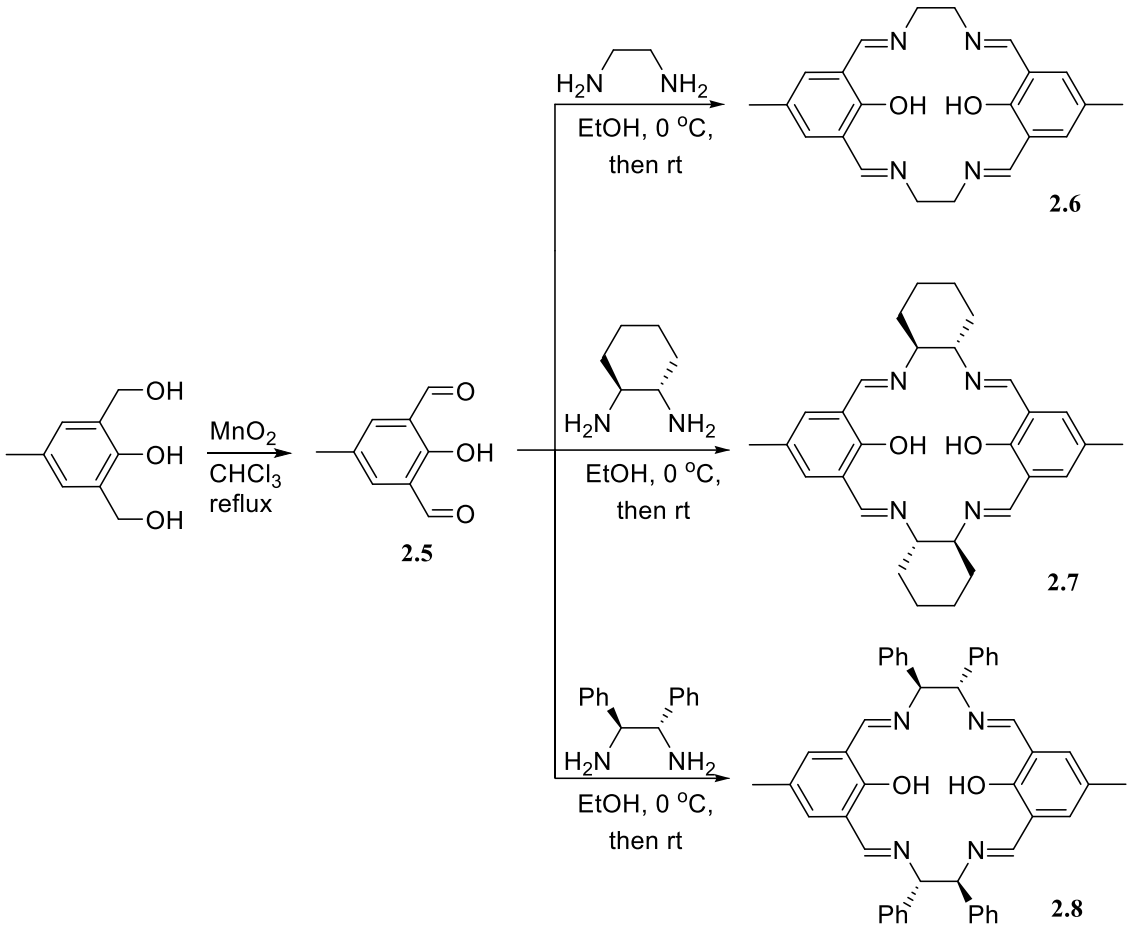

Scheme 2.3. Synthesis of phenyl-substituted Schiff base macrocycles

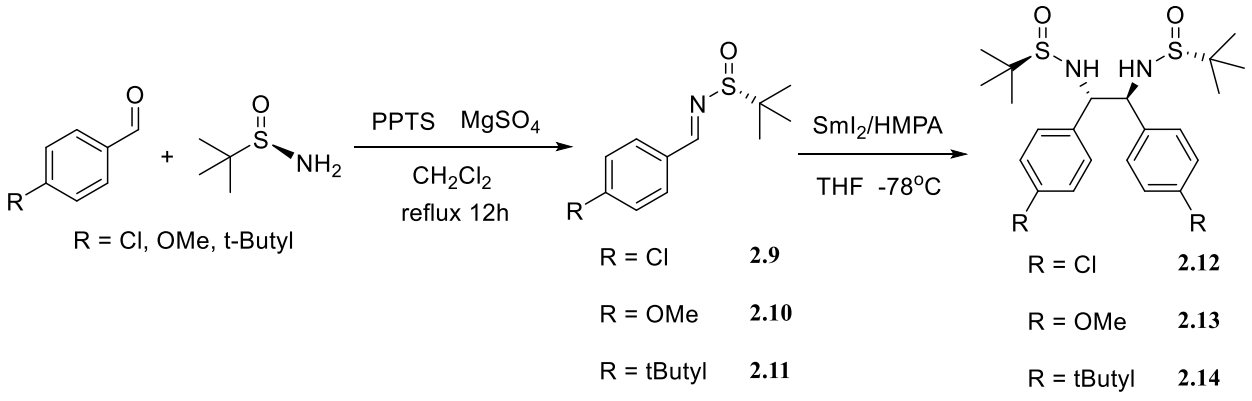

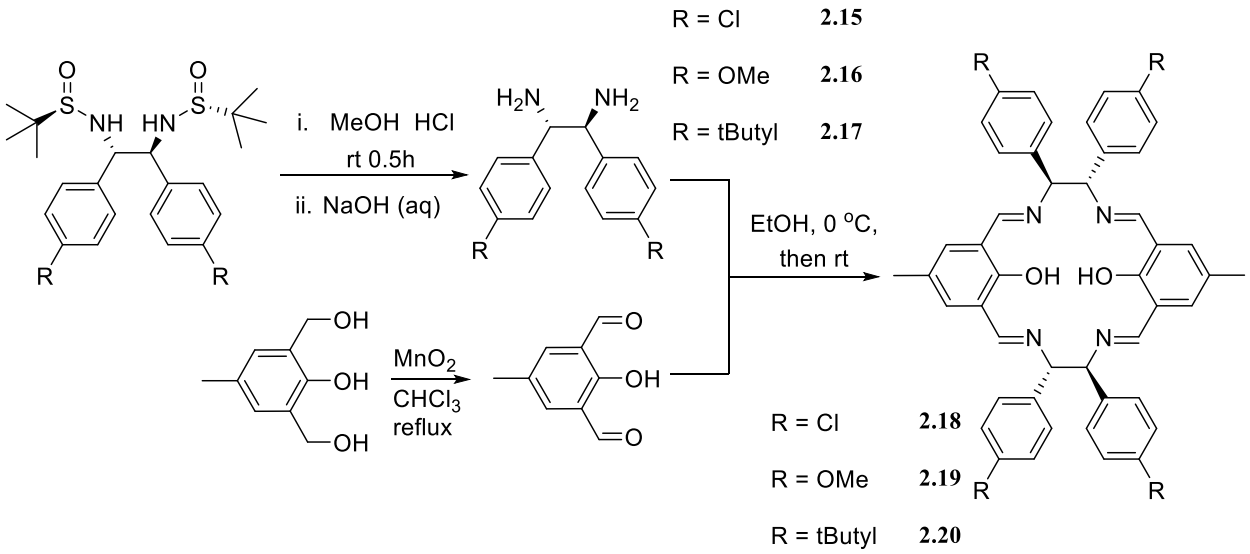

3. Investigation of Stereocontrolled ATRP Conditions

There are various parameters that can influence the conversion and tacticity of the polymerization results. The concentration of monomer could affect the polymerization rate, the conversion and the tacticity of polymer. The ligand structure could influence the total reactivity of the metal complex and further change the equilibrium constant of ATRP. The temperature and solvent also play important roles. As mentioned in the previous chapter, the temperature can significantly influence the tacticity of polymer and reaction rate. In addition, the polarity of solvent could change the effectiveness of coordination between monomer and metal triflate and further affect the tacticity of polymers. Different type and concentration of metal triflates might have different coordination effects with monomers, which will have an impact on the tacticity.

First, the three commercially available diamine derived Schiff base ligands were used to polymerize DMAA following the procedure in the literature[4] to compare their effectiveness on the stereocontrolled ATRP. Methanol was used as solvent to form a 1:1 volume ratio solution with DMAA. Ethyl 2-bromoisobutyrate was used as initiator and

CuBr as copper salt. $Yb(OTf)_3$ was added as Lewis acid to control the stereochemistry of polymer. The concentration of each reactant was [DMAA]: [Yb(III)]: [CuBr]: [Initiator] :[Ligand] = 100: 5: 2: 2: 1. The polymerization underwent at room temperature (20℃). After 24 hours, polymerization was quenched by exposing to air and the conversion and tacticity were determined by proton NMR. **Table 2.1** shows the results of the polymerization using three different ligands. The tacticity and conversion are comparable for each ligand, and 1,2-diphenylethylenediamine derived Schiff base macrocycle **2.8** shows slightly better isotacticity and higher conversion. Therefore, it is chosen as the ligand for the optimization of polymerization conditions.

Table 2.1. Polymerization of DMAA by using ligand **2.6**, **2.7**, and **2.8**

Ligand	**2.6**	**2.7**	**2.8**
Isotacticity %	85	85	89
Conversion %	60	80	87

Solvent: MeOH, 103μL. DMAA: 1 mmol, 103μL. [DMAA] = 4.85M. [DMAA]: [$Yb(OTf)_3$]: [CuBr]: [Initiator]: [Ligand] = 100: 5: 2: 2: 1. ATRP at 20℃, 24h. Conversion and isotacticity were measured by 600MHz ^{1}H NMR.

Tacticity of PDMAA was determined by ^{1}H NMR**. Figure 2.2** shows an example proton NMR spectrum of isotactic PDMAA. If the methylene group is in an *m* dyad, the two methylene protons are in different chemical environment and lead to two broad peaks with same area at 1.61 and 1.06 ppm. If the methylene group is in an *r* dyad, the two protons are equivalent and only shows a single broad peak at 1.41 ppm. This *r* peak overlaps with the *m* peak at 1.61 ppm. But the *m* peak at 1.06 ppm is separated from other peaks. Therefore, the isotacticity is equal to twice the integral of *m* peak at 1.06 divided by the integration of both *m* and *r* peaks.

Figure 2.2. ^{1}H NMR spectrum of isotactic PDMAA (DMSO – d_6, 25℃)

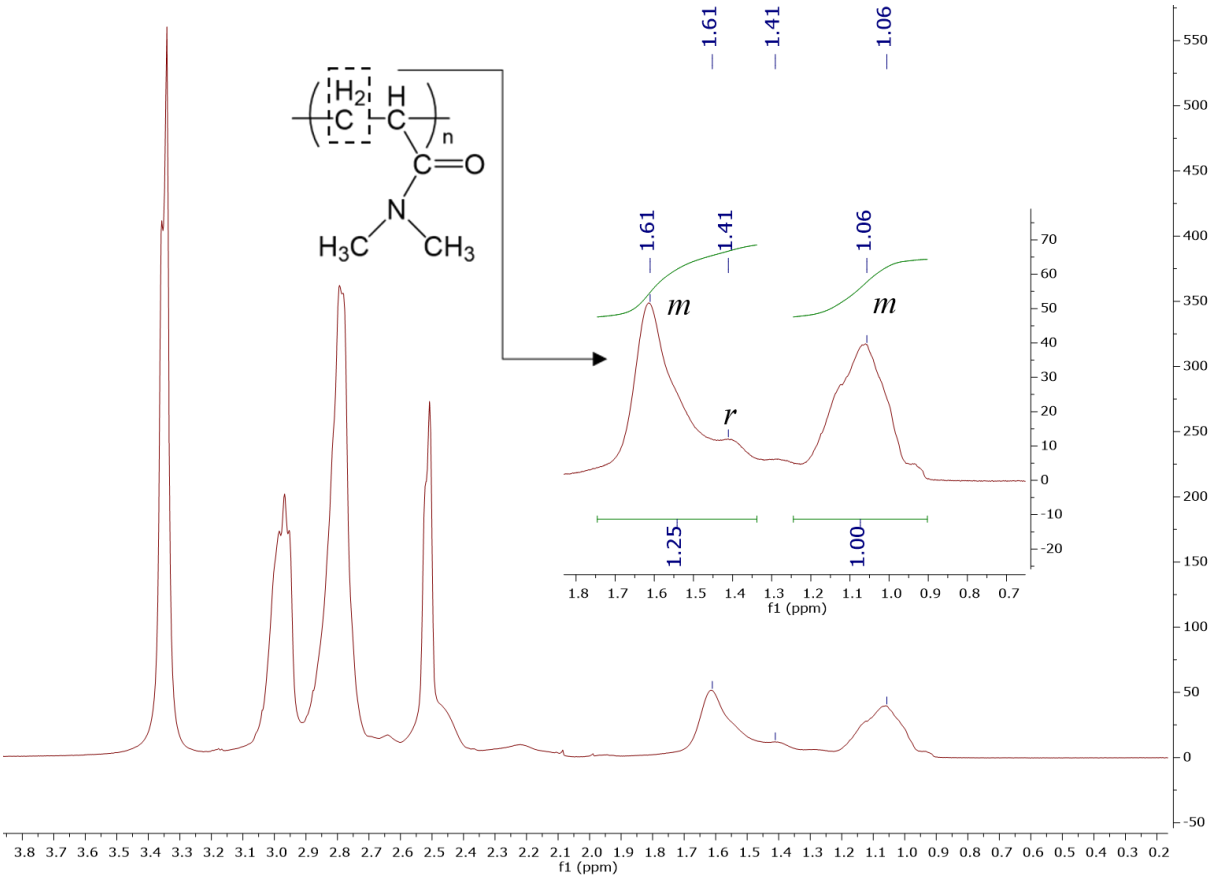

Table 2.2 shows the results of the influence of the Lewis acids on polymerization. It is concluded that 5 mol % of $Yb(OTf)_3$ has the best ability to increase the isotacticity of the polymer. This can be explained that when the concentration of the metal triflates is high in the solution, the carbonyl groups on the propagating chain ends and incoming monomers have a high probability to coordinate with the Lewis acids and control the stereochemistry of the polymer chain. When the concentration of the metal triflates is lower, less Lewis acids are involved in the propagating process, leading to less isotacticity for the polymers.

Table 2.2. Influence of the amount and type of Lewis acid on the polymerization

Amount (equiv)	Isotacticity (%)/Conversion (%) obtained with various Lewis acids				
	$Yb(OTf)_3$	$Y(OTf)_3$	$La(OTf)_3$	$Eu(OTf)_3$	$Zn(OTf)_2$
5	89/87	82/80	88/98	85/80	57/53
3	81/10	78/66	82/50	84/66	54/33
1	N/A	72/35	N/A	79/32	51/24

Solvent: MeOH, 103μL. DMAA: 1 mmol, 103μL. [DMAA] = 4.85M. [DMAA]: [Lewis acid]: [CuBr]: [Initiator]: [Ligand] = 100: 5: 2: 2: 1. ATRP at 20℃, 24h. Conversion and isotacticity were measured by 600MHz ^{1}H NMR.

Table 2.3 shows the influence of common solvents on the tacticity of the polymer. As the polarity of solvents increases (toluene to methanol), the isotacticity of the polymer increases significantly. However, if the polarity of the solvent is too high, such as DMF, the isotacticity decreases. The possible reason is that as the polarity of the solvent increases, the solubility of the metal triflate becomes better, which can facilitate the coordination between the monomers and the Lewis acid, resulting in the increase in isotacticity. However, the Lewis acid could coordinate with the high polarity solvent such as DMF more tightly than with the monomer, which in turn should impede the coordination between the Lewis acid and the monomer, leading to the decrease of the isotacticity. Therefore, methanol was chosen as the optimized solvent, which is consistent with the previous work[4,5].

Table 2.3. Influence of solvent on the tacticity of polymer

Solvent	Toluene	THF	Methanol	DMF
Isotacticity %	70	82	89	74

Solvent: 103μL. DMAA: 1 mmol, 103μL. [DMAA] = 4.85M. [DMAA]: [$Yb(OTf)_3$]: [CuBr]: [Initiator]: [Ligand] = 100: 5: 2: 2: 1. ATRP at 20℃, 24h. Isotacticity was measured by 600MHz ^{1}H NMR.

Table 2.4 shows the influence of the reaction temperature on the polymerization. At room temperature (20℃), a polymer with the highest isotacticity was obtained. When the temperature is lower, the isotacticity gradually decreases. This might be due to the kinetic control of the propagation at lower temperature. At lower temperature, the polymerization rate decreases, and the addition of the monomer will choose the kinetically more favorable pathway. The side groups of the polymer chain end and incoming monomer tend to repulse each other and align on the opposite side of the polymer chain plane, which is kinetically favorable. Therefore, at lower temperature, more syndiotactic dyads exist in the polymer chain, causing the decrease in isotacticity. Further increasing the temperature did not really increase the isotacticity. It demonstrates that the polymerization at room temperature can generate highly isotactic polymers. The advantage of the polymerization at room temperature is that no heating or cooling devices are needed, which simplifies the procedure.

Table 2.4. Influence of temperature on polymerization

Temperature (℃)	0	10	20	30
Isotacticity %	83	86	89	88
Conversion %	31	70	87	85

Solvent: MeOH, 103μL. DMAA: 1 mmol, 103μL. [DMAA] = 4.85M. [DMAA]: [$Yb(OTf)_3$]: [CuBr]: [Initiator]: [Ligand] = 100: 5: 2: 2: 1. ATRP for 24h. Conversion and isotacticity were measured by 600MHz ^{1}H NMR.

Table 2.5 shows the influence of the monomer concentration on polymerization. By changing the volume ratio of methanol and monomer, the concentration of monomer was also changed. When the volume ratio of methanol: monomer is larger than 1, the isotaciticity is always higher than 88%. Higher monomer concentration leads to polymer with lower isotacticity. This can be explained that the rate of polymerization increases

when the monomer concentration is higher. In this case, the Lewis acid may not fully coordinate with monomers before their addition to polymer chain radical. As a result, the stereocontrolled effect of Lewis acid is weaken, leading to less isotactic polymers.

Table 2.5. Influence of monomer concentration on polymerization

Methanol: monomer (volume ratio)	0.25	0.5	1	1.25	1.5	2
Isotacticity %	67	84	89	90	90	89
Conversion %	90	70	87	50	70	59

Solvent: MeOH. DMAA: 1 mmol, 103μL. [DMAA]: [$Yb(OTf)_3$]: [CuBr]: [Initiator]: [Ligand] = 100: 5: 2: 2: 1. ATRP at 20℃, 24h. Conversion and isotacticity were measured by 600MHz ^{1}H NMR.

In addition, changing the ratio of CuBr: ligand did not have a big influence on the isotacticity of polymer. The isotacticity keeps similar when the ratio changed from 1:1 (*m* = 86%) to 2:1 (*m* = 89%) to 3:1 (*m* = 87%). And the ratio of CuBr: ligand = 2:1 was chosen. A controlled experiment, which means no ligand was present in the reaction system, was also conducted. As expected, no polymerization occurred, proving the necessity of ligand in ATRP system.

In conclusion, the optimized reaction condition is: [Monomer]: [Lewis acid]: [CuBr]: [Initiator]: [Ligand] = 100: 5: 2: 2: 1, the solvent is methanol and volume ratio of methanol: monomer is 1.5 (concentration of monomer: 3.9mol/L). In addition, the polymerization takes place room temperature (20℃), which simplifies the operation process as no heating or cooling apparatus are needed.

Other Schiff base ligands were also tested under optimized reaction condition to evaluate their effectiveness on the polymerization of DMAA. As shown in **Table 2.6**,

polymerization using other imine ligands gave both good tacticity control and high conversion.

Table 2.6. Schiff base ligands on polymerization of DMAA

Ligand	**2.6**	**2.7**	**2.18**	**2.19**	**2.20**
Isotacticity %	86	86	88	89	88
Conversion %	54	80	51	90	90

Solvent: MeOH, 154μL. DMAA: 1 mmol, 103μL. [DMAA] = 3.9M. [DMAA]: [$Yb(OTf)_3$]: [CuBr]: [Initiator]: [Ligand] = 100: 5: 2: 2: 1. ATRP at 20℃, 24h. Conversion and isotacticity were measured by 600MHz ^{1}H NMR.

4. Stereocontrolled ATRP of NIPAM and Other Acrylamide Monomers

4.1. Introduction of PNIPAM

Inspired by the results of the DMAA polymerization, we intended to apply these ligands to the stereocontrolled ATRP of NIPAM. This is not only because highly isotactic PNIPAM (*m* > 85%) has not been synthesized by the ATRP method, but also because of its unique thermal properties in aqueous solutions[6]. PNIPAM is soluble in water at low temperature, when the temperature rises to a certain degree, PNIPAM will precipitate out of the solution abruptly. This temperature is called lower critical solution temperature (LCST). At LCST, there is a transition of PNIPAM structure from hydrophilic to hydrophobic, which is driven by hydrophobic effect. The LCST of NIPAM is between about 30 and 35℃, depending on the microstructure of PNIPAM. This temperature is very close to the temperature of human body, which is usually around 37℃. Therefore, it has a promising potential in drug delivery applications[7,8].

The general idea of the PNIPAM drug delivery system is that drugs are delivered by PNIPAM micelles, which requires the copolymerization of hydrophilic NIPAM with

other hydrophobic monomers to form a core-shell structure in aqueous solution[9]. The hydrophobic drugs are carried in the hydrophobic core, surrounded by the hydrophilic PNIAPM shell. Below LCST, the micelles are stable in aqueous environment and the inner drug can be delivered to the desired location of the body. By local heating, the temperature will be above LCST and PNIPAM becomes hydrophobic, leading to the dissociation of the micelles. The drugs can be released consequently.

There have been several studies on the influence of tacticity and MW on the LCST of NIPAM. Stover et al. reported the influence of MW on LCST[10]. The PNIPAM was synthesized by using the ATRP method, with Me_6TREN/CuCl as the catalyst and various initiators. The polymers showed an inverted relationship between MW and LCST. For example, the LCST of the PNIPAM initiated by ethyl 2-chloropropionate decreased from 40.6 to 33.3℃ when the MW increased from 3000 to 15200. Kubosaki et al. reported the influence of tacticity on LCST[11]. PNIPAMs with various isotacticity were synthesized by using RAFT polymerization. The study revealed that increase in tacticity will decrease the LCST. For example, the atactic PNIPAM with an isotacticity of 46% had LCST at 33℃. However, when the isotacticity increased to 64%, the LCST decreased to 25℃. This discovery demonstrated that higher isotactic PNIPAM are more hydrophobic, leading to the decrease in LCST.

As the stereocontrolled ATRP is able to control the MW and tacticity at the same time, it is possible to fine tune the LCST of PNIPAM and apply it in multiple drug delivery. Therefore, stereocontrolled ATRP of NIPAM is mecessary.

4.2. Stereocontrolled ATRP of NIPAM and Other Acrylamide Derived Monomers

We are delighted to find that these copper-ligands complexes showed excellent catalytic activity towards the ATRP of NIPAM under the optimized conditions ([NIPAM]: [$Yb(OTf)_3$]: [CuBr]: [Initiator]: [Ligand] = 100: 5: 2: 2: 1, [NIPAM] = 3.9 mol/L). PNIPAM with high conversion and high isotacticity were produced, as shown in **Table 2.7**. This is the first time that a highly isotactic PNIPAM is synthesized by an ATRP method.

Table 2.7. Schiff base ligands on polymerization of NIPAM

Ligand	**2.6**	**2.7**	**2.8**	**2.18**	**2.19**	**2.20**
Isotacticity %	85	88	89	89	89	89
Conversion %	44	83	89	63	85	97

Solvent: MeOH, 257μL. NIPAM: 1 mmol. [NIPAM] = 3.9M. [NIPAM]: [$Yb(OTf)_3$]: [CuBr]: [Initiator]: [Ligand] = 100: 5: 2: 2: 1. ATRP at 20℃, 24h. Conversion and isotacticity were measured by 600MHz ^{1}H NMR.

Figure 2.3 shows how the isotacticity of PNIPAM is determined. The method is the same as what is used to determine the isotacticity of PDMAA. The isotacticity is equal to twice the integral of *m* peak at 1.62 divided by the integration of both *m* and *r* peaks.

Figure 2.3. ^{1}H NMR spectrum of isotactic PNIPAM (DMSO – d_6, 100℃)

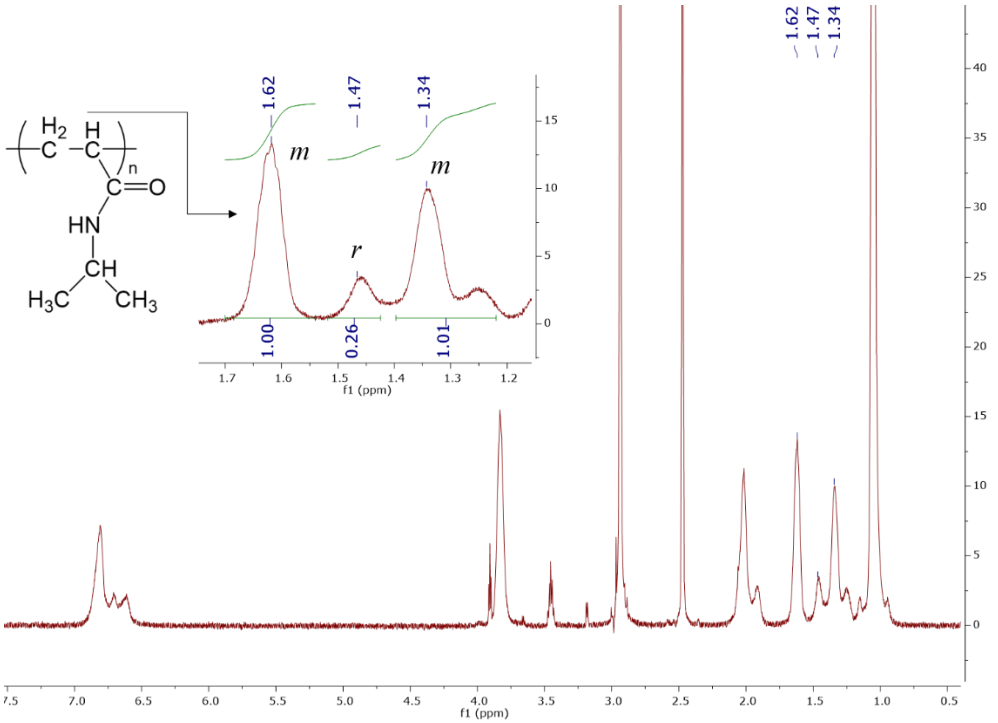

Then we tried to further expand the substrates to other acrylamides. **Figure 2.4** shows the structure of all the monomers tested. We found that the stereocontrolled ATRP of the other acrylamides using ligand **2.8** was not as good as that observed for DMAA and NIPAM. The polymerization of *N*,*N*-diethylacrylamide (DEAA) gave low conversion (35%), although the tacticity is relatively high (*m* = 80%). The ATRP of other acrylamides did not yield any or gave only trace amount of polymers. Therefore, new ligands able to catalyze these polymerizations needs to be developed.

Figure 2.4. Structure of acrylamide monomers

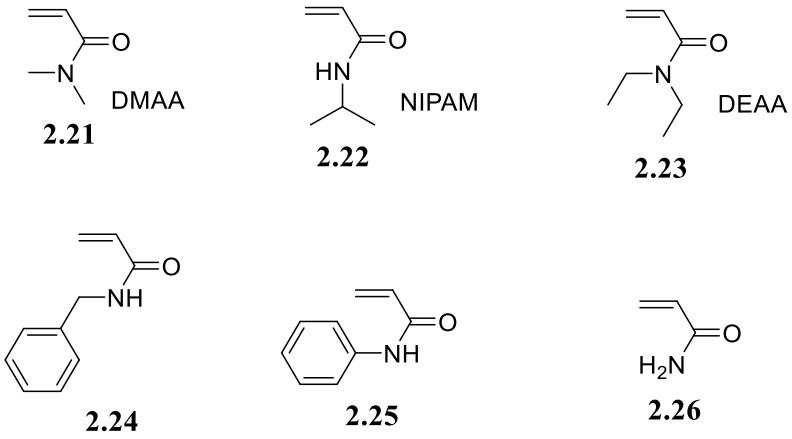

Changing ligand structure can change the redox potential of the metal complex, and can thus greatly influence the reactivity of the catalysts[12]. The Schiff base macrocycles have four carbon-nitrogen double bonds, which makes the nitrogen atom relatively electron deficient. If these double bonds can be reduced, the resulting nitrogen atoms could be more electron rich, which might lead to more electron-rich copper atom for the corresponding Cu(I) complexes. It would be easier to oxidize these more electron rich Cu(I) complexes to the corresponding Cu(II) complexes by abstracting the halogen atom from R-X. That is, such Cu(I) complexes could be more active in generating radicals for polymerization. Therefore, the carbon-nitrogen double bonds of these Schiff base macrocycles were reduced by sodium borohydride ($NaBH_4$) (**Scheme 2.4**) to generate the corresponding macrocyclic amine compounds (**Figure 2.5**). Whether these reduced Schiff base macrocycles could work better for various substrates was then examined.

Scheme 2.4. Reduction of Schiff base macrocycles

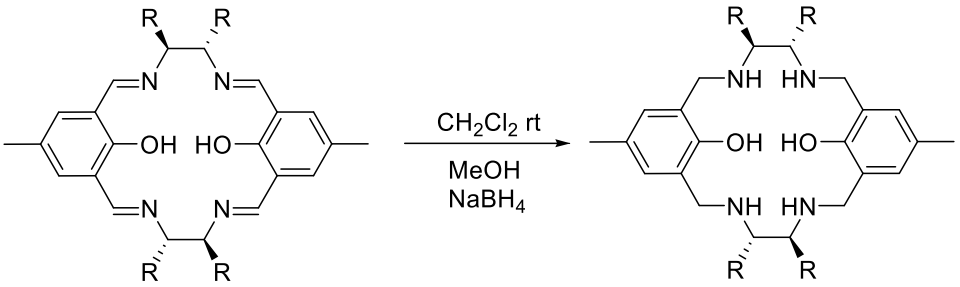

Figure 2.5. Structures of macrocyclic amine compounds

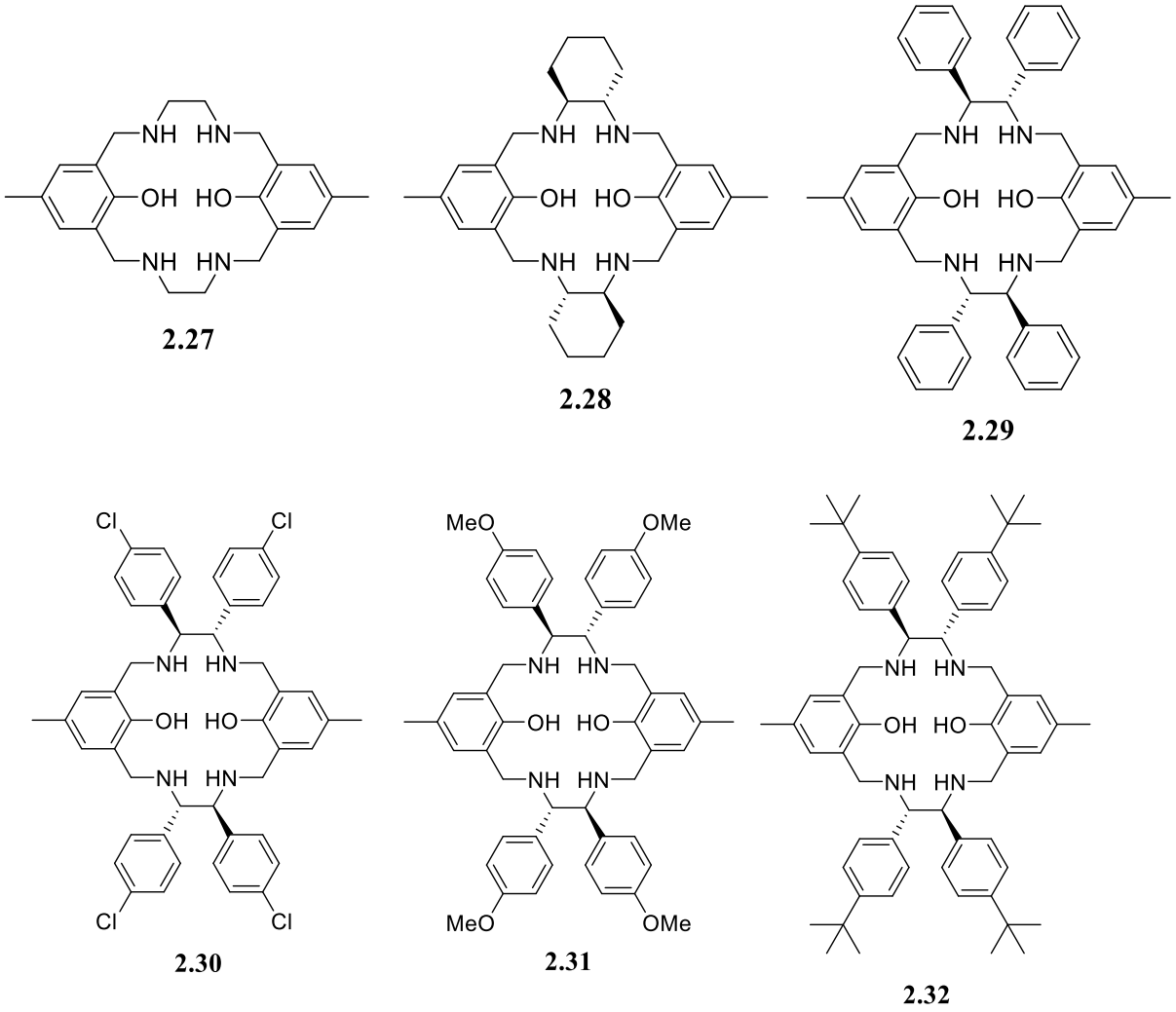

Table 2.8. Polymerization of various monomers using ligand **2.29**

Monomer	**2.21**	**2.22**	**2.23**	**2.24**	**2.25**	**2.26**
Isotacticity %	90	90	80	85	67	66
Conversion %	97	99	89	42	55	40

Solvent: MeOH, 257μL. Monomer: 1 mmol. [Monomer] = 3.9M. [Monomer]: [$Yb(OTf)_3$]: [CuBr]: [Initiator]: [Ligand] = 100: 5: 2: 2: 1. ATRP at 20℃, 24h. Conversion and isotacticity were measured by 600MHz ^{1}H NMR.

The polymerization results were quite promising. The ligand **2.29**, which was reduced from ligand **2.8**, showed good reactivity to all six substrates under the optimized polymerization conditions (**Table 2.8**). The conversions of DMAA, DEAA and NIPAM are all higher than polymerizations induced by ligand **2.8**, while the tacticity of the resulting polymers is maintained. Then, the other macrocyclic amine ligands were used for ATRP under the optimized conditions and good conversions were observed for various monomers (**Table 2.9**). These results demonstrate that this type of copper-amine complexes have very high reactivity and can be applied to multiple acrylamide derivatives. The ATRP of N-benzylacrylamide also gave highly isotactic polymer (*m* = 87%). For acrylamide and N-phenylacrylamide, the ATRP of these two monomer did not produce polymer with high isotacticity. This might be because that the coordination between $Yb(OTf)_3$ and the carbonyl group of the monomers is weaker than other monomers, leading to the decrease in polymer tacticity. Overall, this type of new cyclic amine ligand proved to be very effective for copper-mediated stereocontrolled ATRP.

Table 2.9. ATRP of various monomers using other cyclic amine ligands

	2.21	**2.22**	**2.23**	**2.24**	**2.25**	**2.26**
2.27 (m% / c%)	86 / 98	88 / 92	80 / 66	87 / 30		67 / 51
2.28 (m% / c%)	86 / 99	88 / 83	78 / 36			
2.30 (m% / c%)	86 / 73	86 / 99	80 / 60			
2.31 (m% / c%)	89 / 97	88 / 99	80 / 26	85 / 50	64 / 99	65 / 86
2.32 (m% / c%)	90 / 76	89 / 80	80 / 68			

Solvent: MeOH, 257μL. Monomer: 1 mmol. [Monomer] = 3.9M. [Monomer]: [$Yb(OTf)_3$]: [CuBr]: [Initiator]: [Ligand] = 100: 5: 2: 2: 1. ATRP at 20℃, 24h. Conversion and isotacticity were measured by 600MHz ^{1}H NMR.

We then compared the effectiveness of our reaction system with the one reported by Matyjaszewski et al. Their ATRP system used Me_6TREN/CuCl as the metal catalyst and methyl 2-chloropropionate as the initiator, and the polymerization took place at 30℃. Four monomers, DMAA, DEAA, NIPAM and *N*-benzylacrylamide were applied in their reaction system because their polymers showed high isotacticity under our ATRP system. The reaction temperature was set to room temperature (20℃) and follow the procedure described in the literature[4]. After 24 hours, the conversion and tacticity were determined by proton NMR. **Table 2.10** gives the results of polymerization. It shows that the polymerization of DMAA gave high isotacticity and moderate conversion, and those of NIPAM and *N*-benzylacrylamide also yielded high tacticity but with very low conversions. For DEAA, no polymerization was observed. These results demonstrate that our new catalysts are much more efficient than the previous one in the ATRP of acrylamides

Table 2.10. ATRP of various monomers using Me_6TREN/CuCl as the catalyst

Monomer	**2.21**	**2.22**	**2.23**	**2.24**
Isotacticity %	86	87	No polymerization	85
Conversion %	50	18		22

Solvent: MeOH, 103μL. Monomer: 1 mmol. [Monomer] = 4.85M. [Monomer]: [$Yb(OTf)_3$]: [CuCl]: [Initiator]: [Me_6TREN] = 100: 5: 1: 1: 1. ATRP at 20℃, 24h. Conversion and isotacticity were measured by 600MHz ^{1}H NMR.

The results from **Table 2.7** and **Table 2.9** also show that the tacticity of the polymers was hardly influenced by the chirality of the ligand. That is, the PDMAA and PNIPAM obtained by using the achiral ligands **2.6** and **2.27** have isotacticity similar to that of the polymers by using the chiral metal complexes. Polymerization of NIPAM using ligand **2.8** and **2.29** in the absence of a Lewis acid was also studied. The reaction was conducted under the optimized conditions but without the addition of $Yb(OTf)_3$. **Table 2.11** shows the polymerization result. The PNIPAMs have an isotacticity of 46% for both polymerizations, which is the same as the tacticity of PNIPAM synthesized by free radical polymerization[13]. This result demonstrates that the chirality of the ligand has little influence on the tacticity of the polymer. This indicates that the chiral centers of the metal complex might also be far from the propagating chain radical as previously observed[14].

Table 2.11. ATRP of NIPAM in the absence of Lewis acid

Ligand	**2.8**	**2.29**
Isotacticity %	46	46
Conversion %	95	75

Solvent: MeOH, 257μL. NIPAM: 1 mmol. [NIPAM] = 3.9M. [NIPAM]: [CuBr]: [Initiator]: [Ligand] = 100: 5: 2: 2: 1. ATRP at 20℃, 24h. Conversion and isotacticity were measured by 600MHz ^{1}H NMR.

The MALDI-TOF mass spectroscopic method was applied to analyze the MW and MW distribution of PNIPAM and other polymers. **Table 2.12** shows the MW and PDI of some polymers obtained by using the ligand **2.29**-copper complex under the optimized conditions. In general, the PDI is narrow for all polymers, which shows a controlled manner for the polymerization. However, the MW of PNIPAM from the mass spectrum is much lower than the value by theoretical calculation. This might be due to the very high viscosity of the reaction system when the conversion is high, which will impede the addition of monomer to the polymer chain end and results in low MW polymers.

Table 2.12. Molecular weight and distribution of polymers catalyzed by ligand **2.29**

Monomer	**2.21**	**2.22**	**2.23**	**2.24**	**2.25**
$M_{n,\ theoretical}$	5152	5796	5283	3601	4242
$M_{n,\ MALDI\text{-}TOF}$	6877	1606	3882	4414	4381
PDI	1.05	1.05	1.08	1.06	1.08

Polymerization conditions. Solvent: MeOH, 257μL. Monomer: 1 mmol. [Monomer] = 3.9M. [Monomer]: [$Yb(OTf)_3$]: [CuBr]: [Initiator]: [Ligand] = 100: 5: 2: 2: 1. ATRP at 20℃, 24h. Conversion and isotacticity were measured by 600MHz ^{1}H NMR.

To further investigate the controlled/living property for the polymerization of NIPAM, several experiments were performed. Kinetic studies can provide the evidence for a living polymerization. The rate of propagation can be expressed by using the following equation:

$$-\frac{d[M]}{dt} = k_p[P\cdot][M]$$

By integration, the equation can be changed to:

$$\ln\frac{[M_0]}{[M]} = k_p[P\cdot]t$$

This equation demonstrates the relationship between conversion and reaction time. In an ATRP system, the concentration of a propagating chain radical is very low and can be regarded as constant once the equilibrium is reached. Therefore, $k_p[P\cdot]$ can be regarded as constant. Consequently, the relationship between $\ln\frac{[M_0]}{[M]}$ and time should be linear for an ATRP system[15].

The kinetic study of the ligand **2.8** catalyzed polymerization was investigated. The study was made under the optimized polymerization conditions ([NIPAM]: [$Yb(OTf)_3$]: [CuBr]: [Initiator]: [Ligand] = 100: 5: 2: 2: 1, [NIPAM] = 3.9M. Solvent: MeOH. 20℃.). Once the polymerization started, after a certain time, a small fraction of the reaction mixture was taken out and exposed to air to quench the reaction, then the conversion of the mixture was determined by ^{1}H NMR. **Figure 2.6** shows good linear relationship between $\ln\frac{[M_0]}{[M]}$ and time when the conversion is lower than 70% as R^2 = 0.9893. When the conversion is higher than 70%, the more viscous system might slow down the reaction and the relationship is deviated from linear. **Figure 2.7** reveals the relationship between conversion and time. 70% conversion was reached within 10 min, indicating a high reactivity of the catalyst for the polymerization of NIPAM.

Figure 2.6. Relationship between $\ln\frac{[M_0]}{[M]}$ and time (**Ligand 2.8**)

Figure A: Total $\ln\frac{[M_0]}{[M]}$ verse time

Figure B: Linear region of Figure A (first 10min, conversion less than 70%, $R^2 = 0.9893$)

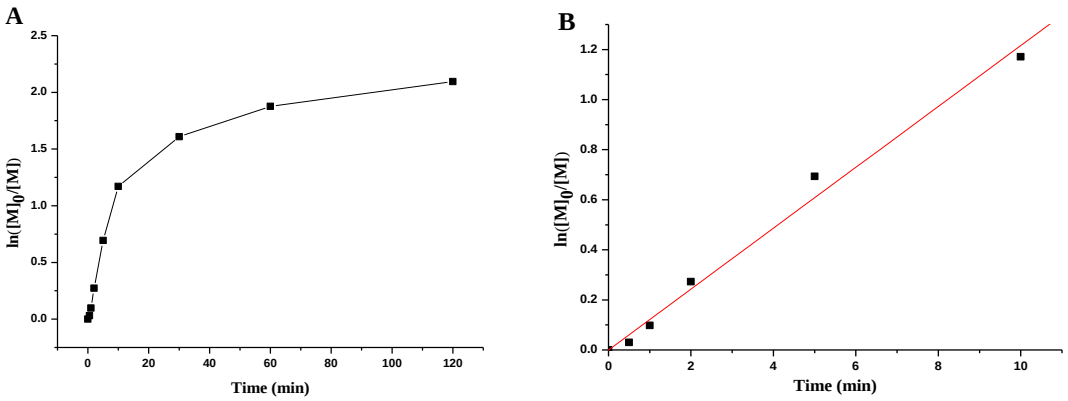

Figure 2.7. Relationship between conversion and time (**Ligand 2.8**)

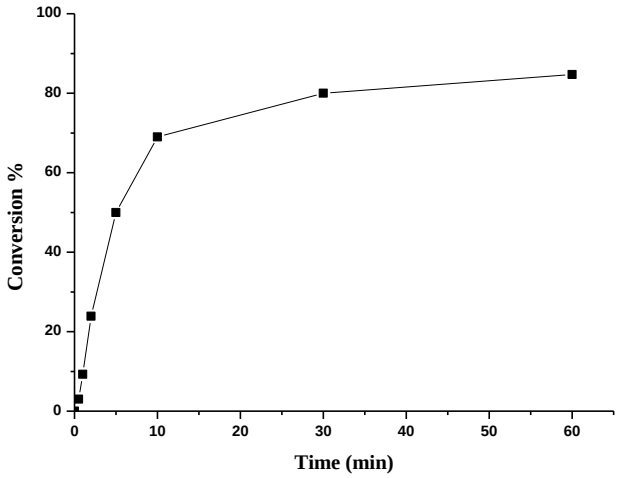

The kinetic study for the use of ligand **2.29** was also carried out under the optimized conditions in order to compare the effectiveness of the two catalytic systems. For ligand **2.29**, the relationship between $\ln\frac{[M_0]}{[M]}$ and time keeps linear even when the conversion is

large than 95% (**Figure 2.8**). In addition, the conversion of the monomer reached 80% within 7 minutes (**Figure 2.9**), which means the polymerization rate is much faster using the macrocyclic amine ligand based catalyst. Overall, this macrocyclic amine catalytic system is more effective than the corresponding Schiff base-based one.

Figure 2.8. Relationship between $\ln \frac{[M_0]}{[M]}$ and time (R^2 = 0.9211, **Ligand 2.29**)

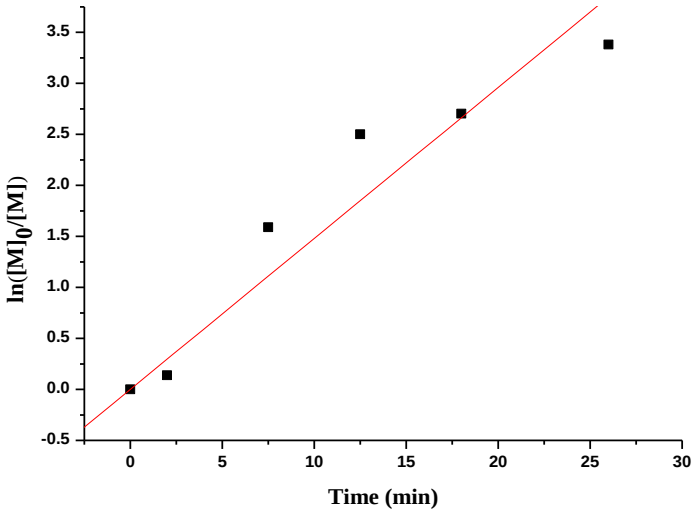

Figure 2.9. Relationship between conversion and time (**Ligand 2.29**)

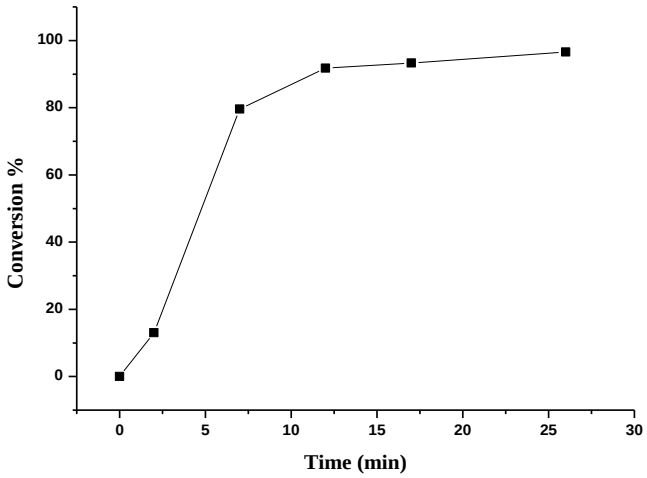

If the polymerization is a living system, when all the remaining monomers are consumed, the addition of new monomers will be polymerized in a controlled manner as well. Therefore, the relationship between MW and conversion should keep linear all the time. To examine this, an experiment was carried out. First, ATRP of 1 mmol NIPAM in 250μL methanol was initiated in the presence of 0.01 mmol Ligand **2.29** and 0.05 mmol $Yb(OTf)_3$. After 1 hour, a small amount of sample was analyzed by proton NMR. The NMR spectra showed that the conversion is higher than 99%, and the tacticity was about 89%. Then, another solution with 1 mmol NIPAM and 0.05 mmol $Yb(OTf)_3$ in 250μL methanol was added to the ATRP system. After 20 hours, the polymerization was quenched in air. By proton NMR analysis, the total conversion is 97% and the final tacticity of polymer is 88%. The MALTI-TOF analysis was applied to measure the MW and PDI of two samples. **Figure 2.10** and **2.11** are the raw data of MALDI-TOF analysis and **Table 2.13** shows the analysis results of the polymers. The MW of second PNIPAM sample is almost doubled compared to the first PNIPAM sample. However, the mass spectrum of the second sample contains another MW distribution with lower MW, which means some polymer chains terminated earlier than others. This observation reveals that this copper complex catalyzed polymerization exhibits a partially living character, and the system needs to be refined to perform a better controlled property.

Figure 2.10. MALDI-TOF analysis data, first sample

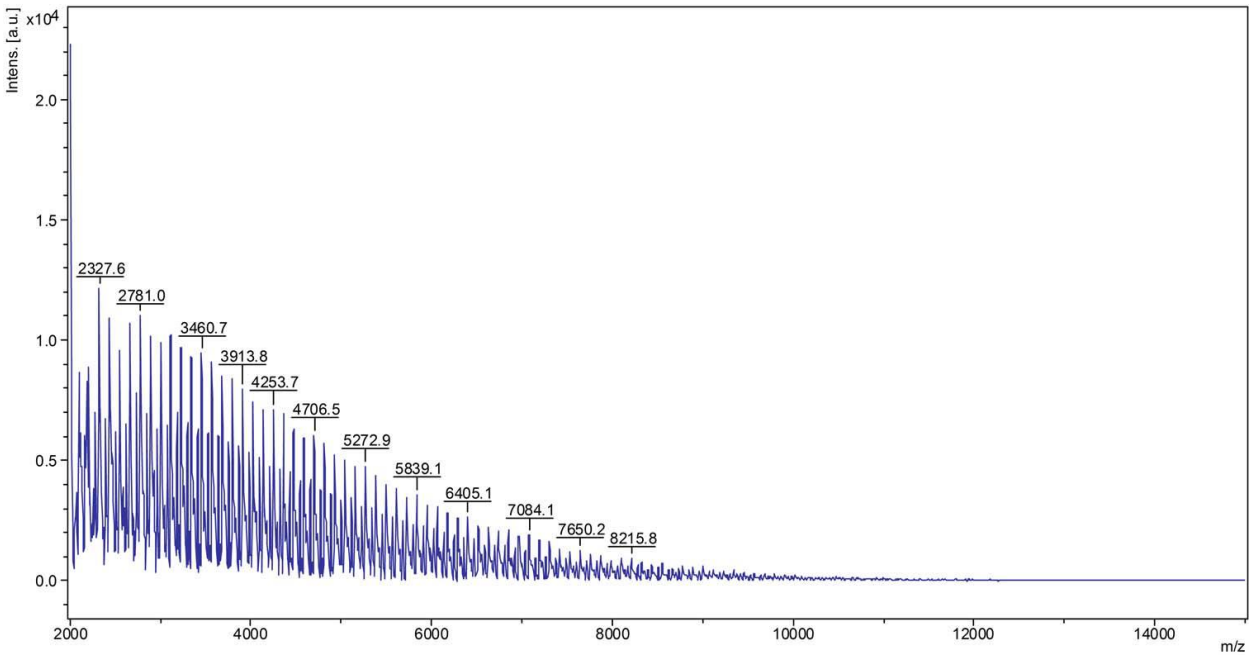

Figure 2.11. MALDI-TOF analysis data, second sample

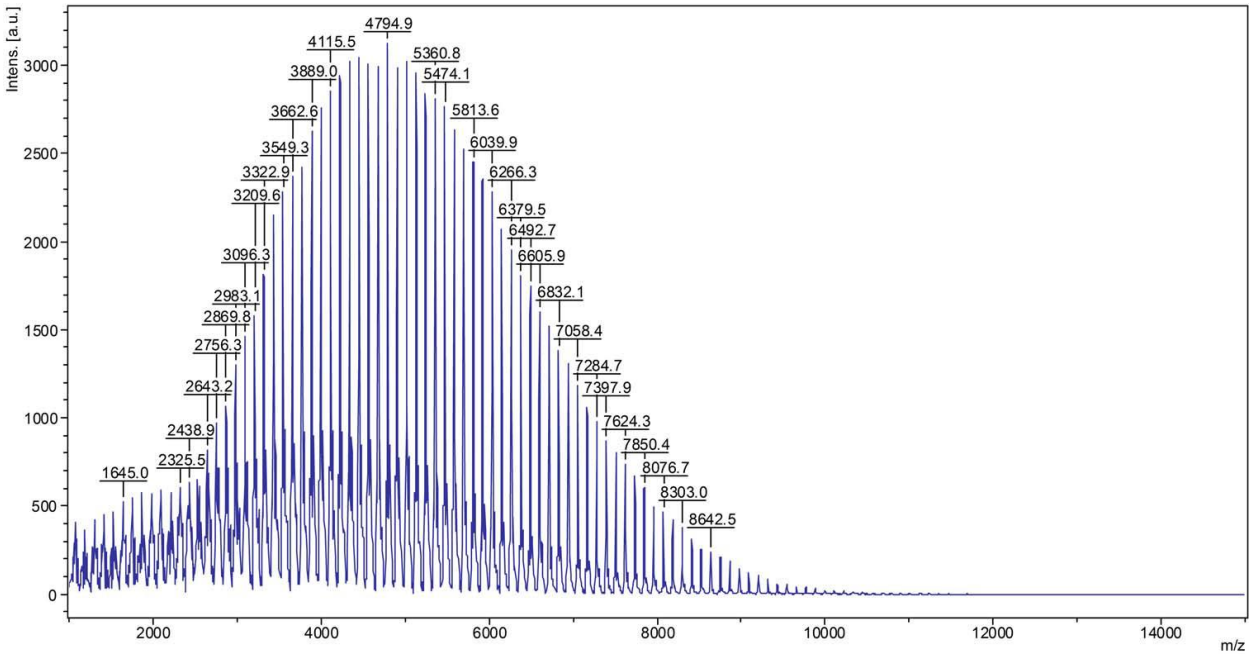

Table 2.13. Tacticity and MALDI-TOF analysis of PNIPAM

PNIPAM	Tacticity %	Conversion %	$M_{n,\ theoretical}$	$M_{n,\ MALDI\text{-}TOF}$	PDI
First sample	89	99	5796	2866	1.04
Second sample	88	97	11454	5211	1.07

First sample. Solvent: MeOH, 257μL. NIPAM: 1 mmol. [NIPAM] = 3.9M. [NIPAM]: [$Yb(OTf)_3$]: [CuBr]: [Initiator]: [Ligand] = 100: 5: 2: 2: 1. ATRP at 20℃, 1h. Conversion and isotacticity were measured by 600MHz ^{1}H NMR. MW and PDI were measured by MALDI-TOF analysis.
Second sample. Add a mixture of 1 mmol NIPAM, 0.05 mmol $Yb(OTf)_3$ and 257μL MeOH to the ATRP system 1 hour after the start of first polymerization. Then ATRP at 20℃ for 24 hours. Conversion and isotacticity were measured by 600MHz ^{1}H NMR. MW and PDI were measured by MALDI-TOF analysis.

In order to refine the system and better control the MW of PNIPAM, a mixed solvent was used. In the stereocontrolled RAFT polymerization of NIPAM, a methanol/toluene mixed solvent was used with the volume ratio equal to 1:1, and PNIPAM with good MW control was achieved. Therefore, in our system, solvent with volume ratio of methanol/toluene equals to 3:1 and 1:1 were examined. 1mmol of NIPAM was dissolved in 400μL solvent. **Figure 2.12** and **2.13** shows the MALDI-TOF analysis data and **Table 2.14** shows the analysis results. The results are very promising. The ATRP of NIPAM using the mixed solvent shows good MW control and narrow PDI, which means the mixed solvent is a better choice for the ATRP of NIPAM. However, from the mass spectra, it is revealed that there is another MW distribution for both solvent systems, even though the intensity is low compared with the major MW distribution. This demonstrates that a small portion of polymer chain might not obey the controlled propagation manner, and the ATRP system needs to be further improved.

Figure 2.12. MALDI-TOF analysis data, MeOH: Toluene = 1:1 (v/v)

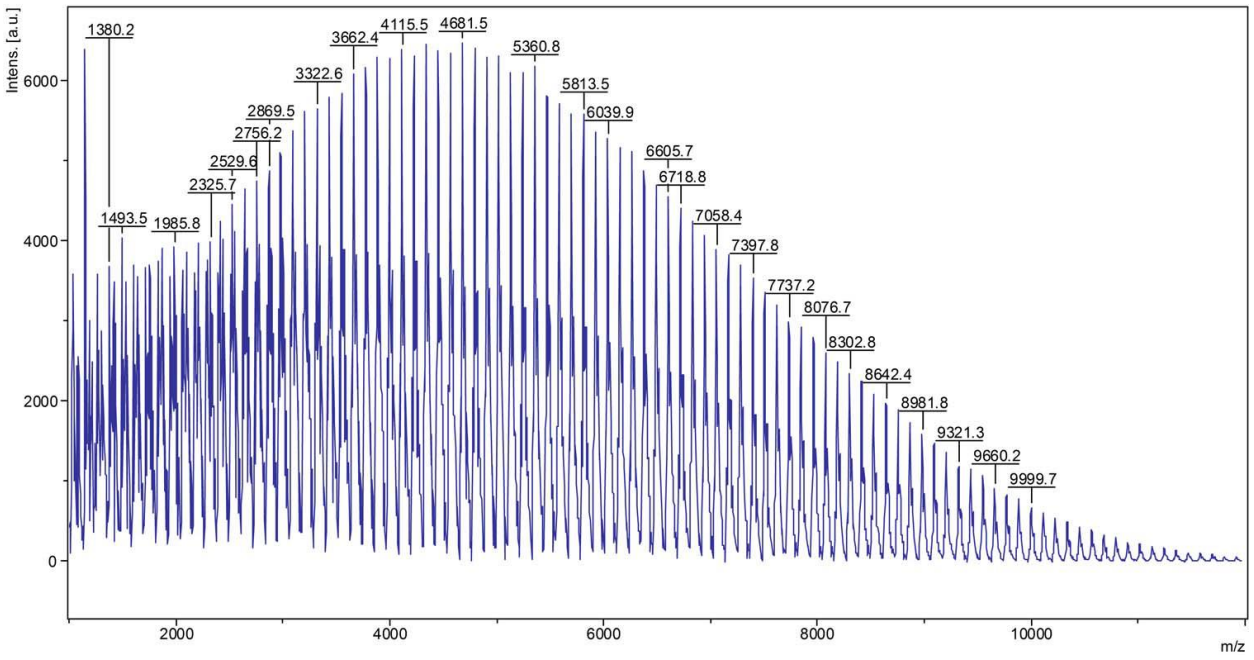

Figure 2.13. MALDI-TOF analysis data, MeOH: Toluene = 3:1 (v/v)

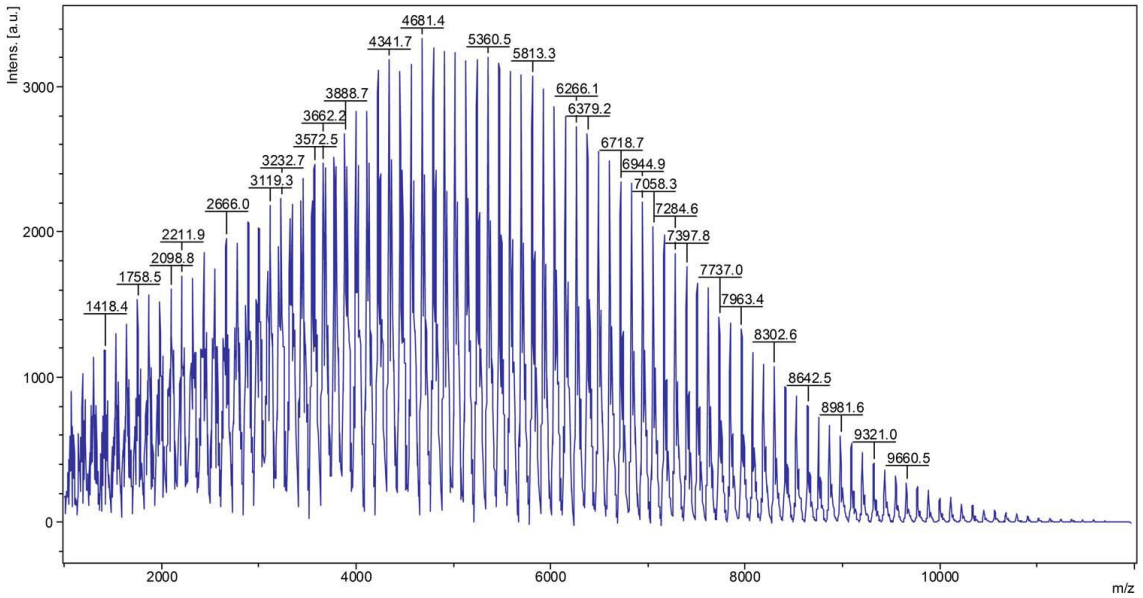

Table 2.14. Polymerization of NIPAM using mixed solvent

Solvent	Tacticity %	Conversion %	$M_{n,\ theoretical}$	$M_{n,\ MALDI\text{-}TOF}$	PDI
MeOH: Toluene (v/v = 1:1)	88	89	5231	5599	1.12
MeOH: Toluene (v/v = 3:1)	89	62	3703	5802	1.07

Polymerization conditions. Solvent: 400μL. NIPAM: 1 mmol. [NIPAM] = 2.5M. [NIPAM]: [$Yb(OTf)_3$]: [CuBr]: [Initiator]: [Ligand] = 100: 5: 2: 2: 1. ATRP at 20℃, 24h. Conversion and isotacticity were measured by 600MHz ^{1}H NMR. MW and PDI were measured by MALDI-TOF analysis.

5. Summary

In summary, the ATRP of various acrylamides was successfully conducted. The new copper-ligand catalytic system shows both good control on tacticity and MW distribution of the polymers. In addition, for the first time, the highly isotacitic PNIPAM was synthesized by using the ATRP method, which is a breakthrough for the stereocontrolled CRP of NIPAM, as PNIPAM has potential applications in drug delivery. We will continue explore the potential of this new catalytic system in the ATRP of functional α-olefins.

Experimental and Characterization

1. Analytical Instruments

NMR: Bruker 600 MHz.

Polarimeter: Jasco Digital Polarimeter P-2000.

High resolution mass spectrometer: Waters Q-TOF Ultima ESI.

MALDI-TOF analysis: Bruker Daltonics UltrafleXtreme MALDI TOF.

2. General Data

All commercial chemicals were used without further purification unless otherwise noted. Tetrahydrofuran (THF) was distilled over sodium and benzophenone under nitrogen. Methanol, toluene and dimethylformamide (DMF) were dried over molecular sieve and distilled. *N*,*N*-dimethylacrylamide and *N*,*N*-diethylacrylamide were dried over molecular sieve and distilled. *N*-isopropylacrylamide and acrylamide were recrystallized using toluene/hexane = 1:1 solvent.

3. General procedure

3.1 Synthesis of macrocyclic ligands

a. Synthesis of chiral *N*-sulfinyl aldimines[16] (2.9, 2.10, 2.11)

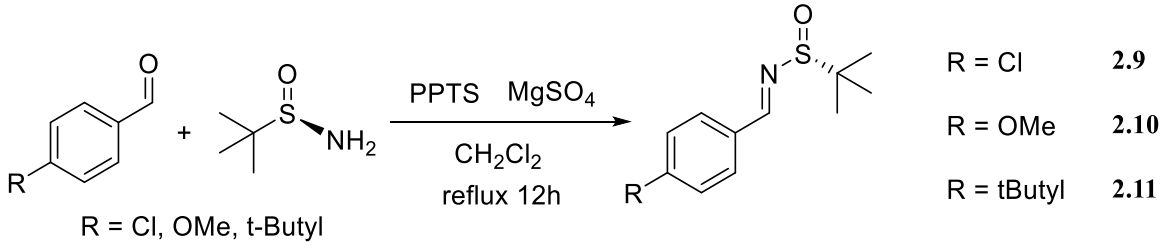

General Procedure

(*R*)-2-Methyl-2-propanesulfinamide (97 mg, 0.8 mmol, 1.0 equiv) was dissolved in 10 mL dichloromethane (DCM), then pyridinium *p*-toluenesulfonate (PPTS) (101 mg, 0.4 mmol, 0.5 equiv) was added followed by $MgSO_4$ (481 mg, 4 mmol, 5 equiv) and the aldehyde (0.8 mmol, 2.0 equiv). The mixture was stirred and refluxed for 20 h, then filtered and washed with 10 mL DCM for three times. The filtrate was concentrated in vacuum and the residue was purified by column chromatography on silica gel (Hexane: EtOAc = 9: 1) to afford the desired product.

(*R*,*E*)-*N*-(4-chlorobenzylidene)-2-methylpropane-2-sulfinamide, 2.9

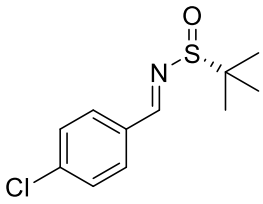

126.7 mg. Yield: 65%. ^{1}H NMR (600 MHz, Chloroform-*d*) δ 8.54 (s, 1H), 7.78 (d, *J* = 8.5 Hz, 2H), 7.44 (d, *J* = 8.5 Hz, 2H), 1.25 (s, 9H).

(*R*,*E*)-N-(4-methoxybenzylidene)-2-methylpropane-2-sulfinamide, 2.10

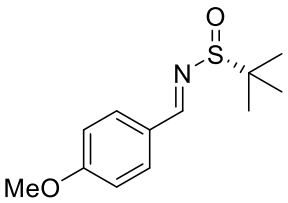

181.9 mg. Yield: 95%. ^{1}H NMR (600 MHz, Chloroform-*d*) δ 8.50 (s, 1H), 7.79 (d, *J* = 8.8 Hz, 2H), 6.96 (d, *J* = 8.8 Hz, 2H), 3.86 (s 3H), 1.24 (s, 9H).

(*R*,*E*)-N-(4-(*tert*-butyl)benzylidene)-2-methylpropane-2-sulfinamide, 2.11

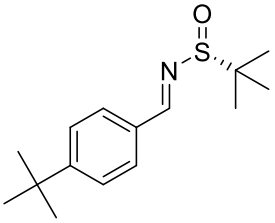

195.3 mg. Yield: 92%. ^{1}H NMR (600 MHz, Chloroform-*d*) δ 8.55 (s, 1H), 7.78 (d, *J* = 8.5 Hz, 2H), 7.49 (d, *J* = 8.5 Hz, 2H), 1.34 (s, 9H), 1.25 (s, 9H).

b. General Procedure for the Homocoupling of Chiral *N-tert*-butylsulfinyl imines[2] **(2.12, 2.13, 2.14)**

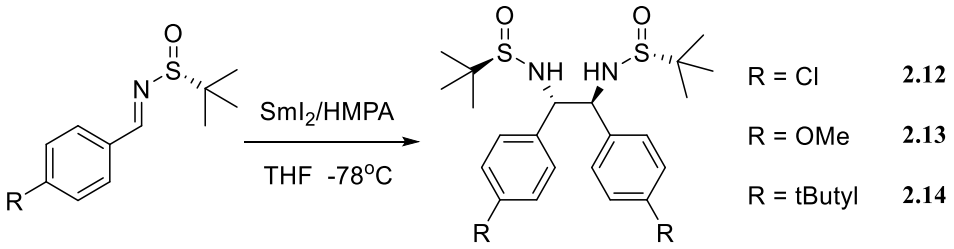

Under nitrogen, hexamethylphosphoramide (HMPA) (537.6 mg, 3.0 mmol, 6 equiv) was added to 5 mL freshly prepared SmI_2 in THF solution (0.2 M) at -78℃. After approximately 30 min, 0.5 mmol of sulfinyl imine in 6 mL THF was then added dropwise. The mixture was stirred at -78 ℃ for another 8 h. The reaction was monitored by TLC, and quenched with 5 mL of saturated aqueous $Na_2S_2O_3$ solution after the reaction reached completion. Extraction with ethyl acetate and purification by flash column chromatography on silica gel (Hexane: EtOAc = 5: 1) afforded the desired homocoupling product.

Homocoupling product 2.12

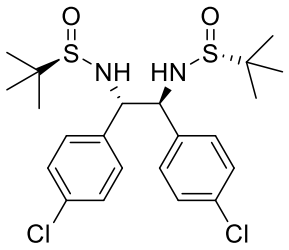

91.8 mg. Yield: 75%. ^{1}H NMR (600 MHz, Chloroform-*d*) δ 7.18 (dd, *J* = 8.5, 1.7 Hz, 1H), 7.07 (dd, *J* = 8.5, 1.7 Hz, 1H), 5.93 (s, 2H), 4.85 (s, 2H), 1.11 (s, 18H).

Homocoupling product 2.13

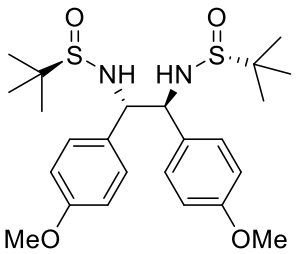

96.1 mg. Yield: 80%. ^{1}H NMR (600 MHz, Chloroform-*d*) δ 7.10 (m, 4H), 6.73 (m, 4H), 5.84 (s, 2H), 4.91 (s, 2H), 3.74 (s, 6H), 1.13 (s, 18H).

Homocoupling product 2.14

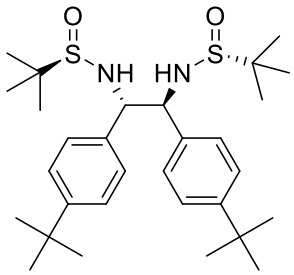

86.6 mg. Yield: 65%. ^{1}H NMR (600 MHz, Chloroform-*d*) δ 7.20 (d, *J* = 8.4 Hz, 1H), 7.11 (d, *J* = 8.4 Hz, 1H), 5.69 (s, 2H), 4.92 (s, 2H), 1.25 (s, 18H), 1.13 (s, 18H).

c. General procedure for the synthesis of chiral diamine

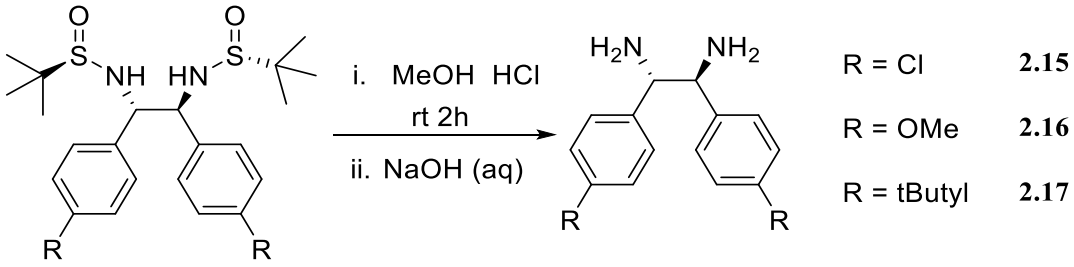

The obtained homocoupling product **(**0.2 mmol) was dissolved in 2.0 mL of methanol, then 0.5 mL of 4 N HCl (2.0 mmol) was added to the solution. The mixture was stirred for 2 hours at room temperature and then concentrated under vacuum. The resulting solid was recrystallized using a mixture of methanol and ethyl ether to provide the diamine salt. Then the diamine salt (0.2 mmol) was dissolved in 30ml DI water, NaOH solid was added to the aqueous solution until white precipitate (free diamine) came out. Diamine was extracted by ethyl acetate and concentrated under vacuum to get the free diamine.

(1*S*,2*S*)-1,2-bis(4-chlorophenyl)ethane-1,2-diamine, 2.15

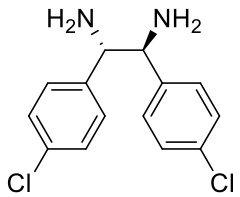

39.4 mg. Yield: 70%. ^{1}H NMR (600 MHz, Methanol-d_4) δ 7.17 (d, *J* = 8.5 Hz, 4H), 7.07 (d, *J* = 8.5 Hz, 4H), 3.89 (s, 2H).

(1*S*,2*S*)-1,2-bis(4-methoxyphenyl)ethane-1,2-diamine, 2.16

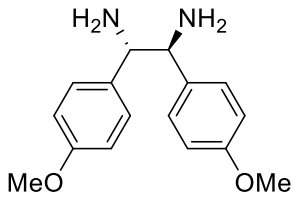

40.9 mg. Yield: 75%. ^{1}H NMR (600 MHz, Methanol-d_4) δ 7.00 (d, J = 8.7 Hz, 4H), 6.73 (d, J = 8.7 Hz, 4H), 3.87 (s, 2H), 3.70 (s, 6H).

(1*S*,2*S*)-1,2-bis(4-(tert-butyl)phenyl)ethane-1,2-diamine, 2.17

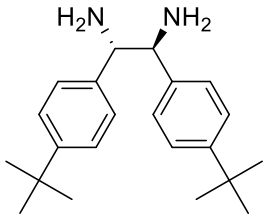

46.7 mg. Yield: 72%. ^{1}H NMR (600 MHz, Methanol-d_4) δ 7.24 (d, J = 8.3 Hz, 1H), 7.06 (d, J = 8.3 Hz, 1H), 3.96 (s, 2H), 1.24 (s, 18H).

d. General Procedure for the Yynthesis of Dialdehyde 2.5[17]

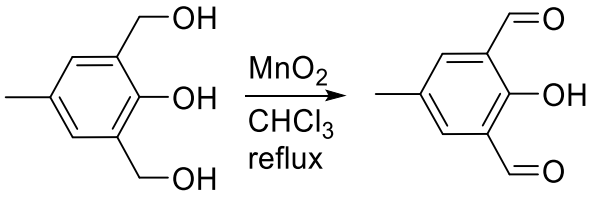

2.5

Manganese (IV) oxide (8.0 g, 92 mmol) and 50 mL chloroform were added into a 250 mL round bottom flask. The mixture was heated at reflux for 15 min and 2,6-Bis(hydroxymethyl)-*p*-cresol (1.0 g, 5.95 mmol) was added. The reaction was heated at reflux for 8 h. Then the mixture was cooled to room temperature and filtered by vacuum filtration then washed by 50 mL chloroform for three times. The filtrated solution was concentrated and purified by column chromatography on silica gel (hexane: ethyl acetate = 5: 1) to afford the desired product (0.36 g, yield: 37%). ^{1}H NMR (600 MHz, Chloroform-*d*) δ 11.44 (s, 1H), 10.20 (s, 2H), 7.76 (s, 2H), 2.38 (s, 3H).

e. Synthesis of Schiff Base Macrocycle[1] (2.6 - 2.8, 2.18 - 2.20)

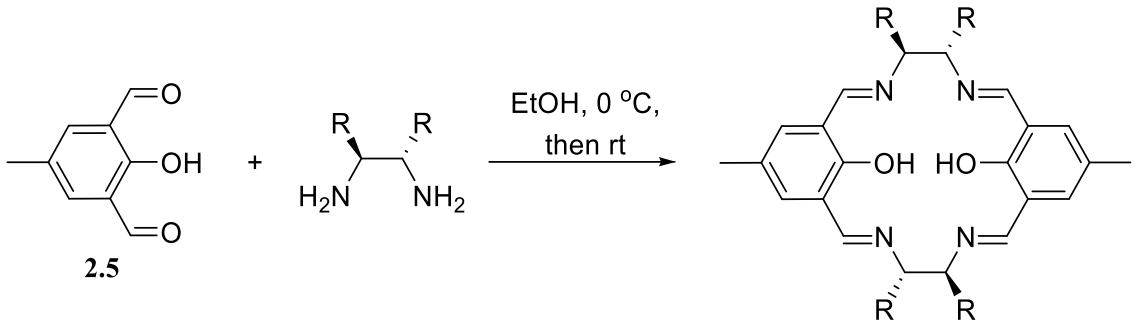

General Procedure

To an ethanol solution (50 mL) of **2.5** (65.7 mg, 0.4 mmol, 1 equiv) at 0 °C, chiral diamine (0.4 mmol, 1 equiv) in 15 mL ethanol was added dropwise. The reaction mixture was stirred at 0 ℃ for 4 h and then at room temperature for 18 h. Yellow precipitate was generated and was separated by centrifugation. The wet product was dried under reduce pressure to afford the desired product.

Ligand 2.6

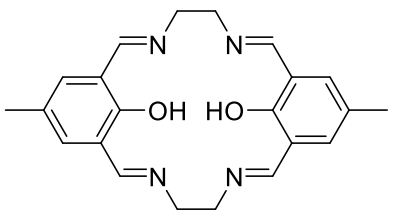

52.7 mg. Yield: 70%. ^{1}H NMR (600 MHz, DMSO-d_6) δ 14.14 (s, 2H), 8.45 (s, 4H), 7.42 (s, 4H), 3.90 (s, 8H), 2.14 (s, 6H).

HRMS (ESI) for $C_{22}H_{25}N_4O_2$ (MH^+) Cacld: 377.1978, Found: 377.1969.

Ligand 2.7

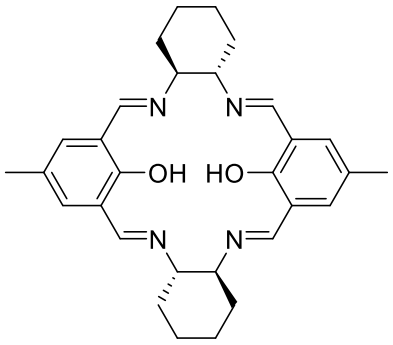

77.5 mg. Yield: 80%. ^{1}H NMR (600 MHz, Chloroform-*d*) δ 13.84 (s, 2H), 8.65 (s, 2H), 8.18 (s, 1H), 7.54 (s, 2H), 6.87 (s, 2H), 3.34 (d, J = 29.8 Hz, 4H), 2.06 (s, 6H), 1.74 (m, 12H), 1.45 (m, 4H).

^{13}C NMR (151 MHz, Chloroform-*d*) δ 163.39, 159.30, 156.10, 134.09, 129.50, 126.84, 123.02, 118.77, 75.41, 73.38, 33.45, 33.17, 24.42, 24.33, 19.99.

HRMS (ESI) for $C_{30}H_{37}N_4O_2$ (MH^+) Cacld: 485.2917, Found: 485.2905.

Ligand 2.8

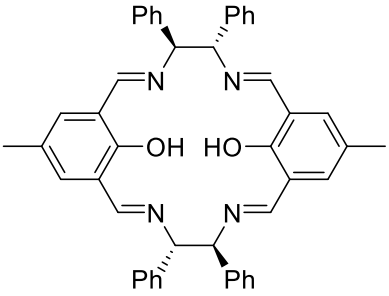

111.7 mg. Yield: 82%. ^{1}H NMR (600 MHz, DMSO-d_6) δ 14.11 (s, 2H), 8.80 (s, 2H), 8.59 (s, 2H), 7.49 (s, 2H), 7.34 – 7.03 (m, 22H), 5.00 (d, *J* = 54.6 Hz, 4H), 1.81 (s, 6H).

^{13}C NMR (151 MHz, Chloroform-*d*) δ 164.83, 159.07, 156.70, 140.88, 140.02, 134.60, 130.11, 128.21, 128.07, 127.93, 127.81, 127.24, 127.11, 126.97, 123.07, 118.90, 82.43, 81.25, 20.19.

HRMS (ESI) for $C_{46}H_{41}N_4O_2$ (MH^+) Cacld: 681.3230, Found: 681.3220.

Ligand 2.18

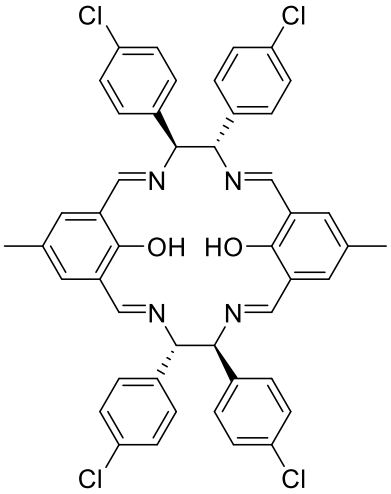

131 mg. Yield: 80%. ^{1}H NMR (600 MHz, Chloroform-*d*) δ 13.57 (s, 2H), 8.79 (s, 2H), 8.34 (s, 2H), 7.76 (s, 2H), 7.13 (m, 8H), 7.09 (s, 4H), 7.02 (s, 6H), 4.63 (d, *J* = 21.6 Hz, 4H), 2.21 (s, 6H).

^{13}C NMR (151 MHz, Chloroform-*d*) δ 165.22, 158.96, 156.92, 139.05, 138.16, 134.92, 133.28, 132.95, 130.29, 129.26, 128.98, 128.58, 128.29, 127.42, 122.89, 118.80, 81.56, 80.50, 20.25.

HRMS (ESI) for $C_{46}H_{37}N_4O_2Cl_4$ (MH^+) Cacld: 817.1671, Found: 817.1654.

Ligand 2.19

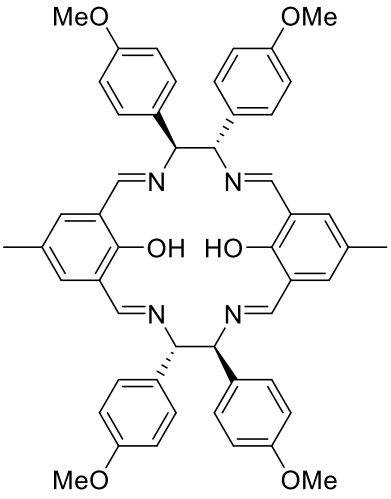

124.9 mg. Yield: 78%. ^{1}H NMR (600 MHz, Chloroform-*d*) δ 13.83 (s, 2H), 8.79 (s, 2H), 8.34 (s, 2H), 7.74 (s, 2H), 7.07 (s, 4H), 7.02 (s, 4H), 6.96 (s, 2H), 6.68 (s, 8H), 4.67 (d, *J* = 9.2 Hz, 2H), 4.61 (d, *J* = 9.0 Hz, 2H), 3.70 (s, 12H), 2.19 (s, 6H).

^{13}C NMR (151 MHz, Chloroform-*d*) δ 164.41, 159.08, 158.54, 158.38, 156.29, 134.41, 133.34, 132.42, 130.02, 128.99, 128.78, 126.97, 123.14, 118.90, 113.62, 113.35, 81.76, 80.55, 55.12, 55.10, 20.23.

HRMS (ESI) for $C_{50}H_{49}N_4O_6$ (MH^+) Cacld: 801.3652, Found: 801.3633.

Ligand 2.20

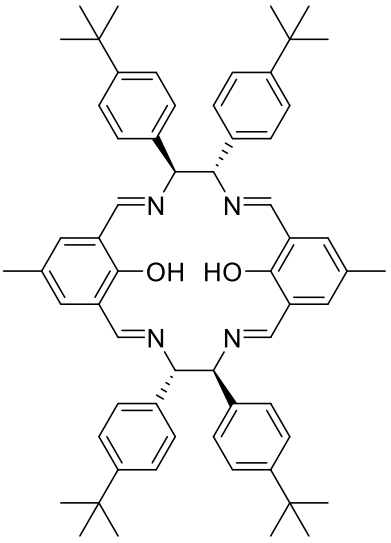

144.8 mg. Yield: 80%. ^{1}H NMR (600 MHz, Chloroform-*d*) δ 13.86 (s, 2H), 8.83 (s, 2H), 8.36 (s, 2H), 7.75 (s, 2H), 7.11 (m, 8H), 7.06 (m, 4H), 7.00 (m, 4H), 6.93 (s, 2H), 4.70 (d, *J* = 35.2 Hz, 4H), 2.15 (s, 6H), 1.20 (s, 36H).

^{13}C NMR (151 MHz, Chloroform-*d*) δ 164.55, 159.13, 156.53, 149.93, 149.58, 137.97, 137.13, 134.39, 129.99, 127.62, 127.40, 126.92, 124.87, 124.60, 123.12, 118.93, 82.18, 80.78, 34.32, 34.27, 31.27, 31.23, 20.17.

HRMS (ESI) for $C_{62}H_{73}N_4O_2$ (MH^+) Cacld: 905.5734, Found: 905.5741.

f. Synthesis of Macrocyclic Amine Compounds[18] (2.27 – 2.32)

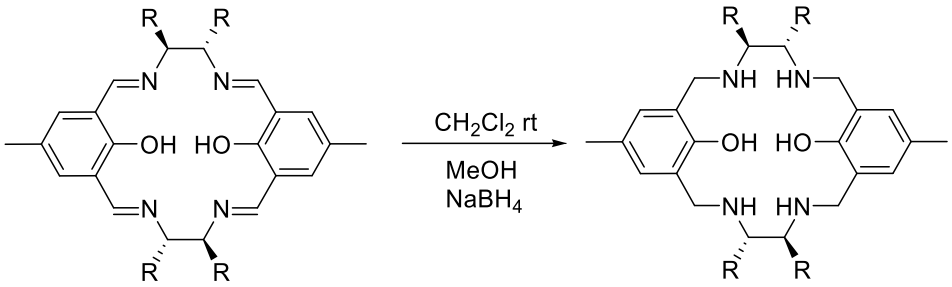

General Procedure

A Schiff base ligand (0.1 mmol, 1 equiv) was dissolved in a mixture of solvents containing 15 mL DCM and 5 mL MeOH. $NaBH_4$ (15.1 mg, 0.4 mmol, 4 equiv) was added to the solution. The mixture was stirred for 12 h under nitrogen and then quenched by 5 mL water. The product was extracted by 20 mL DCM for 3 times and concentrated under vacuum to afford the desired product.

Ligand 2.27

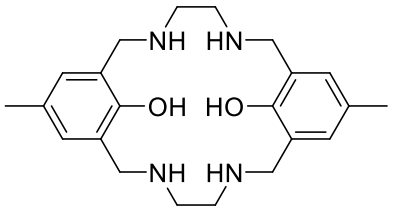

34.6 mg. Yield: 90%. ^{1}H NMR (600 MHz, Chloroform-*d*) δ 6.76 (s, 4H), 3.79 (s, 8H), 2.72 (s, 8H), 2.19 (s, 6H). ^{13}C NMR (151 MHz, Chloroform-*d*) δ 154.14, 128.82, 127.41, 124.41, 50.72, 47.79, 20.39. HRMS (ESI) for $C_{22}H_{33}N_4O_2$ (MH^+) Cacld: 385.2604, Found: 385.2586.

Ligand 2.28

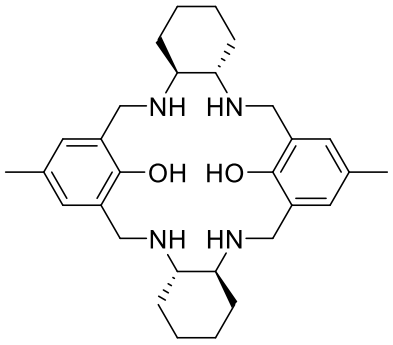

44.8 mg. Yield: 91%. ^{1}H NMR (600 MHz, Chloroform-*d*) δ 6.74 (s, 4H), 3.74 (dd, *J* = 72.2, 13.2 Hz, 8H), 2.31 (m, 4H), 2.17 (s, 6H), 2.06 (m, 4H), 1.68 (m, 4H), 1.21 (m, 4H), 1.11 (m, 4H).

^{13}C NMR (151 MHz, Chloroform-*d*) δ 154.08, 128.10, 127.14, 125.18, 60.45, 47.68, 31.21, 24.97, 20.49.

HRMS (ESI) for $C_{30}H_{45}N_4O_2$ (MH^+) Cacld: 493.3543, Found: 493.3536.

$[\alpha]_D$ = 90.2° (c = 1, $CHCl_3$)

Ligand 2.29

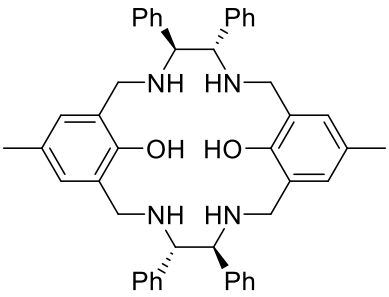

62 mg. Yield: 90%. ^{1}H NMR (600 MHz, Chloroform-*d*) δ 7.15 (m, 8H), 7.12 – 7.08 (m, 4H), 7.07 – 7.03 (m, 8H), 6.59 (s, 4H), 3.81 (s, 4H), 3.67 (d, *J* = 13.4 Hz, 4H), 3.58 (d, *J* = 13.3 Hz, 4H), 2.66 (s, 4H), 2.08 (s, 6H).

^{13}C NMR (151 MHz, Chloroform-*d*) δ 153.77, 140.32, 128.51, 128.06, 127.45, 127.04, 124.60, 68.07, 48.75, 20.31.

HRMS (ESI) for $C_{46}H_{49}N_4O_2$ (MH^+) Cacld: 689.3856, Found: 689.3844.

$[\alpha]_D$ = 76.2° (c = 0.435, $CHCl_3$)

Ligand 2.30

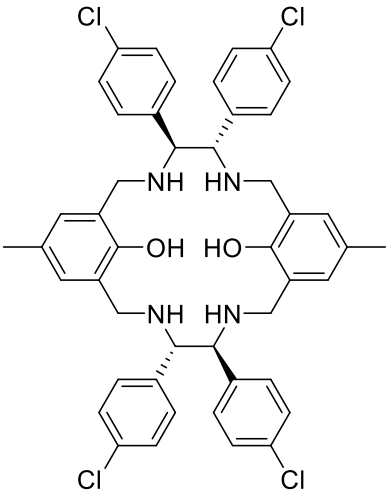

76.1 mg. Yield: 92%. ^{1}H NMR (600 MHz, Chloroform-*d*) δ 7.14 (d, *J* = 8.0 Hz, 8H), 6.96 (d, *J* = 8.0 Hz, 8H), 6.55 (s, 4H), 3.73 (s, 4H), 3.67 (d, *J* = 13.4 Hz, 4H), 3.51 (d, *J* = 13.4 Hz, 4H), 2.62 (s, 4H), 2.08 (s, 6H).

^{13}C NMR (151 MHz, Chloroform-*d*) δ 153.70, 138.57, 132.93, 129.28, 128.84, 128.45, 127.78, 124.23, 67.13, 48.69, 20.28.

HRMS (ESI) for $C_{46}H_{45}N_4O_2Cl_4$ (MH^+) Cacld: 825.2297, Found: 825.2264.

$[\alpha]_D$ = 40.1° (c = 0.335, $CHCl_3$)

Ligand 2.31

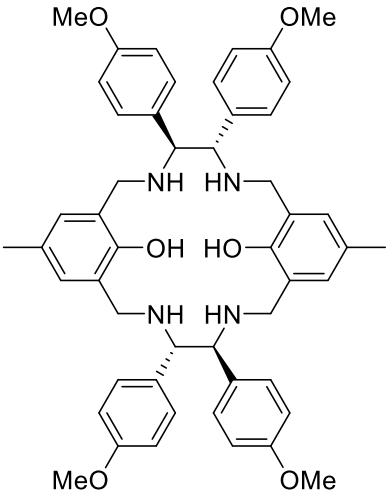

73.6 mg. Yield: 91%. ^{1}H NMR (600 MHz, Chloroform-*d*) δ 6.95 (d, *J* = 8.2 Hz, 8H), 6.69 (d, *J* = 8.2 Hz, 8H), 6.58 (s, 4H), 3.74 (s, 4H), 3.71 (s, 12H), 3.66 (d, *J* = 13.5 Hz, 4H), 3.55 (d, *J* = 13.4 Hz, 4H), 2.08 (s, 6H).

^{13}C NMR (151 MHz, Chloroform-*d*) δ 158.42, 153.81, 132.43, 129.09, 128.43, 127.34, 124.62, 113.45, 67.26, 55.08, 48.58, 20.33.

HRMS (ESI) for $C_{50}H_{57}N_4O_6$ (MH^+) Cacld: 809.4278, Found: 809.4263.

$[\alpha]_D$ = 31.2° (c = 0.42, $CHCl_3$)

Ligand 2.32

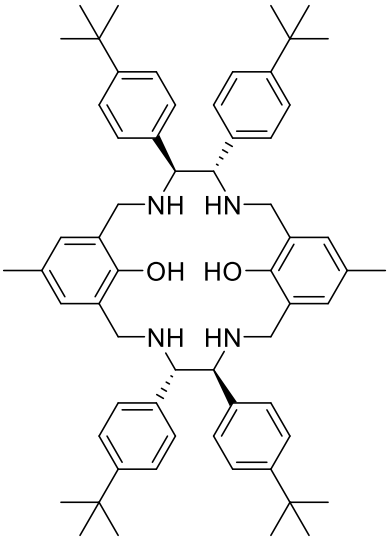

85 mg. Yield: 93%. ^{1}H NMR (600 MHz, Chloroform-*d*) δ 7.11 (d, 8H), 6.93 (d, 8H), 6.61 (s, 4H), 3.77 (s, 4H), 3.65 (d, 4H), 3.62 (d, 4H), 2.09 (s, 6H), 1.21 (s, 36H).

^{13}C NMR (151 MHz, Chloroform-*d*) δ 153.74, 149.62, 137.08, 128.23, 127.65, 127.27, 124.73, 124.67, 67.81, 48.74, 34.30, 31.29, 20.39.

HRMS (ESI) for $C_{62}H_{81}N_4O_2$ (MH^+) Cacld: 913.6360, Found: 913.6334.

$[\alpha]_D = 24.6^o$ (c = 0.492, $CHCl_3$)

3.2. Atom Transfer Radical Polymerization (ATRP) of Monomers

a. Synthesis of Monomer 2.24[19]

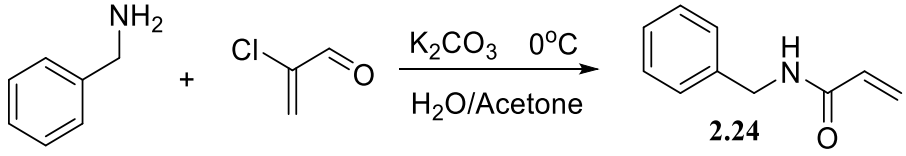

2.24

To a stirred suspension of potassium carbonate (2.76 g, 20.0 mmol, 2 equiv) in distilled water (5 mL) and acetone (20 mL) was added acryloyl chloride (1.81 g, 20.0 mmol, 2 equiv) at 0 °C under nitrogen atomosphere. Benzylamine (1.09 mL, 10.0 mmol, 1 equiv) was then added dropwise to the mixture, and stirred for 1 h at 0 °C. After filtration, the mixture was concentrated under reduced pressure and extracted three times with dichloromethane (3 x 30 mL). The organic layer was dried over Na_2SO_4, and concentrated under reduced pressure. The residue was purified by flash chromatography on silica gel with Hexane: EtOAc = 4: 1 to give the corresponding product (1.45 g, yield: 90%). ^{1}H NMR (600 MHz, Chloroform-*d*) δ 7.35 – 7.24 (m, 5H), 6.30(m, 1H), 6.10 (dd, *J* = 17.0, 10.3Hz, 1H), 5.93 (s, 1H), 5.65 (dd, *J* = 10.3, 1.2 Hz, 0H), 4.50 (d, *J* = 5.8 Hz, 2H).

b. Synthesis of Monomer 2.25[19]

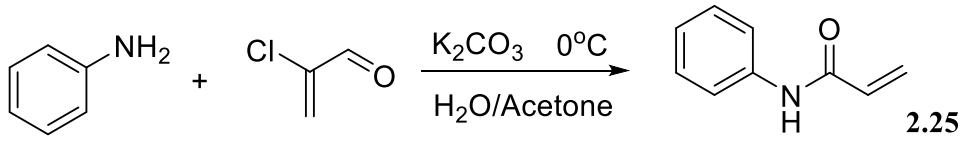

2.25

To a stirred suspension of potassium carbonate (2.76 g, 20.0 mmol, 2 equiv) in distilled water (5 mL) and acetone (20 mL) was added acryloyl chloride (1.81 g, 20.0 mmol, 2 equiv) at 0 °C under nitrogen atomosphere. Aniline (0.91 mL, 10.0 mmol, 1 equiv) was then added dropwise to the mixture, and stirred for 1 h at 0 °C. After filtration, the mixture was concentrated under reduced pressure and extracted three times with dichloromethane (3 x 30 mL). The organic layer was dried over Na_2SO_4, and concentrated under reduced pressure. The residue was purified by flash chromatography on silica gel with Hexane: EtOAc = 4: 1 to give the corresponding product (1.32 g, yield: 90%). ^{1}H NMR (600 MHz, Chloroform-*d*) δ 7.57 (d, *J* = 7.9 Hz, 2H), 7.33 (t, *J* = 7.9 Hz, 2H), 7.12 (t, *J* = 7.4 Hz, 1H), 6.42 (d, *J* = 16.8 Hz, 1H), 6.24 (dd, *J* = 16.8, 10.3 Hz, 1H), 5.76 (dd, *J* = 10.3, 0.9 Hz, 1H).

d. ATRP of DMAA (Example)

N,*N*-Dimethylacrylamide (103 μL, 99.1 mg, 1.0 mmol), methanol (154 μL) and $Yb(OTf)_3$ (31 mg, 0.05 mmol) were added to a Schlenk flask and stirred for 0.5 h. Then ligand **2.29** (6.8 mg, 0.01mmol) was added to the flask and stirred for another 0.5 h. After that, ethyl 2-bromoisobutyrate (3.0 μL, 3.9 mg, 0.02 mmol) was added and the reaction mixture underwent three freeze-pump-thaw cycles for degassing. After the mixture returned to room temperature, CuBr (2.9 mg, 0.02 mmol) were added and the reaction was conducted in dry box for 24 h. After that, a small amount of mixture was used for NMR analysis to determine the tacticity and conversion. The polymer was dissolved in a minimum amount of MeOH and precipitate in excess diethyl ether for three time to purify it. Purified polymer: 82 mg. Isolated yield: 83%.

e. ATRP of NIPAM (Example)

N-Isopropylacrylamide (113 mg, 1.0 mmol), methanol (257 μL) and $Yb(OTf)_3$ (31 mg, 0.05 mmol) were added to a Schlenk flask and stirred for 0.5 hour. Then ligand **2.29** (6.8 mg, 0.01mmol) was added to the flask and stirred for another 0.5 hour. After that, ethyl 2-bromoisobutyrate (3.0 μL, 3.9 mg, 0.02 mmol) was added and the reaction mixture underwent three freeze-pump-thaw cycles for degassing. After the mixture returned to room temperature, CuBr (2.9 mg, 0.02 mmol) were added and the reaction was conducted in dry box for 24 hours. After that, a small amount of mixture was used for NMR analysis to determine the tacticity and conversion. The polymer was hardly dissolved in common solvent except DMSO and DMF. The PNIPAM was put in MeOH to wash out monomers and purified. Purified polymer: 109 mg. Isolated yield: 96%.

f. Polymerization of Other Monomers

The procedure is the same as **3.2.e** and **3.2.f**. Monomer concentration was 3.9 M (1 mmol/257 μL).

3.3. Kinetic Study of ATRP Process

Once the ATRP of NIPAM started, after a certain time, a small amount of reaction mixture was taken out of the glove box and exposed to air to quench the reaction, then the conversion of the mixture was determined by ^1H NMR. The conversion was calculated by compare the integration area of one vinyl proton peak (A_1) and half of the integration area of *m* and *r* peaks (A_2).

$$\text{Conversion } \% = A_2 / (A_1 + A_2) \times 100\%$$

In addition, conversion has direct relationship with the concentration of monomer.

$$\text{Conversion \%} = ([M]_0 - [M]) / [M]_0 = 1 - [M] / [M]_0$$

Therefore, the $[M]_0 / [M]$ value can be calculated based on ^{1}H NMR data, and the $\ln \frac{[M_0]}{[M]}$ verse time plot can be made.

Reference

(1) Wu, J. C.; Tang, N.; Liu, W. S.; Tan, M. Y.; Chan, A. S. C. *Chinese Chem. Lett.* **2001**, *12* (9), 757–760.

(2) Zhong, Y. W.; Izumi, K.; Xu, M. H.; Lin, G. Q. *Org. Lett.* **2004**, *6* (i), 4747–4750.

(3) Dutta, B.; Bag, P.; Adhikary, B.; Flörke, U.; Nag, K. *J. Org. Chem.* **2004**, *69* (16), 5419–5427.

(4) Lutz, J. F.; Neugebauer, D.; Matyjaszewski, K. *J. Am. Chem. Soc.* **2003**, *125* (12), 6986–6993.

(5) Okamoto, Y.; Habaue, S. *Macromol. Symp.* **2003**, *195*, 75–80.

(6) Schild, H. G. *Prog. Polym. Sci.* **1992**, *17*, 163–249.

(7) Convertine, A. J.; Ayres, N.; Scales, C. W.; Lowe, A. B.; McCormick, C. L. *Biomacromolecules* **2004**, *5* (4), 1177–1180.

(8) Ruel-Gariépy, E.; Leroux, J.-C. *Eur. J. Pharm. Biopharm.* **2004**, *58* (2), 409–426.

(9) Wei, H.; Cheng, S.-X.; Zhang, X.-Z.; Zhuo, R.-X. *Prog. Polym. Sci.* **2009**, *34* (9), 893–910.

(10) Xia, Y.; Burke, N. a D.; Sto, H. D. H.; V, M. U.; Ls, C. *Macromolecules* **2006**, *39*, 2275–2283.

(11) Katsumoto, Y.; Kubosaki, N. *Macromolecules* **2008**, *41*, 5955–5956.

(12) Matyjaszewski, K. *Macromolecules* **2012**, *45*, 4015–4039.

(13) Biswas, C. S.; Patel, V. K.; Vishwakarma, N. K.; Tiwari, V. K.; Maiti, B.; Maiti, P.; Kamigaito, M.; Okamoto, Y.; Ray, B. *Macromolecules* **2011**, *44*, 5822–5824.

(14) Iizuka, Y.; Li, Z.; Satoh, K.; Kamigaito, M.; Okamoto, Y.; Ito, J. I.; Nishiyama, H. *European J. Org. Chem.* **2007**, *4* (X), 782–791.

(15) Odian, G. *Principles of Polymerization*, 4th ed.; Wiley, 2004.

(16) Mita, T.; Sugawara, M.; Saito, K.; Sato, Y. *Org. Lett.* **2014**, *16*, 3028–3031.

(17) Huang, W.; Shaohua, G.; Dahua, H.; Qingjing, M. *Synth. Commun.* **2000**, *30* (9), 1555–1561.

(18) Bi, W.-Y.; Lü, X.-Q.; Chai, W.-L.; Song, J.-R.; Wong, W.-Y.; Wong, W.-K.; Jones, R. A. *J. Mol. Struct.* **2008**, *891* (1-3), 450–455.

(19) Chanthamath, S.; Takaki, S.; Shibatomi, K.; Iwasa, S. *Angew. Chemie - Int. Ed.* **2013**, *52* (22), 5818–5821.

Chapter 3. Additional studies of the polymerization

1. Additional Polymerization Methods Explored

We have attempted to conduct the step-wise synthesis of the bimetallic macrocyclic complexes for the ATRP process. As shown in **Scheme 3.1**, ligand **2.8** was first treated with NaH in THF at 0 ^{o}C and then reacted with 1 equiv $Yb(OTf)_3$ to prepare a macrocyclic Yb complex **3.1**. CuBr was added to **3.1** to prepare the bimetallic complex **3.2**. The resulting catalyst mixture was used to promote the polymerization of DMAA in the presence of the initiator ethyl 2-bromoisobutyrate (**Scheme 3.1**). The polymerization was completed in 4 h with 98% conversion as monitored by ^{1}H NMR analysis. The ^{1}H NMR spectrum showed an atactic structure of PDMAA because it contains approximately equal distribution of *m* and *r* diads. The unsuccessful manipulation of taciticty using this method might be because the chirality of the ligand does not have an effect on the stereocontrol of polymerization, and low concentration of Lewis acid is not enough to enhance the isotacticity of polymer.

Scheme 3.1. Step-wise preparation of the bimetallic macrocyclic complex for the polymerization of DMAA

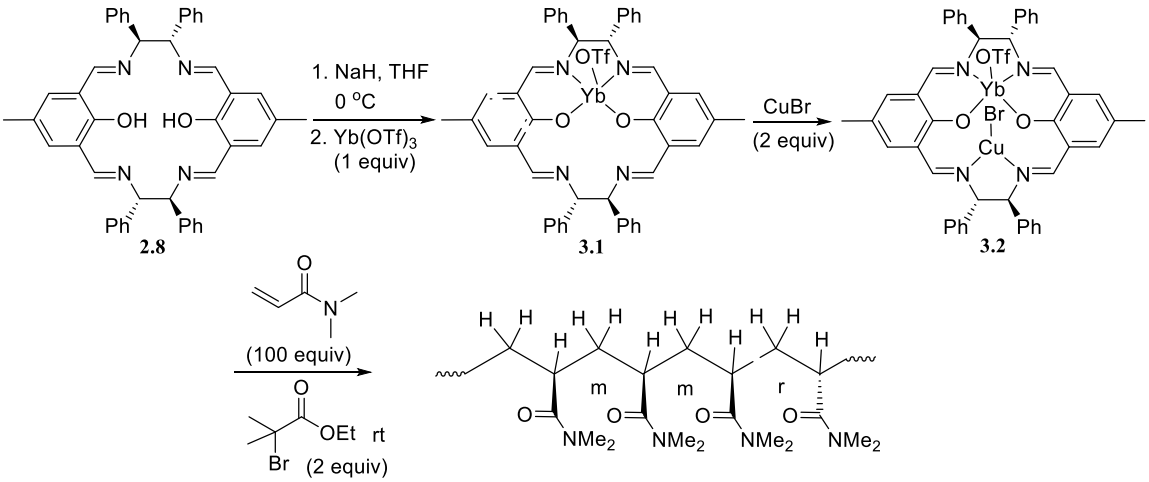

A few acyclic Schiff base compounds were synthesized[1] and their uses for the ATRP were investigated. The synthesis procedure is the same as the macrocycle synthesis. Two equivalent of monoaldehyde was dissolved in ethanol, and one equivalent of diamine in ethanol was added dropwise to the aldehyde. Two different Schiff bases were synthesized (**Scheme 3.2**). Polymerization of DMAA with these acyclic Schiff bases following the optimized condition or using the method of **Scheme 3.1** did not work. This indicates that the macrocyclic structure of ligands is important for their high catalytic activity for the ATRP of acrylamides.

Scheme 3.2. Synthesis of acyclic Schiff base compounds

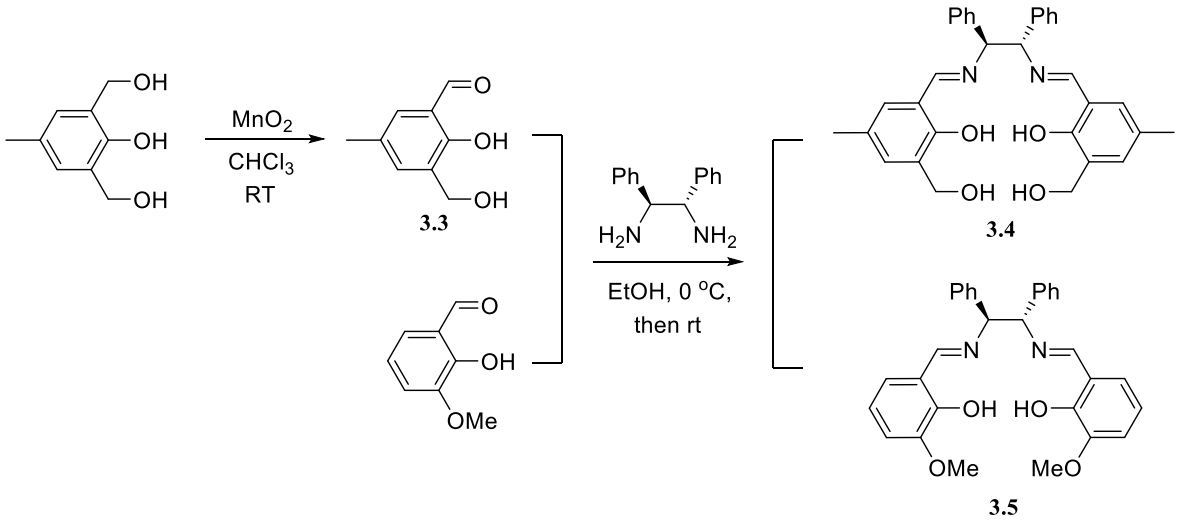

2. Other Monomers Used

Encouraged by the results of the stereocontrolled polymerization of acrylamides, we applied this new catalytic system to other functional olefins. Previously, the stereocontrolled ATRP of acrylates was unsuccessful[2]. No promising results were obtained. Therefore, methyl acrylate was chosen as a substrate to polymerize by using our new catalytic system. However, both the ligand **2.8** and **2.29** based catalytic system did not provide any observable polymerization of methyl acrylate (MA). The reaction in the

presence of ligand **2.8** and 5 mol% $Yb(OTf)_3$ or $Y(OTf)_3$ did not yield any polymer. Polymerization of methyl acrylate using ligand **2.29** was conducted under various reaction conditions, but no polymer formation was observed. **Table 3.1** lists the conditions studied using ligand **2.29**.

Table 3.1. Polymerization of methyl acrylate (MA) using ligand **2.29**

MeOH: MA (v/v) / Temperature (°C)	0: 1	0.5: 1	1: 1	1.5: 1
20	No reaction			
40				
50				

Solvent: MeOH. MA: 1 mmol, 90.1 μL. [MA]: [$Yb(OTf)_3$]: [CuBr]: [Initiator]: [Ligand] = 100: 5: 2: 2: 1. ATRP at 20℃, 24h. Conversion and isotacticity were measured by 600MHz ^{1}H NMR.

Polymerization of styrene was also examined in order to study the effect of the chirality of the ligands on a monomer without the carbonyl group of the acrylamides. Achiral macrocylic ligand **2.27** and chiral ligand **2.29** were used. Polymerizations in the absence and presence of $Yb(OTf)_3$ were performed to compare the influence of the metal triflate on the polymerization of styrene and the results are listed in **Table 3.1**. At room temperature, only the experiment in the presence of ligand **2.27** and without $Yb(OTf)_3$ produced polymer with very low yield, and the polymer was atactic. It might be because the reaction temperature was too low for styrene polymerization. Further studies are still going on.

Table 3.2. Polymerization of styrene under different conditions

	With $Yb(OTf)_3$	Without $Yb(OTf)_3$
Ligand **2.27**	No reaction	13% conversion, atactic polymer
Ligand **2.29**	No reaction	No reaction

Bulk polymerization. Styrene: 2 mmol, 228.8 μL. [Styrene]: [$Yb(OTf)_3$]: [CuBr]: [Initiator]: [Ligand] = 100: 5: 2: 2: 1. ATRP at 20℃, 24h. Conversion and isotacticity were measured by 600MHz ^{1}H NMR.

Experimental and Characterization

1. Analytical Instruments

NMR: Bruker 600 MHz.

2. General Data

All commercial chemicals were used without further purification unless otherwise noted. Methanol was dried over molecular sieve and distilled. Styrene and methyl acrylate were dried over molecular sieve and distilled.

3. General Procedures and Characterization

3.1 Synthesis of Acyclic Schiff Base Compounds

a. Synthesis of 2-hydroxy-3-(hydroxymethyl)-5-methylbenzaldehyde, 3.3[3]

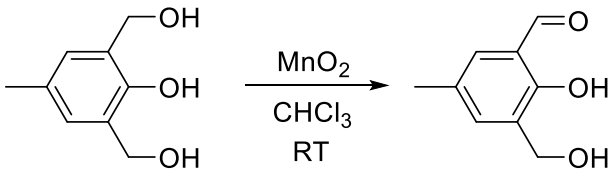

3.3

Manganese (IV) oxide (5.0 g, 58 mmol) and 50 mL chloroform were added into a 250 mL round bottom flask. Then 2,6-Bis(hydroxymethyl)-*p*-cresol (1.5 g, 9 mmol) was added. The reaction was stirred at room temperature for 24 h. Then the mixture was filtered using vacuum filtration then washed by chloroform for three times. The filtrated solution was concentrated and purified by column chromatography on silica gel (hexane: ethyl acetate = 5: 1) to afford the desired product (0.75 g, yield: 50%). ^{1}H NMR (600 MHz, Chloroform-*d*) δ 11.16 (s, 1H), 9.85 (s, 1H), 7.39 (s, 1H), 7.28 (s, 1H), 4.72 (d, *J* = 6.4 Hz, 2H), 2.33 (s, 3H).

b. Synthesis of Acyclic Schiff Base Ligand 3.4

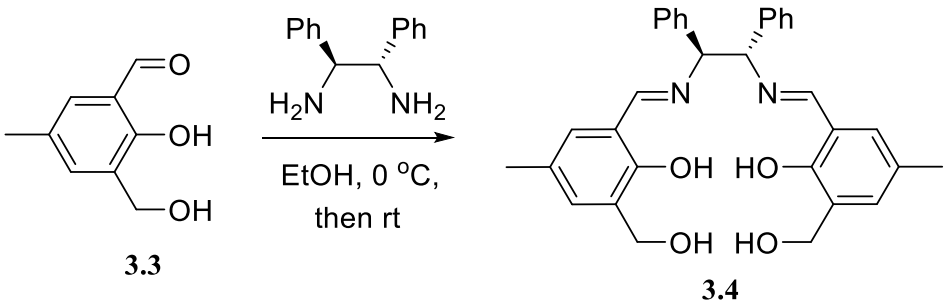

3.3 **3.4**

To an ethanol solution (50 mL) of **3.3** (66.4 mg, 0.4 mmol, 2 equiv) at 0 °C, (1*S*,2*S*)-1,2-diphenylethane-1,2-diamine (42.4 mg, 0.2 mmol, 1 equiv) in ethanol (10 mL) was added dropwise to the aldehyde solution at 0℃. The reaction was stirred at 0℃ for 4 h and then at room temperature for 18 h. Yellow precipitate was generated and was separated by centrifugation. The wet product was dried under reduce pressure to afford the desired product. (71.2 mg, yield: 70%). ^{1}H NMR (600 MHz, DMSO-d_6) δ 13.35 (s, 2H), 8.46 (s, 2H), 7.29 – 7.26 (m, 4H), 7.23 – 7.18 (m, 7H), 7.15 – 7.11 (m, 2H), 6.95 (s, 2H), 5.03 (s, 2H), 4.97 (t, *J* = 5.6 Hz, 2H), 4.47 (d, *J* = 5.5 Hz, 4H), 2.16 (s, 6H).

c. Synthesis of Acyclic Schiff Base Ligand 3.5

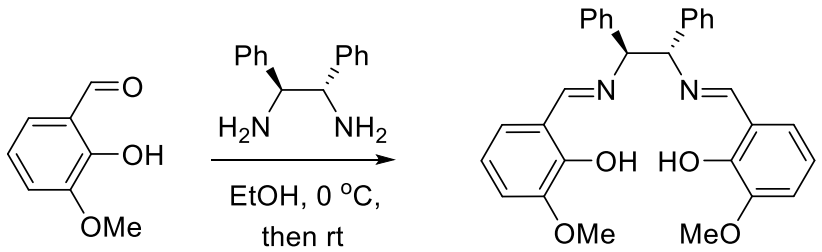

3.5

To an ethanol solution (50 mL) of 2-hydroxy-3-methoxy-5-methylbenzaldehyde (60.8 mg, 0.4 mmol, 2 equiv) at 0 °C, (1*S*,2*S*)-1,2-diphenylethane-1,2-diamine (42.4 mg, 0.2 mmol, 1 equiv) in ethanol (10 mL) was added dropwise. The reaction was stirred at 0℃ for 4 h

and then under room temperature for 18 h. Yellow precipitate was generated and was separated by centrifugation. The wet product was dried under reduce pressure to afford the desired product (72 mg, yield: 75%). ^{1}H NMR (600 MHz, DMSO-d_6) δ 13.46 (s, 2H), 8.48 (s, 2H), 7.28 (m, 3H), 7.22 (m, 2H), 7.15 (m, 1H), 6.98 (m, 1H), 6.87 (m, 1H), 6.74 (m, 1H), 5.06 (s, 2H), 3.74 (s, 6H).

3.2 ATRP of DMAA using Scheme 3.1

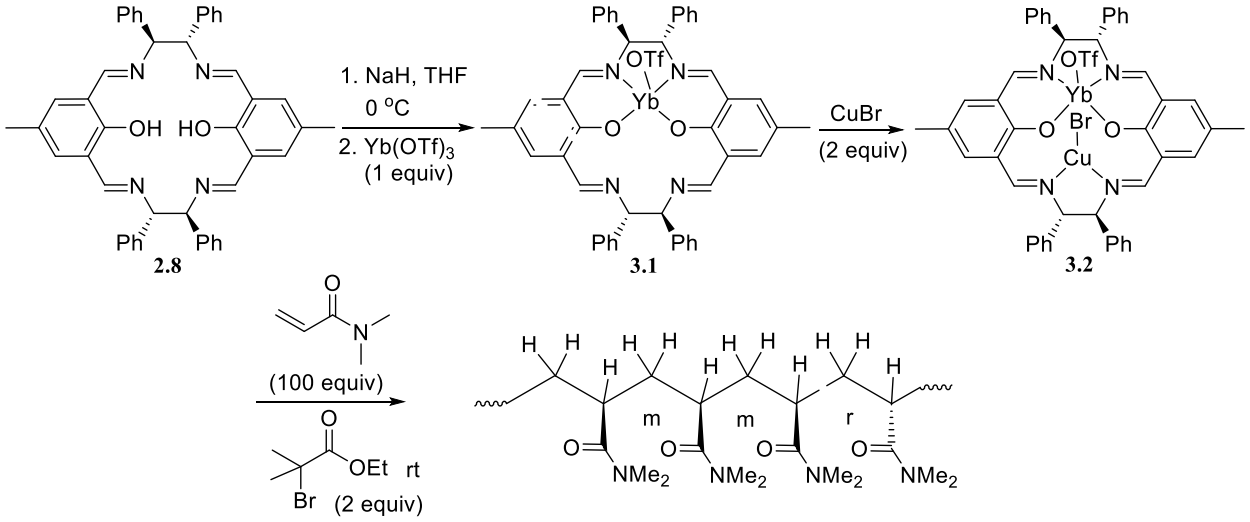

Ligand **2.8** (6.8 mg, 0.01 mmol, 1 equiv) was first treated with NaH (0.5 mg, 0.02 mmol, 2 equiv) in 154μL THF at 0 °C and then reacted with $Yb(OTf)_3$ (6.2 mg, 0.01 mmol, 1 equiv) to prepare a macrocyclic Yb complex **3.1**. CuBr (2.9 mg, 0.02 mmol, 2 equiv) was added to **3.1** to prepare the bimetallic complex **3.2**. DMAA (103 mg, 1 mmol, 100 equiv) was added to the complex **3.2** THF solution followed by adding ethyl 2-bromoisobutyrate (3.9 mg 0.02 mmol, 2 equiv). The polymerization was completed in 4 h with 98% conversion as monitored by ^{1}H NMR analysis. Polymer was purified by dissolving in a minimum amount of MeOH and then precipitating with excess diethyl ether for three time. Tacticity was then determined by ^{1}H NMR.

3.3 ATRP of Methyl Acrylate (Example)

Methyl acrylate (90.1 μL, 86.1 mg, 1.0 mmol), methanol (135 μL) and $Yb(OTf)_3$ (31 mg, 0.05 mmol) were added to a Schlenk flask and stirred for 0.5 h. Then ligand **2.29** (6.8 mg, 0.01mmol) was added to the flask and stirred for another 0.5 h. After that, ethyl 2-bromoisobutyrate (3.0 μL, 3.9 mg, 0.02 mmol) was added and the reaction mixture underwent three freeze-pump-thaw cycles for degassing. After the mixture returned to room temperature, CuBr (2.9 mg, 0.02 mmol) was added and the reaction was conducted in dry box for 24 h. After that, a small amount of mixture was used for ^1H NMR analysis to determine the tacticity and conversion.

3.4 ATRP of Styrene (Example)

Styrene (228.8 μL, 208.2 mg, 2.0 mmol) and $Yb(OTf)_3$ (31 mg, 0.05 mmol) were added to a Schlenk flask and stirred for 0.5 h. Then ligand **2.29** (6.8 mg, 0.01 mmol) was added to the flask and stirred for another 0.5 h. After that, ethyl 2-bromoisobutyrate (3.0 μL, 3.9 mg, 0.02 mmol) was added and the reaction mixture underwent three freeze-pump-thaw cycles for degassing. After the mixture returned to room temperature, CuBr (2.9 mg, 0.02 mmol) were added and the reaction was conducted in dry box for 24 hours. After that, a small amount of mixture was used for ^1H NMR analysis to determine the tacticity and conversion.

Reference

(1) Bi, W.-Y.; Lü, X.-Q.; Chai, W.-L.; Song, J.-R.; Wong, W.-Y.; Wong, W.-K.; Jones, R. A. *J. Mol. Struct.* **2008**, *891* (1-3), 450–455.

(2) Lutz, J. F.; Jakubowski, W.; Matyjaszewski, K. *Macromol. Rapid Commun.* **2004**, *25*, 486–492.

(3) Chandrasekhar, V.; Das, S.; Dey, A.; Hossain, S.; Kundu, S.; Colacio, E. *Eur. J. Inorg. Chem.* **2013**, No. 2, 397–406.

Appendix

^{1}H NMR

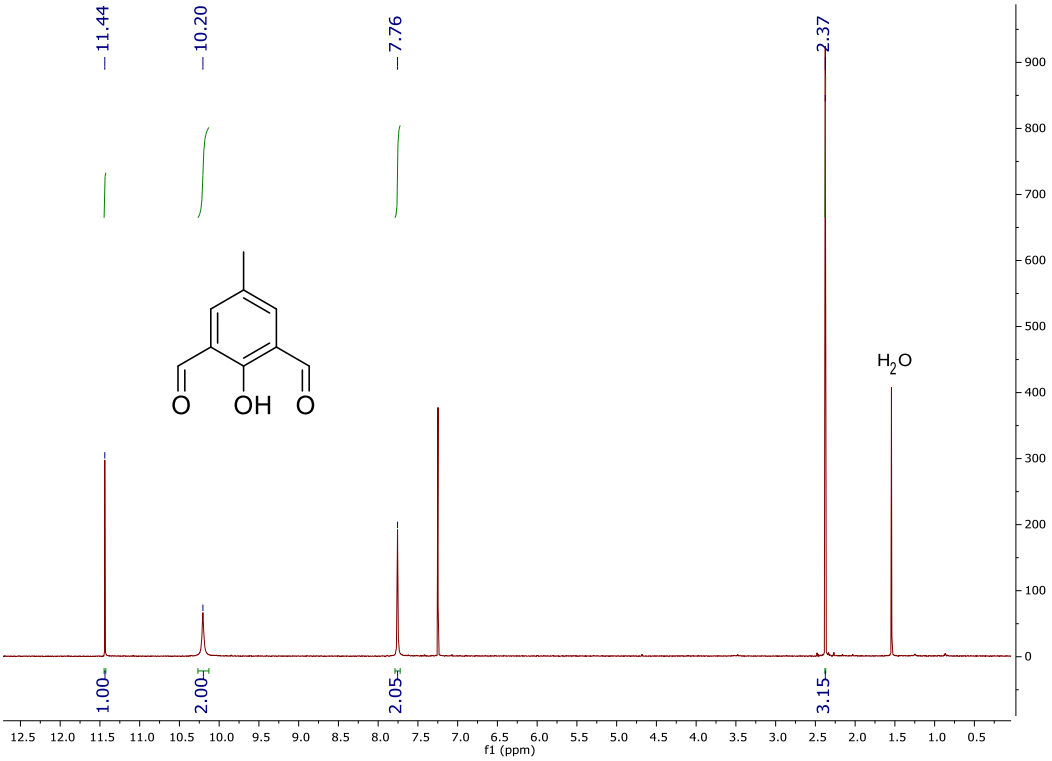
11.44
10.20
7.76
2.37
H2O
O
OH
O
1.00
2.00
2.05
3.15
f1 (ppm)

^{1}H NMR

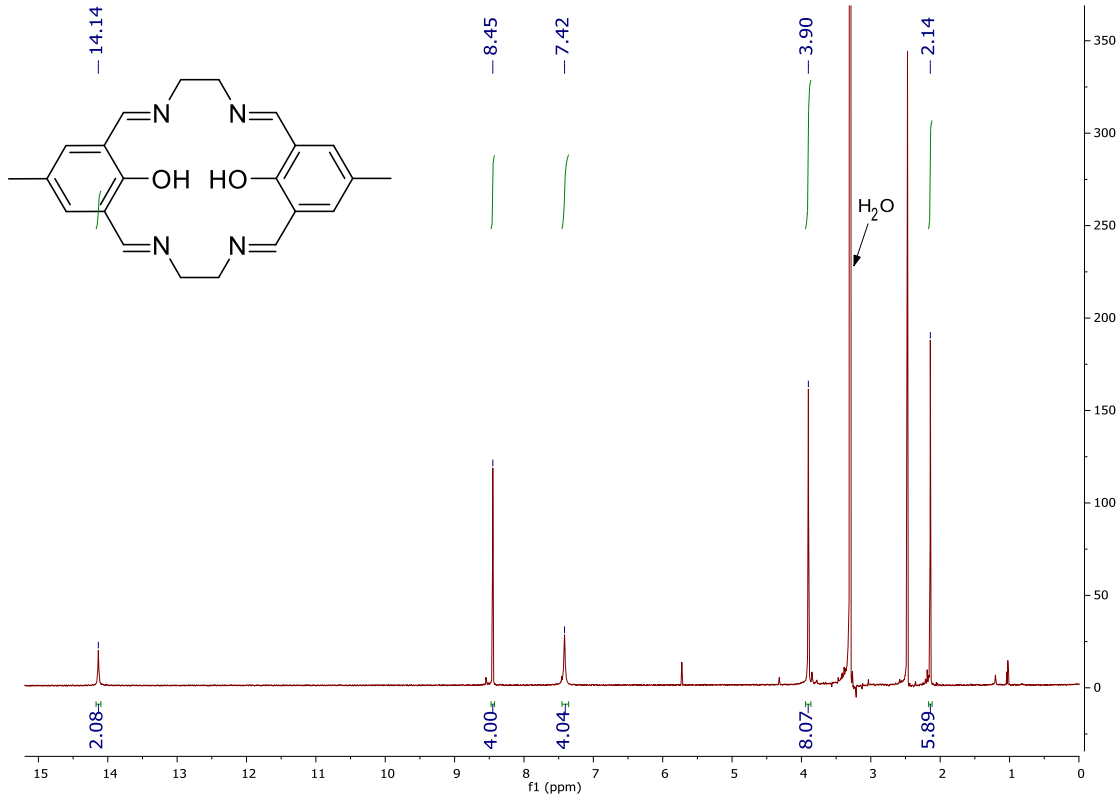
14.14
8.45
7.42
3.90
2.14
N
N
OH
HO
N
N
H2O
2.08
4.00
4.04
8.07
5.89
f1 (ppm)

^{1}H NMR

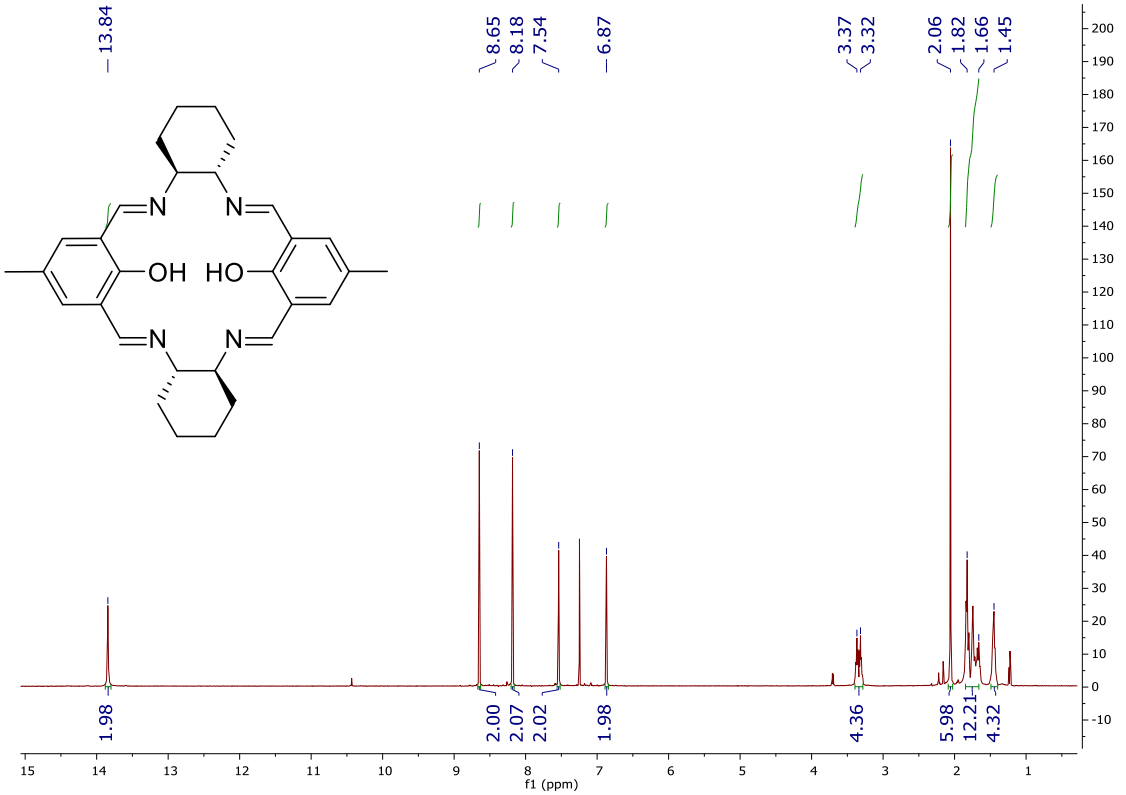

^{13}C NMR

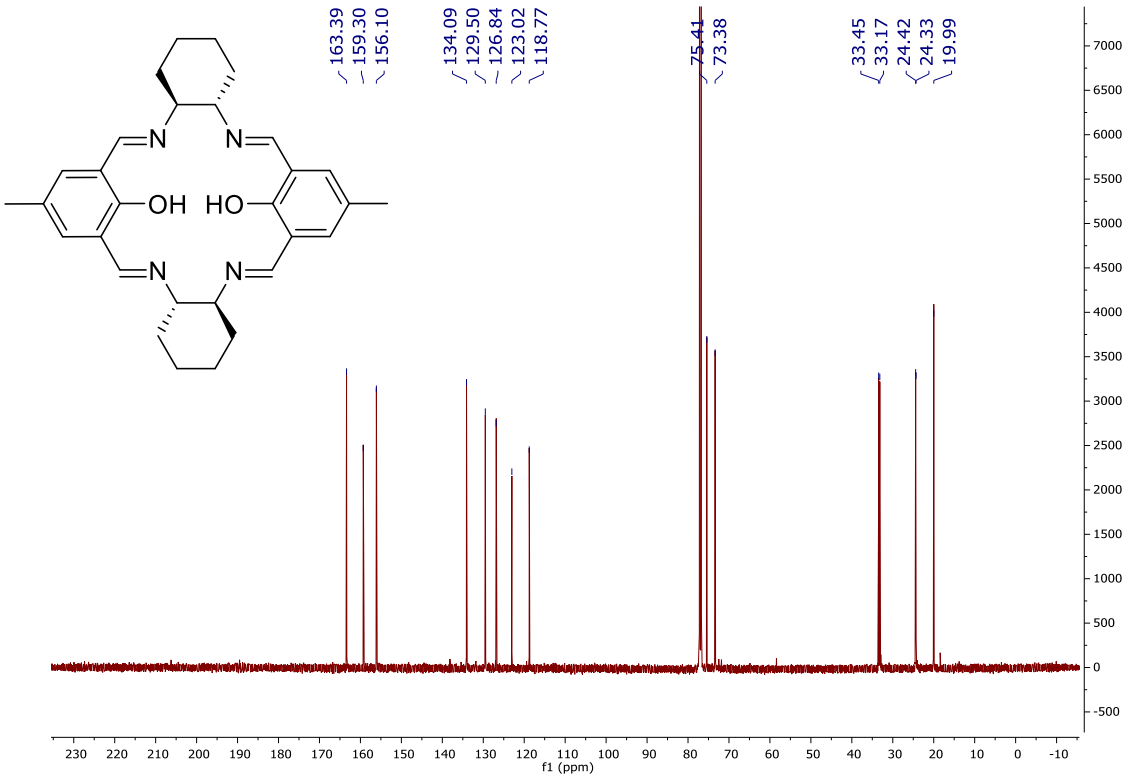

^{1}H NMR

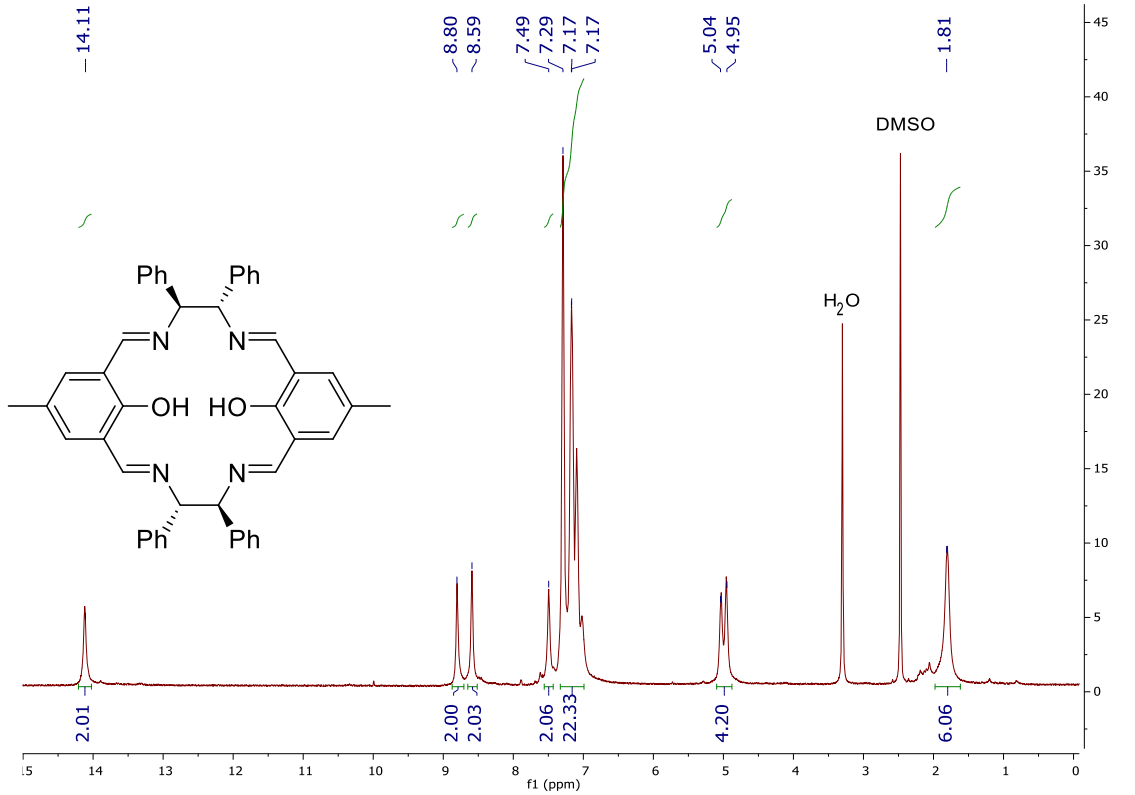

^{13}C NMR

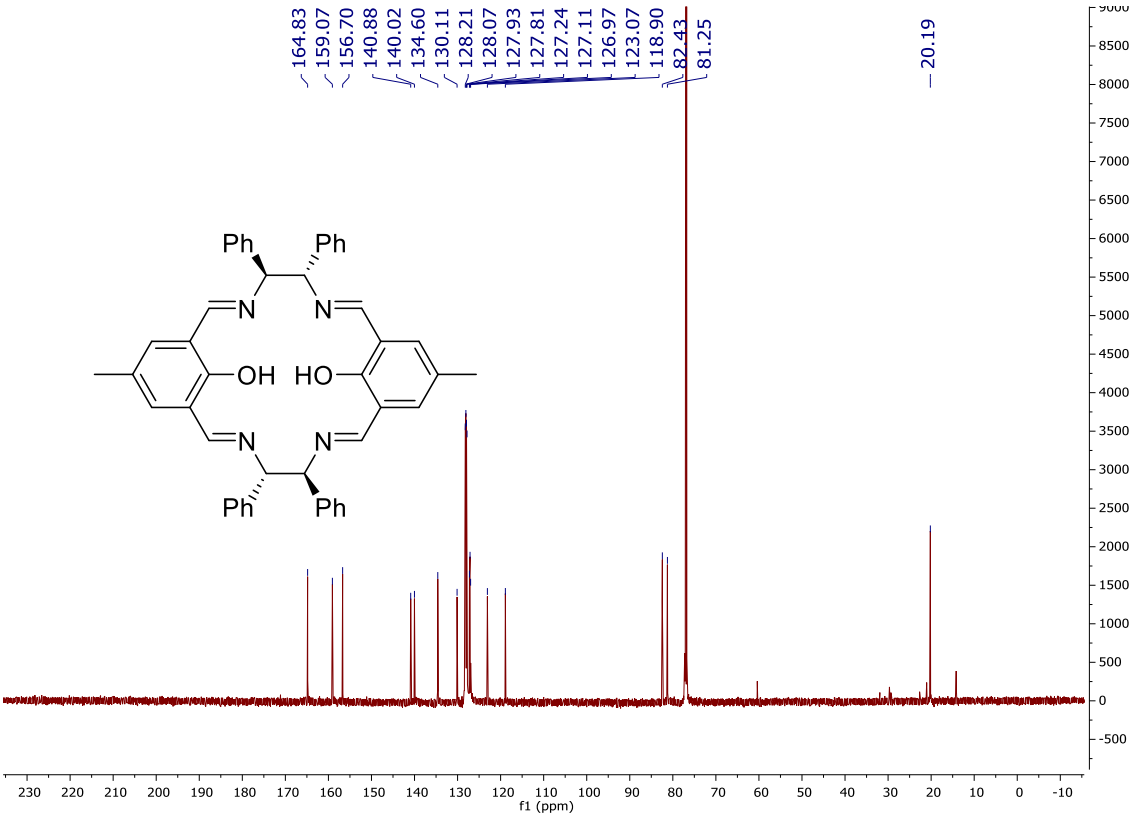

^{1}H NMR

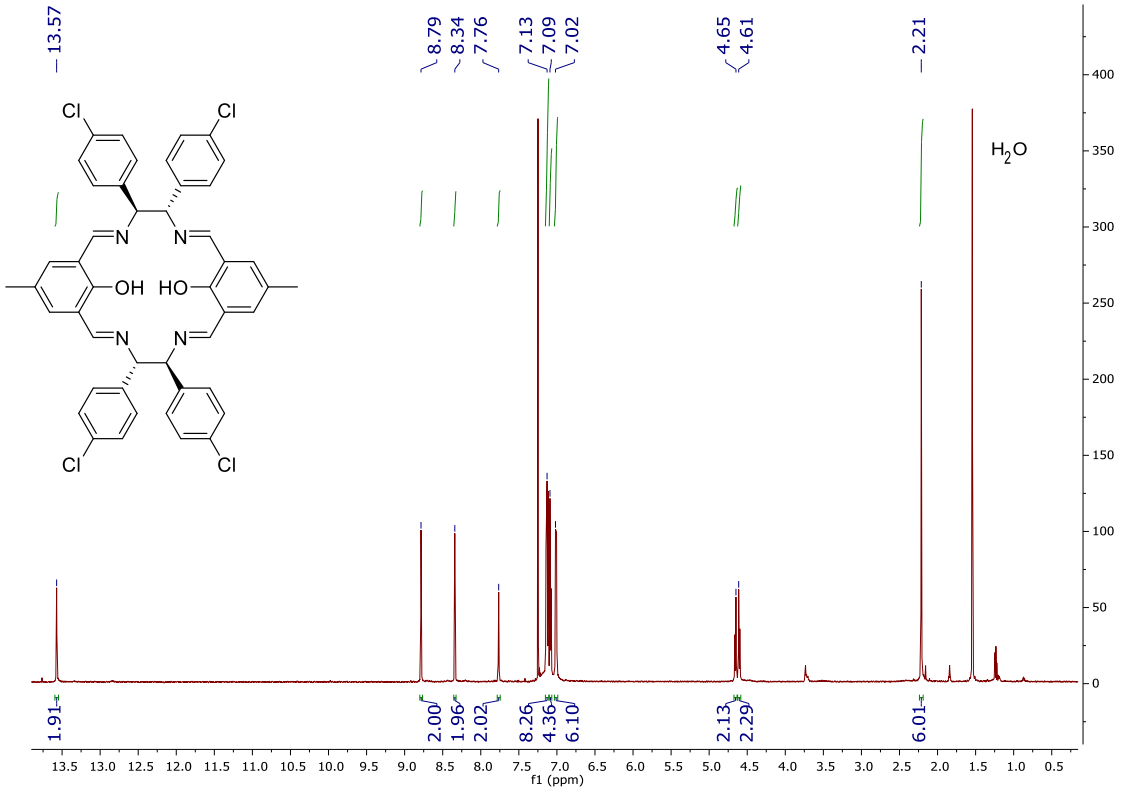

^{13}C NMR

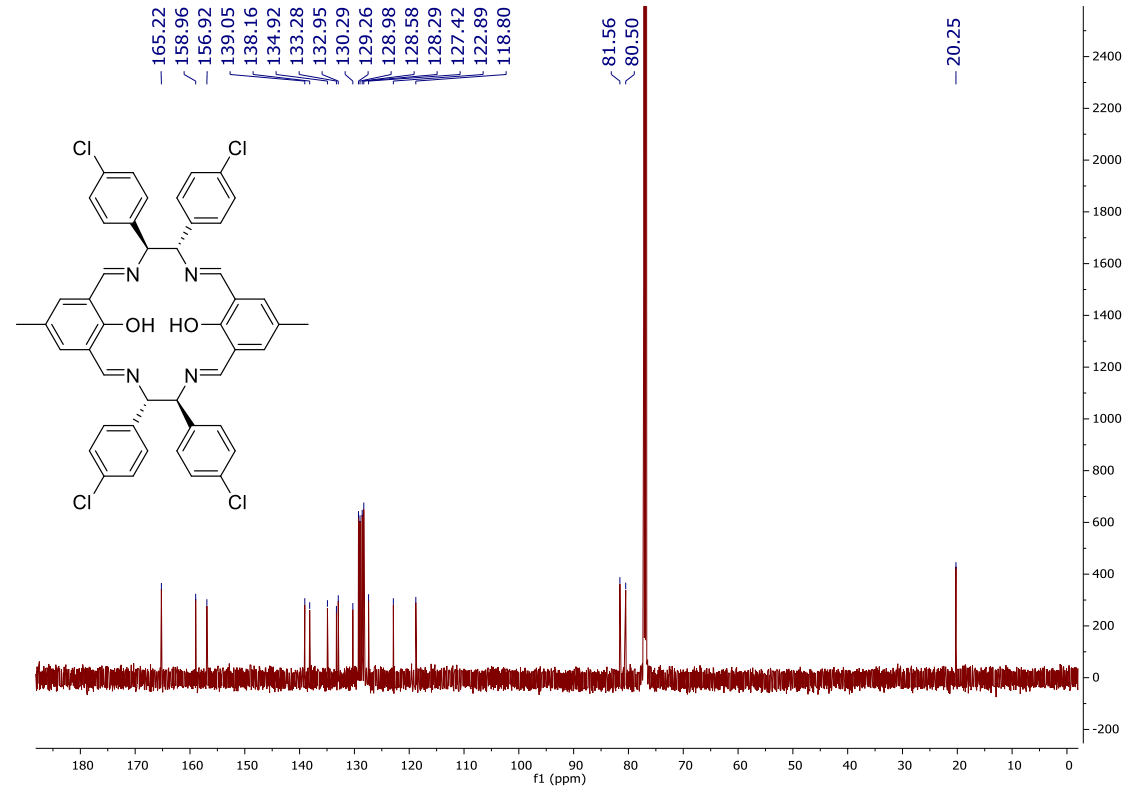

^{1}H NMR

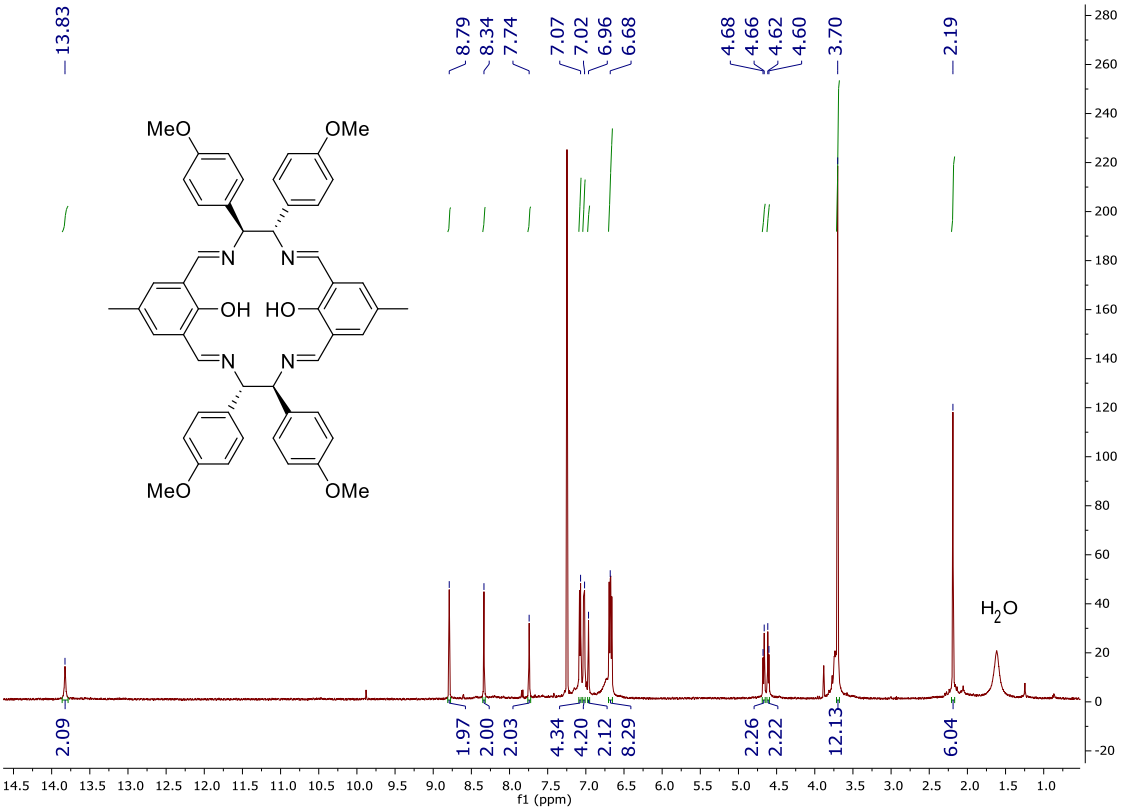

^{13}C NMR

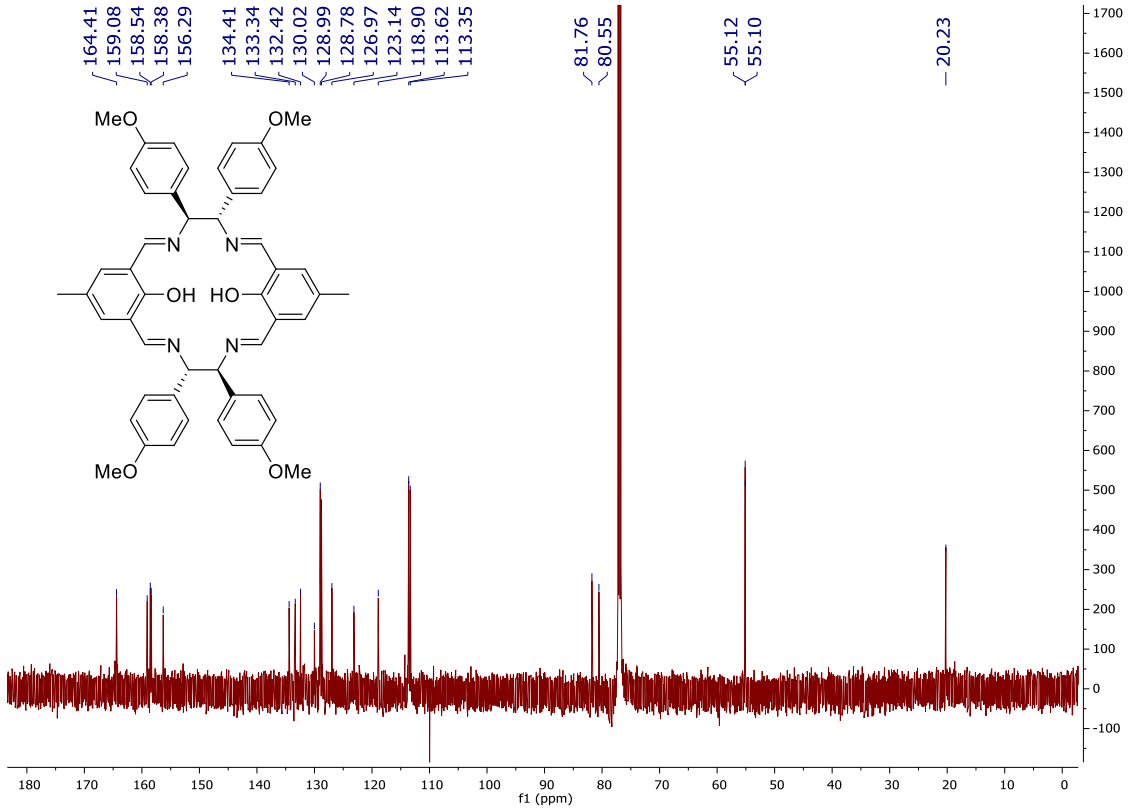

^{1}H NMR

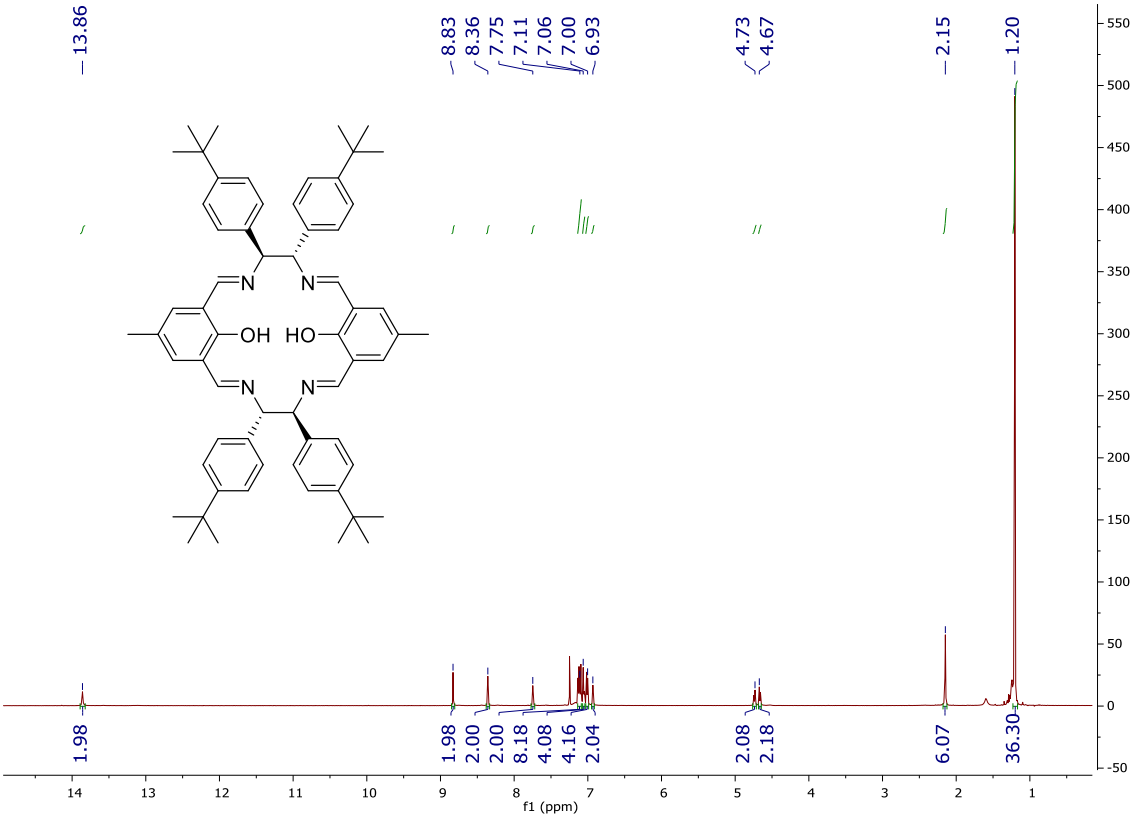

^{13}C NMR

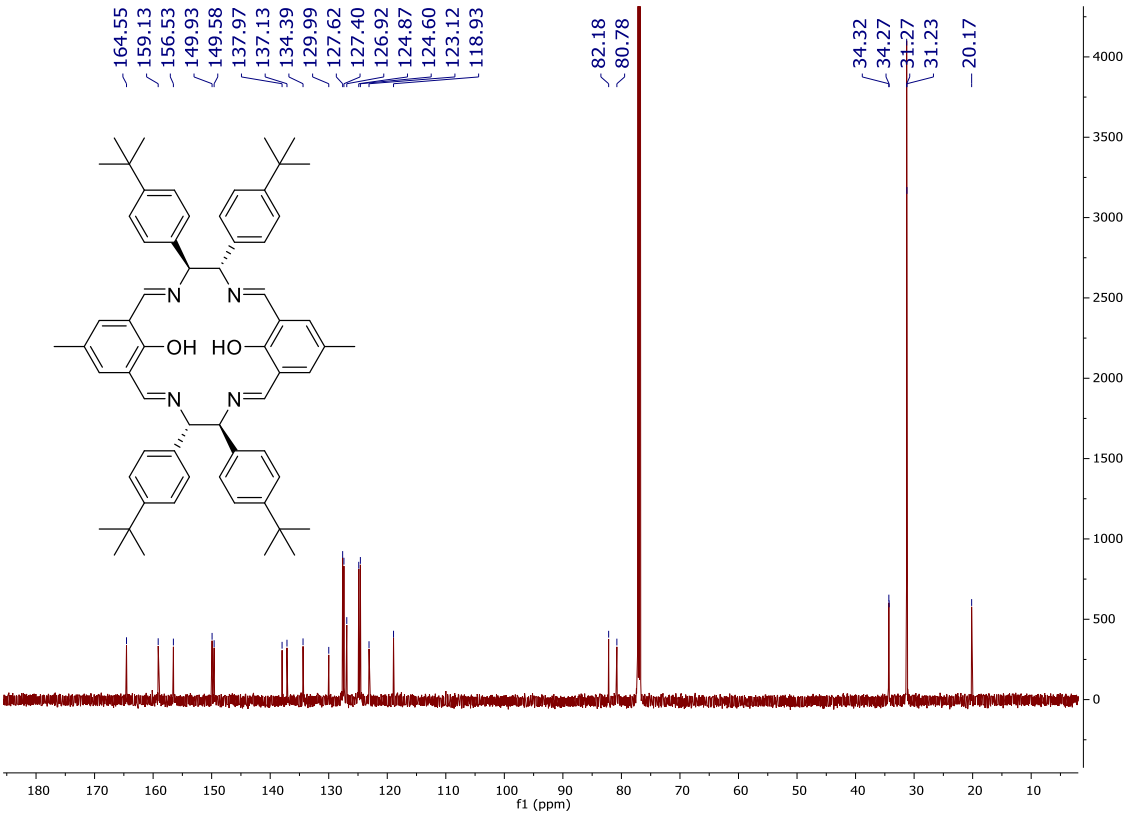

^{1}H NMR

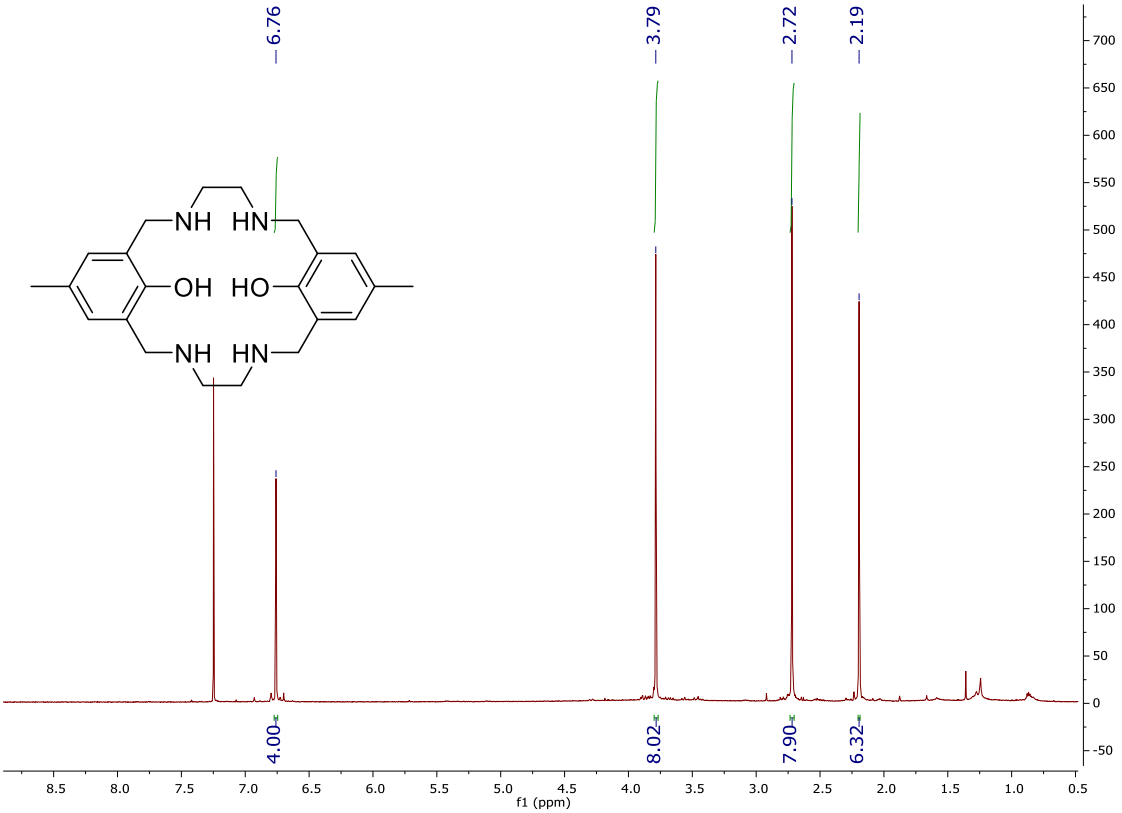

^{13}C NMR

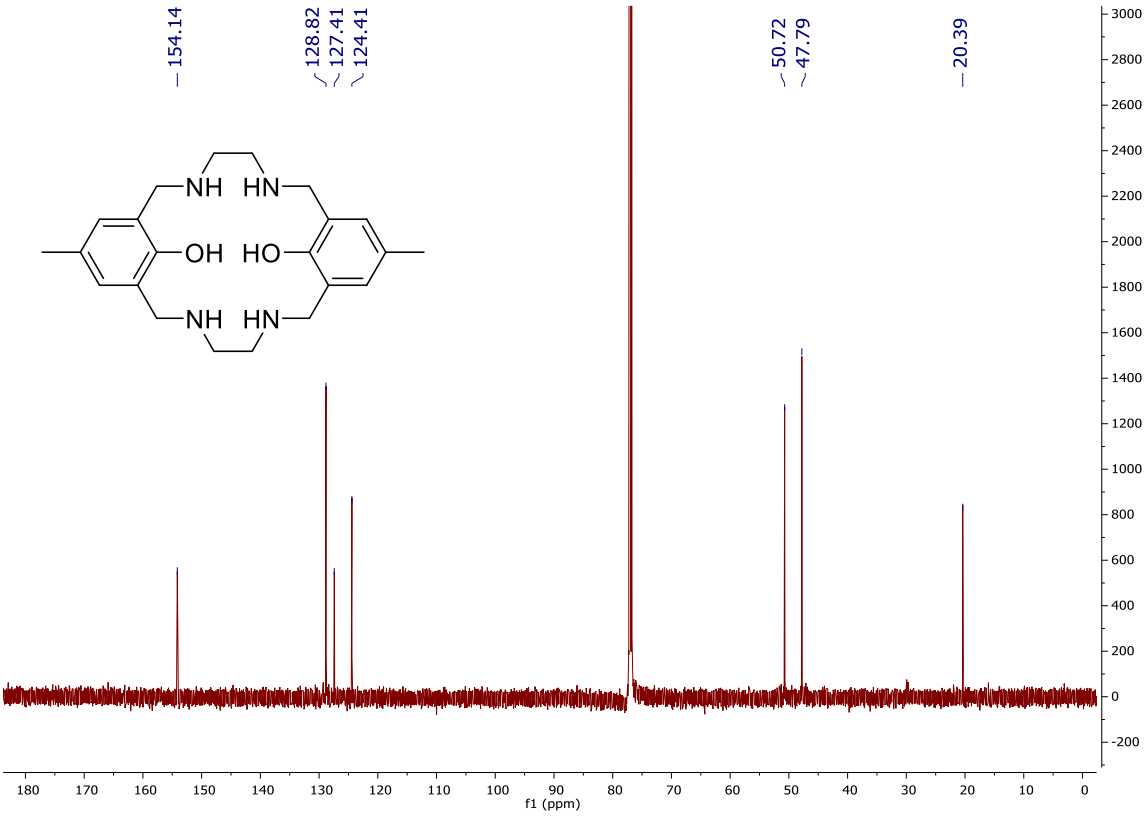

^{1}H NMR

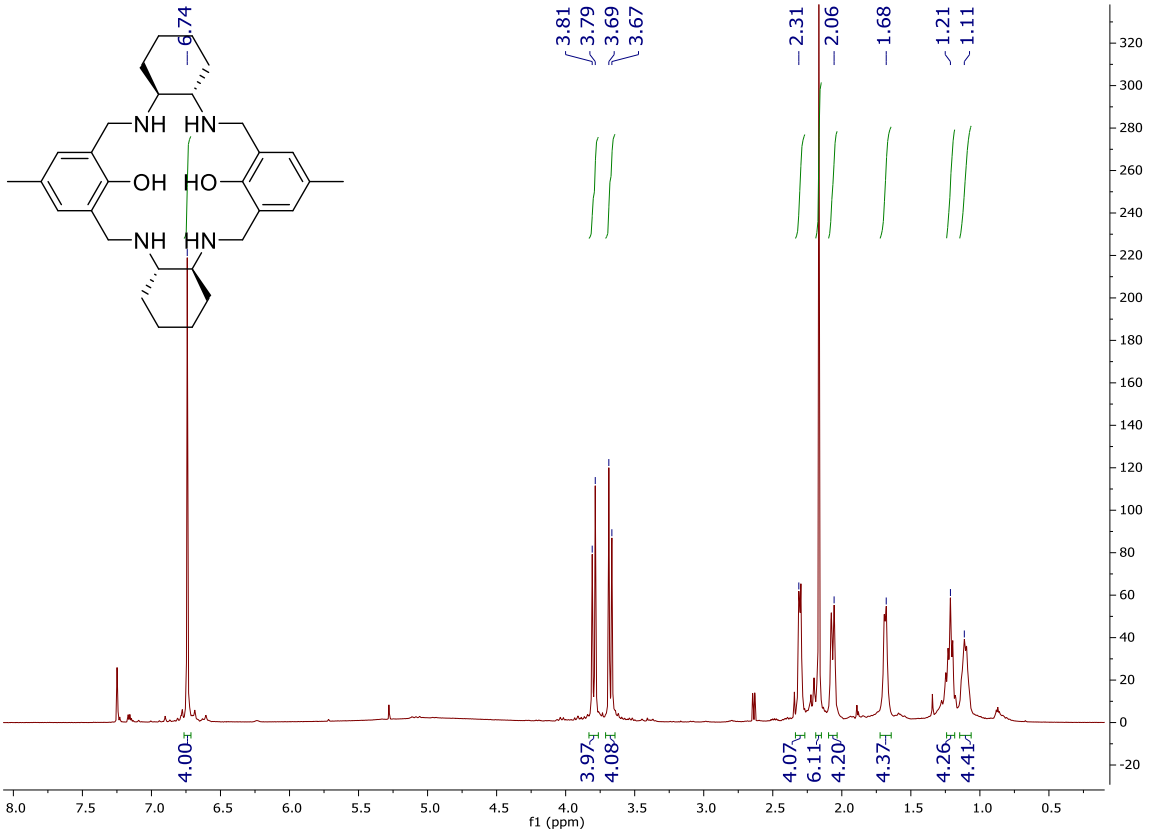

^{13}C NMR

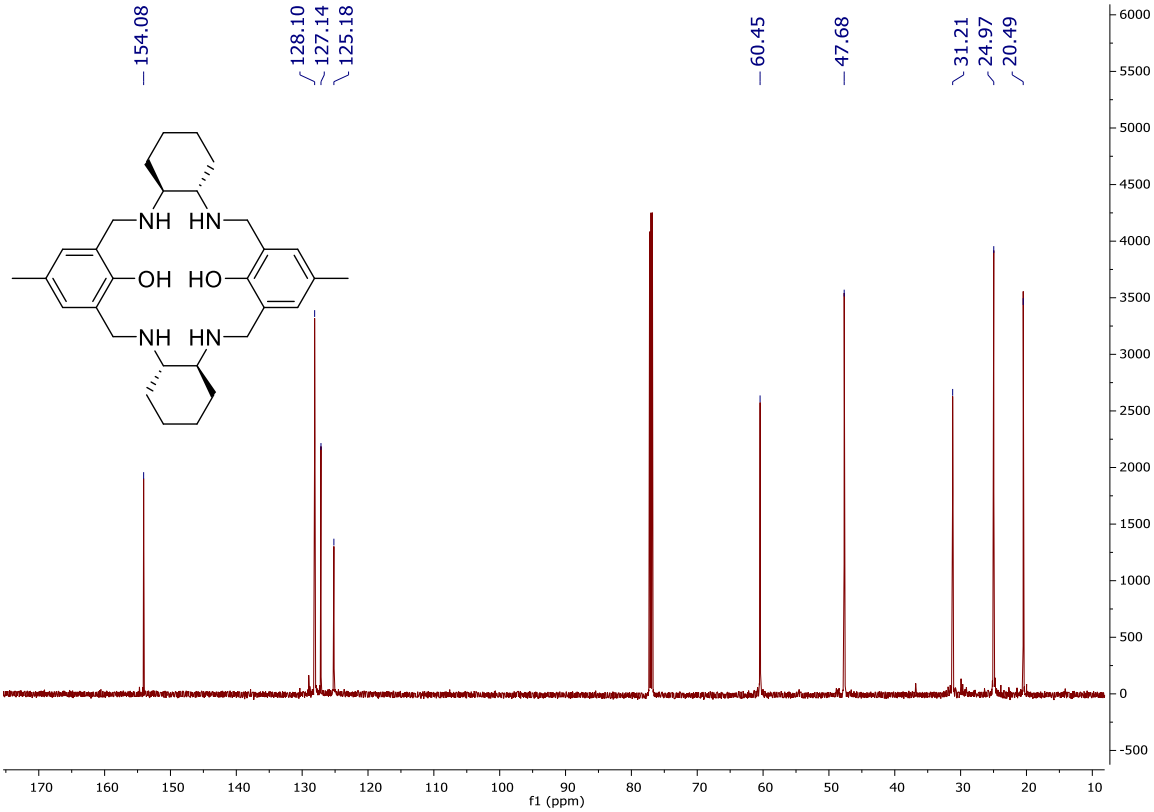

^{1}H NMR

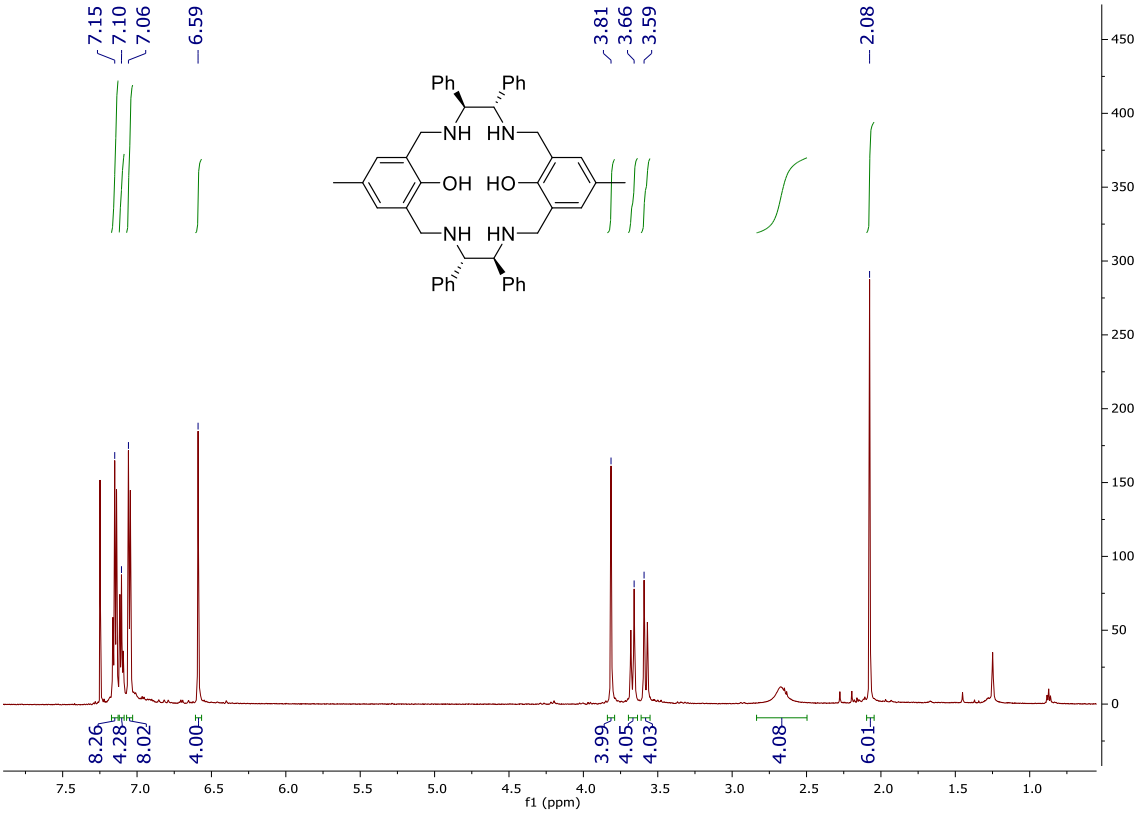

^{13}C NMR

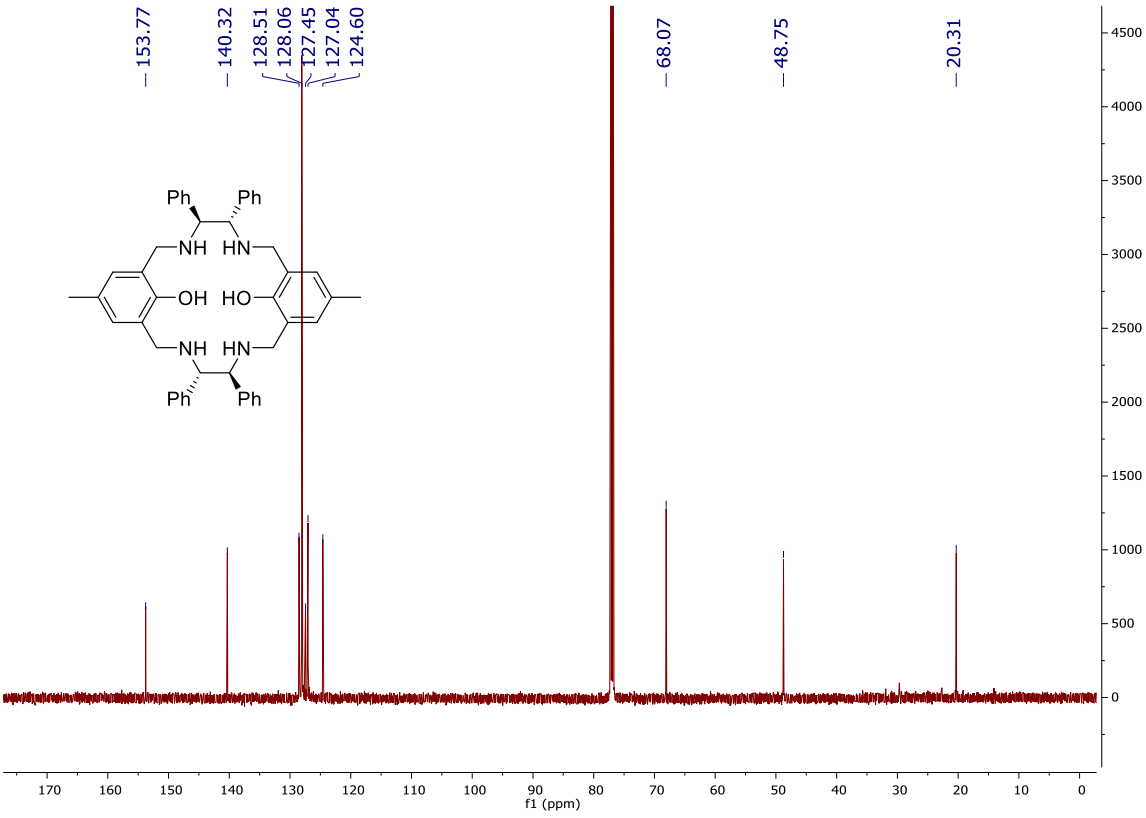

^{1}H NMR

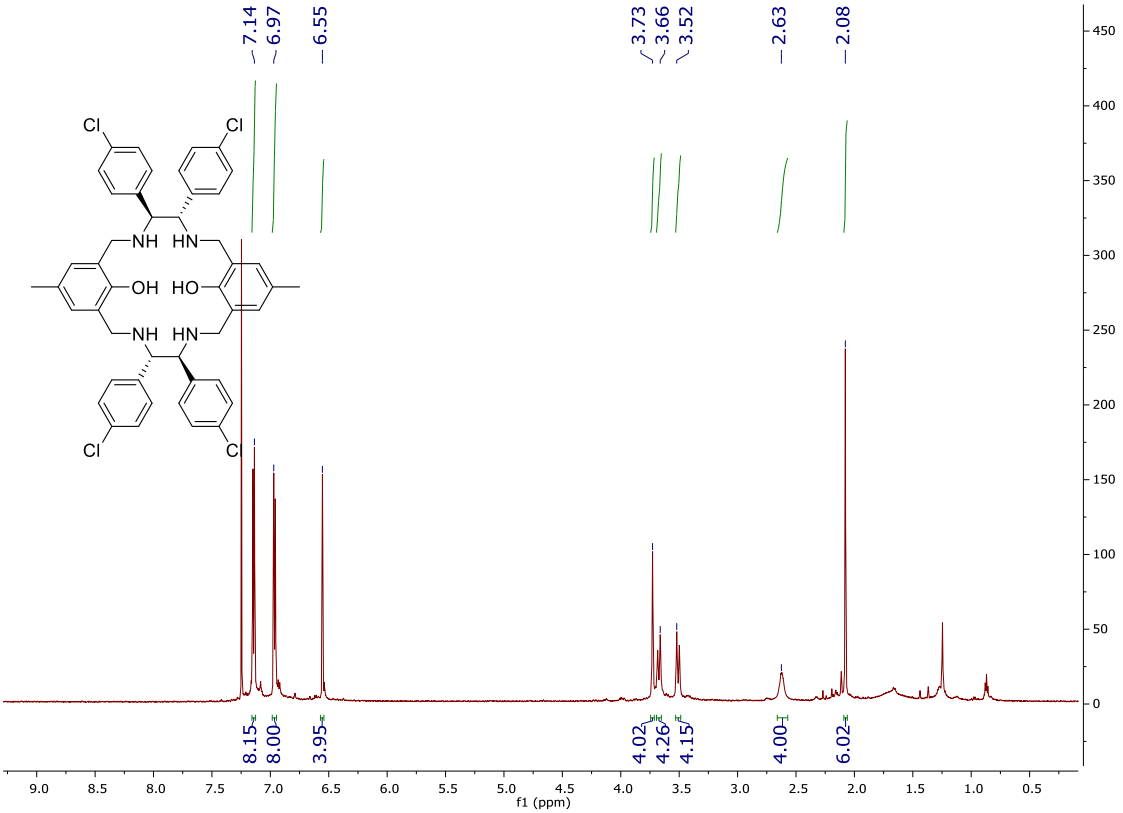

^{13}C NMR

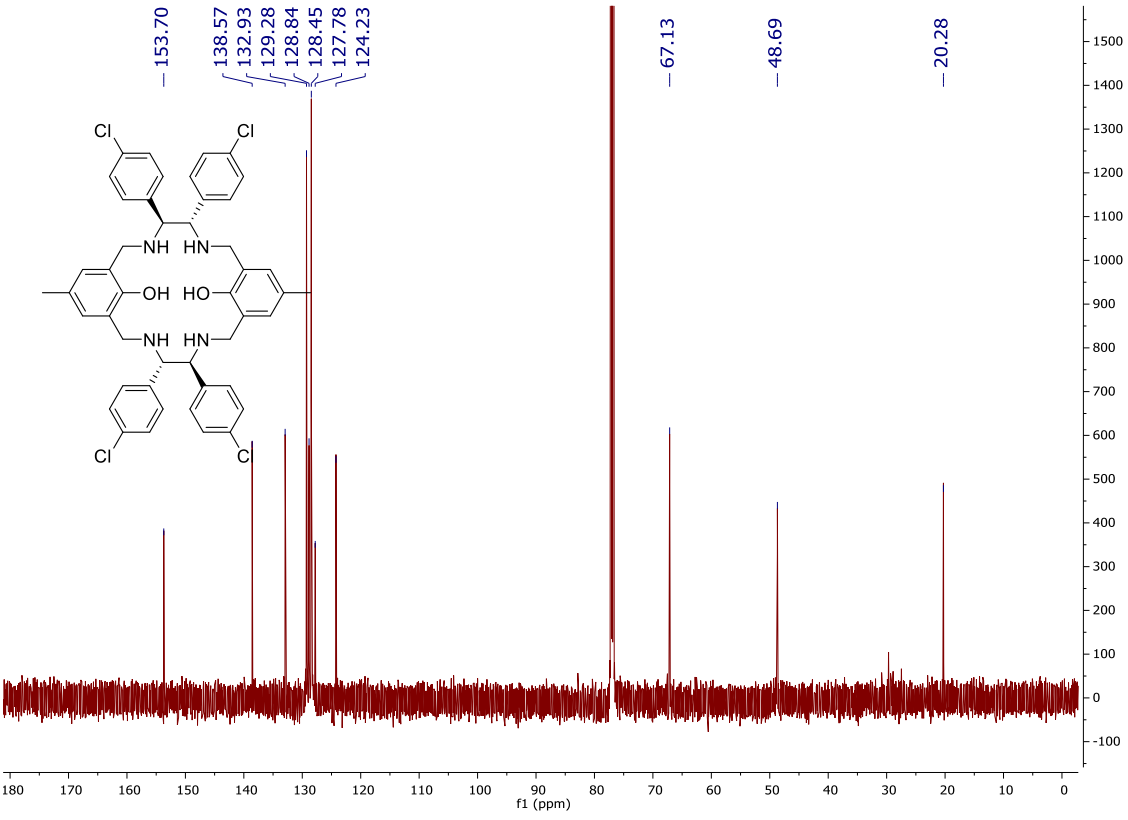

^{1}H NMR

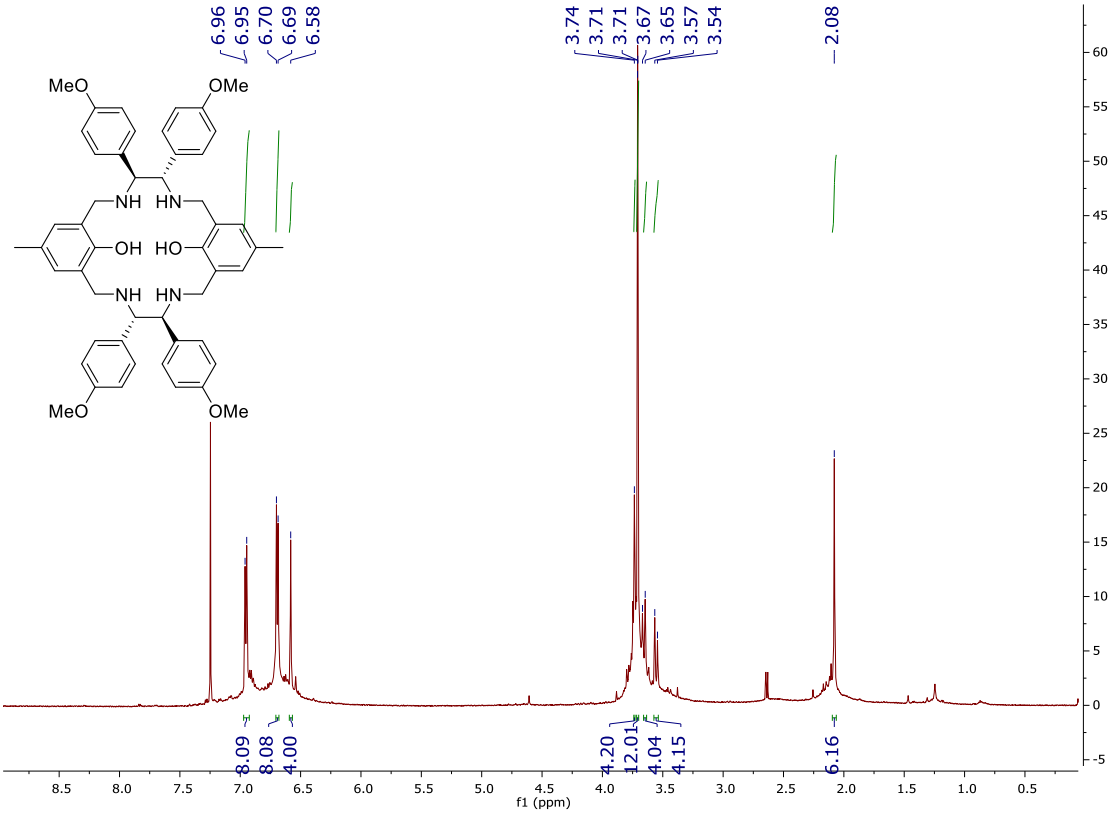

^{13}C NMR

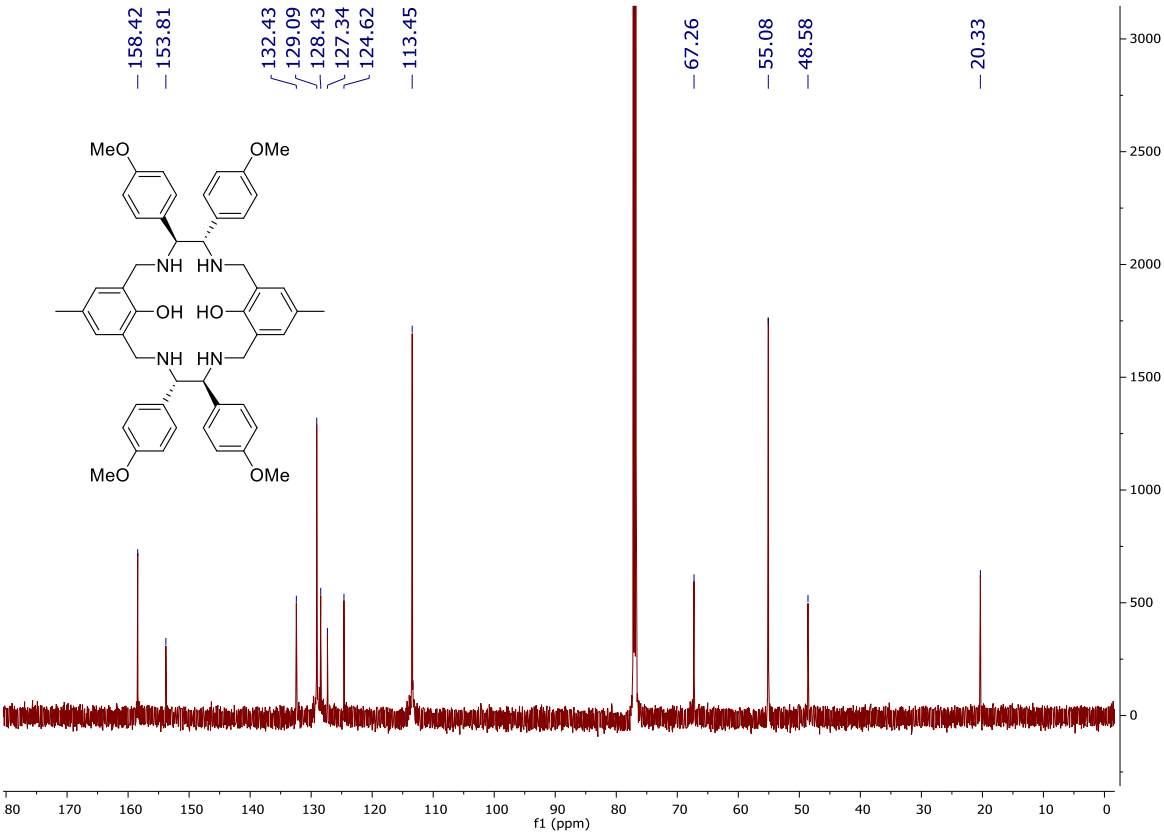

^{1}H NMR

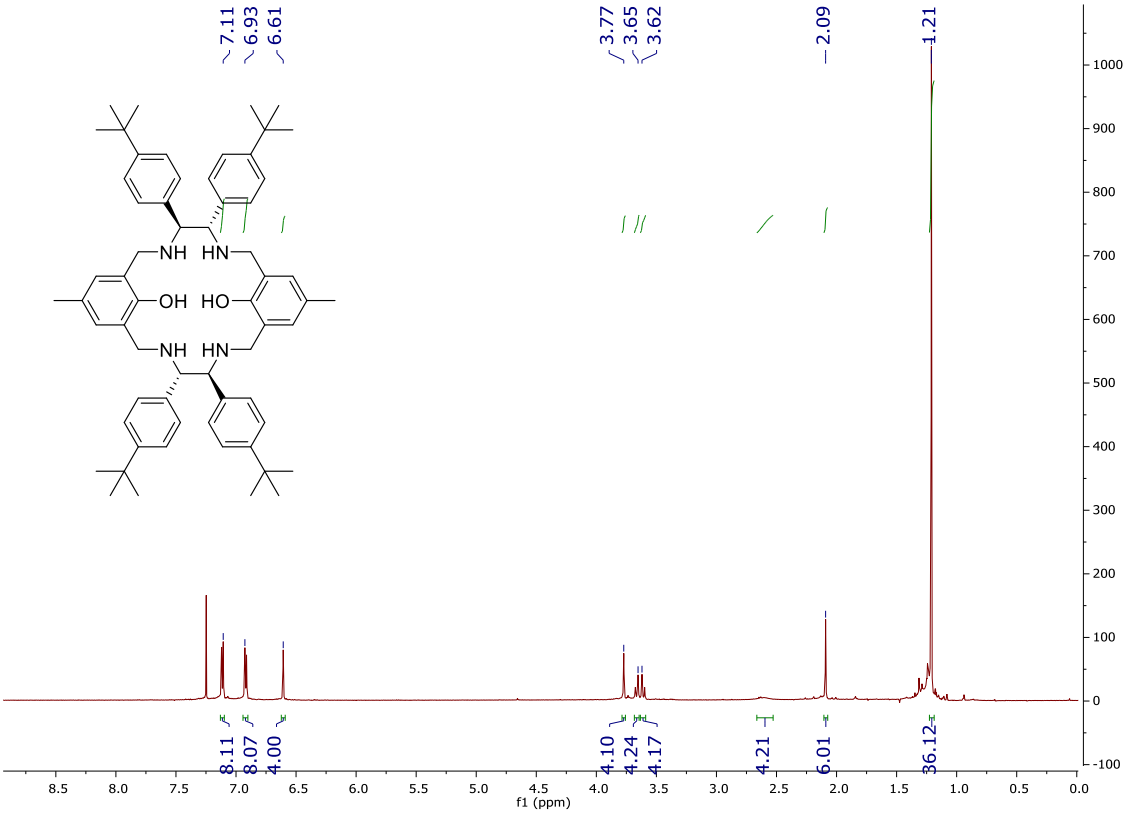

^{13}C NMR

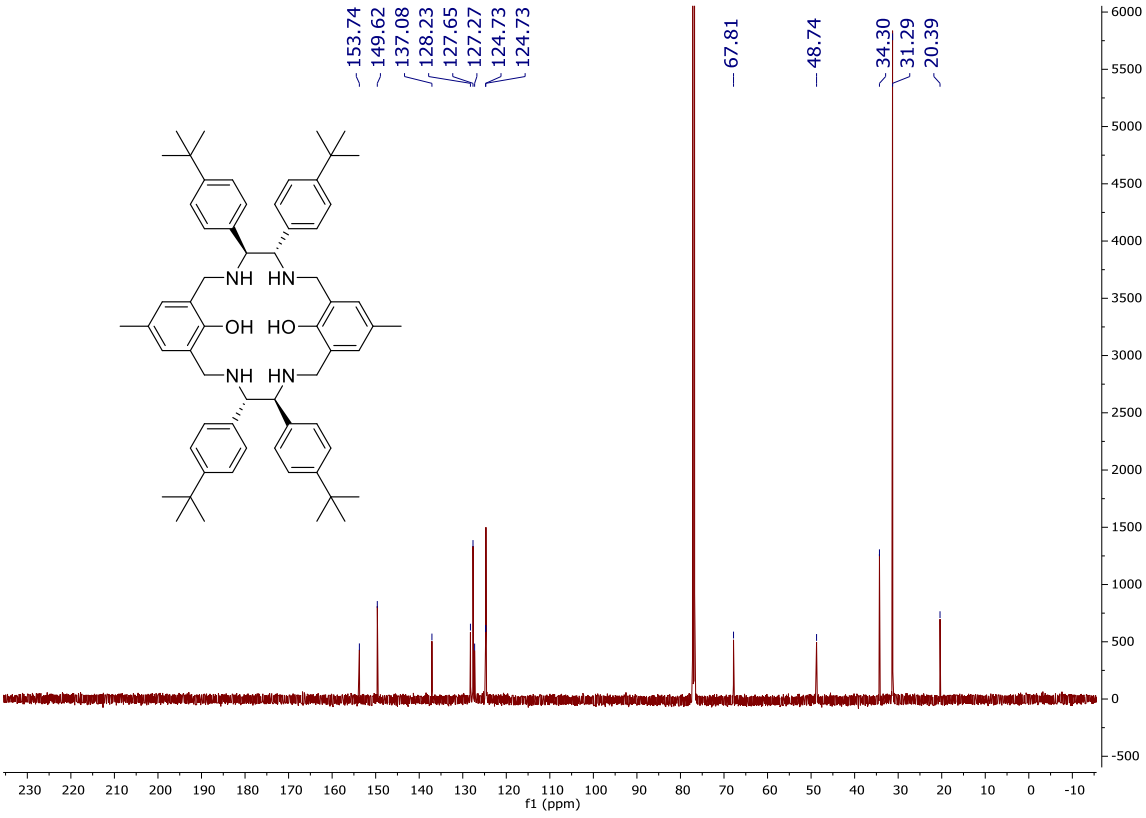

^{1}H NMR

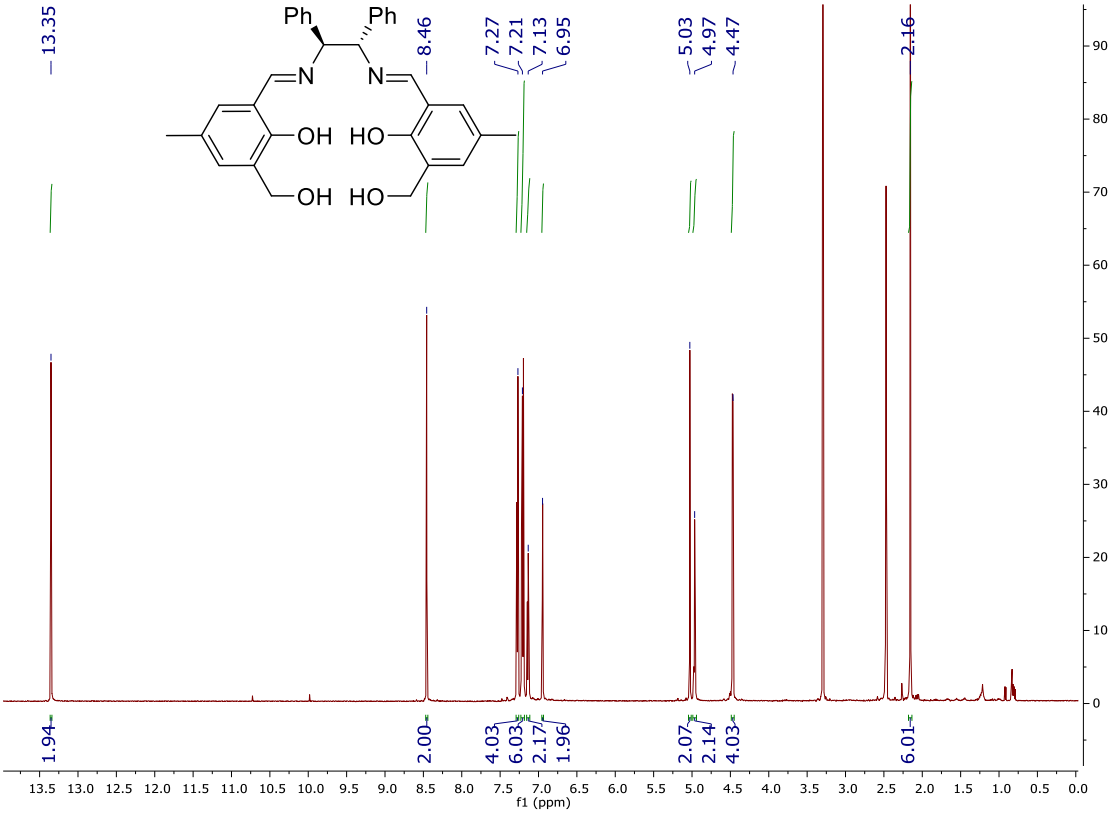
13.35
8.46
7.27
7.21
7.13
6.95
5.03
4.97
4.47
2.16
Ph
Ph
N
N
OH
HO
OH
HO
1.94
2.00
4.03
6.03
2.17
1.96
2.07
2.14
4.03
6.01
f1 (ppm)

^{1}H NMR

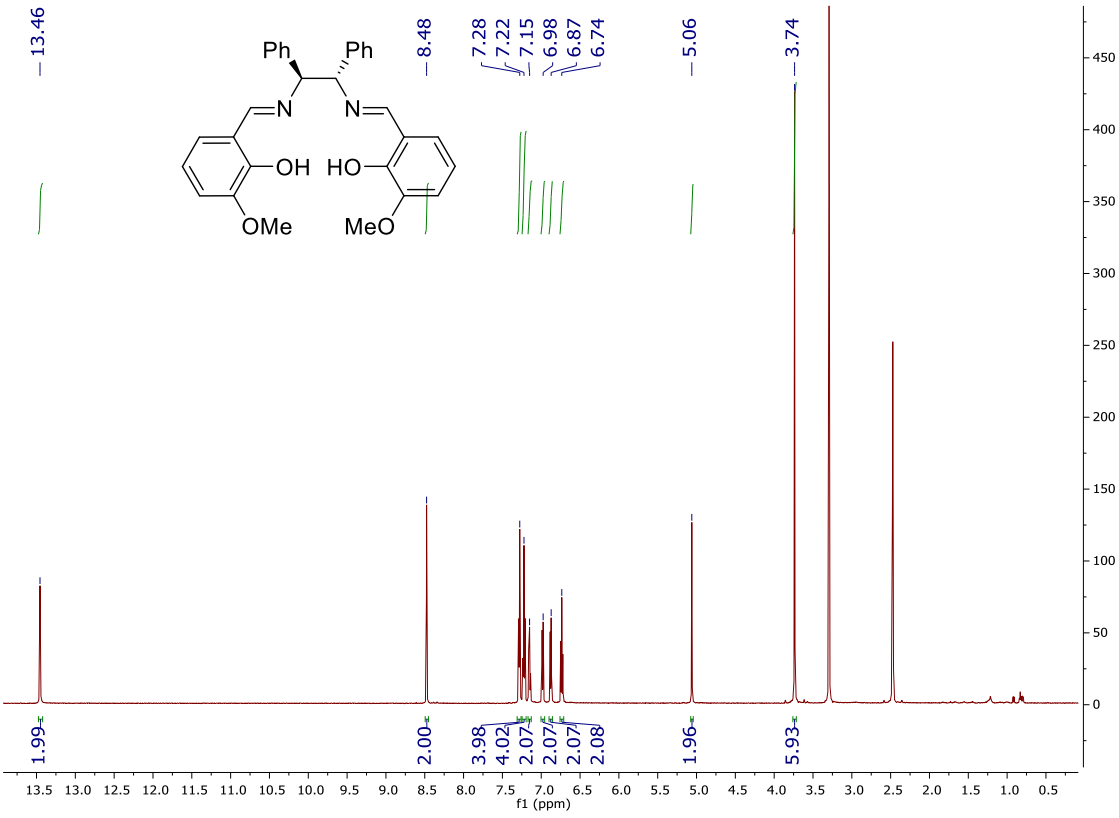
13.46
8.48
7.28
7.22
7.15
6.98
6.87
6.74
5.06
3.74
Ph
Ph
N
N
OH
HO
OMe
MeO
1.99
2.00
3.98
4.02
2.07
2.07
2.07
2.08
1.96
5.93
f1 (ppm)

^{1}H NMR, isotactic PDMAA (DMSO – d_6, 25℃)

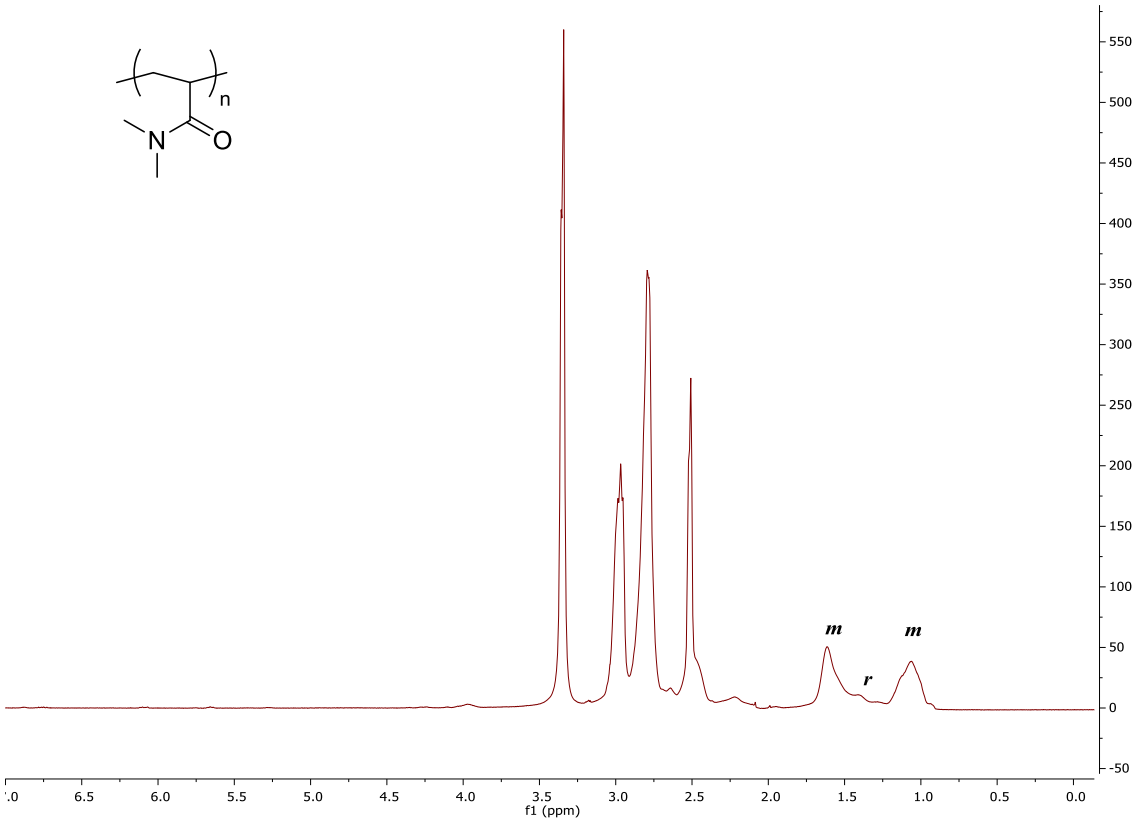

^{1}H NMR, atactic PDMAA (DMSO – d_6, 25℃)

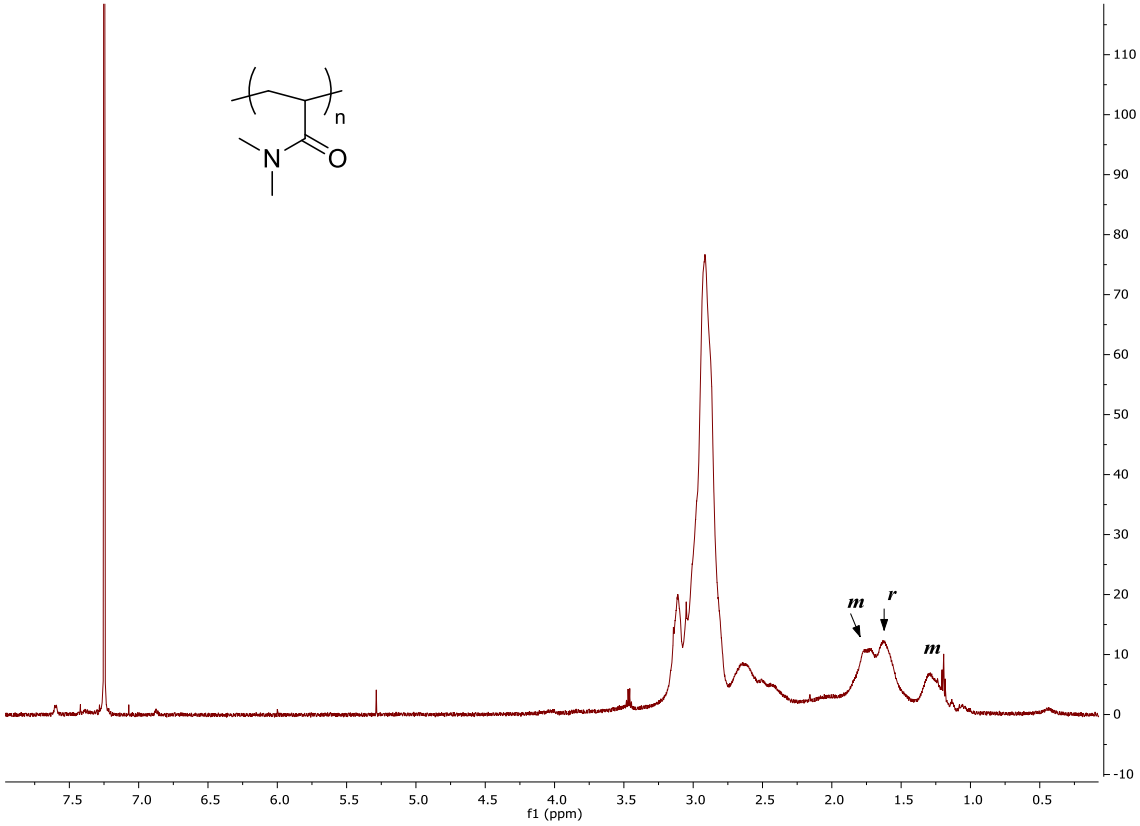

^{1}H NMR, isotactic PNIPAM (DMSO – d_6, 100℃)

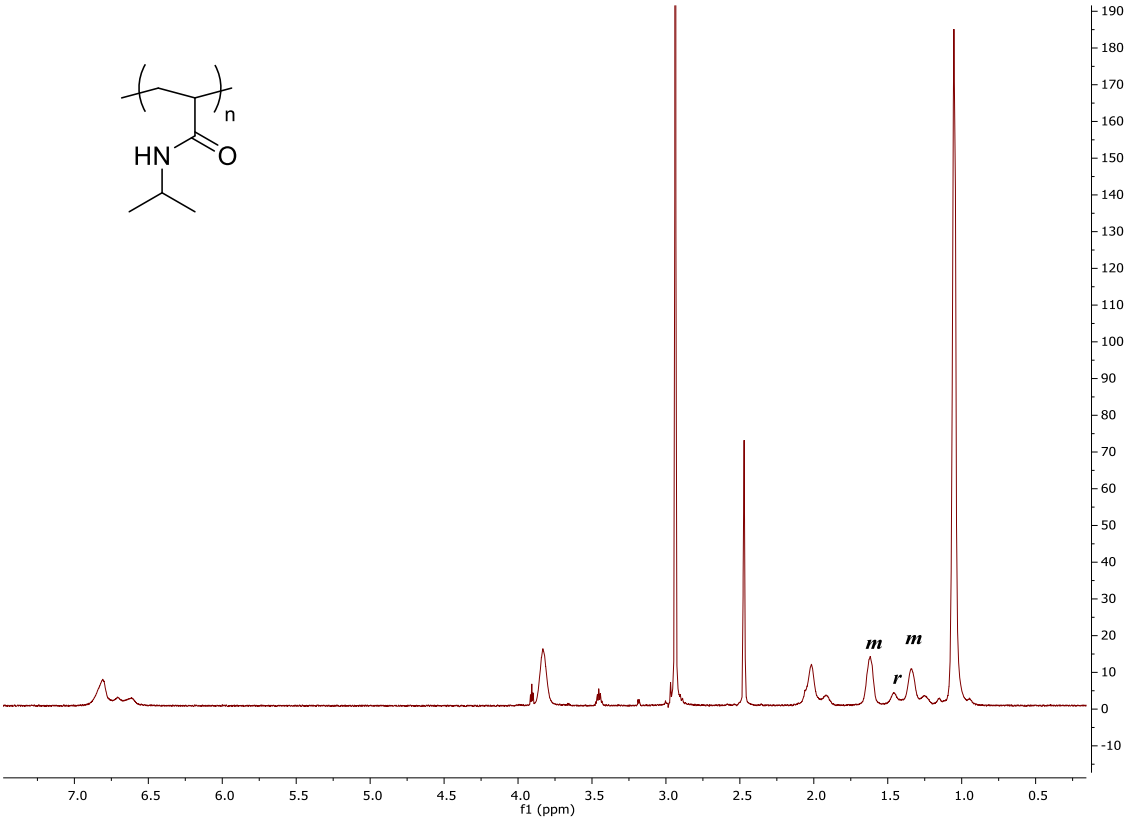

^{1}H NMR, atactic PNIPAM (DMSO – d_6, 100℃)

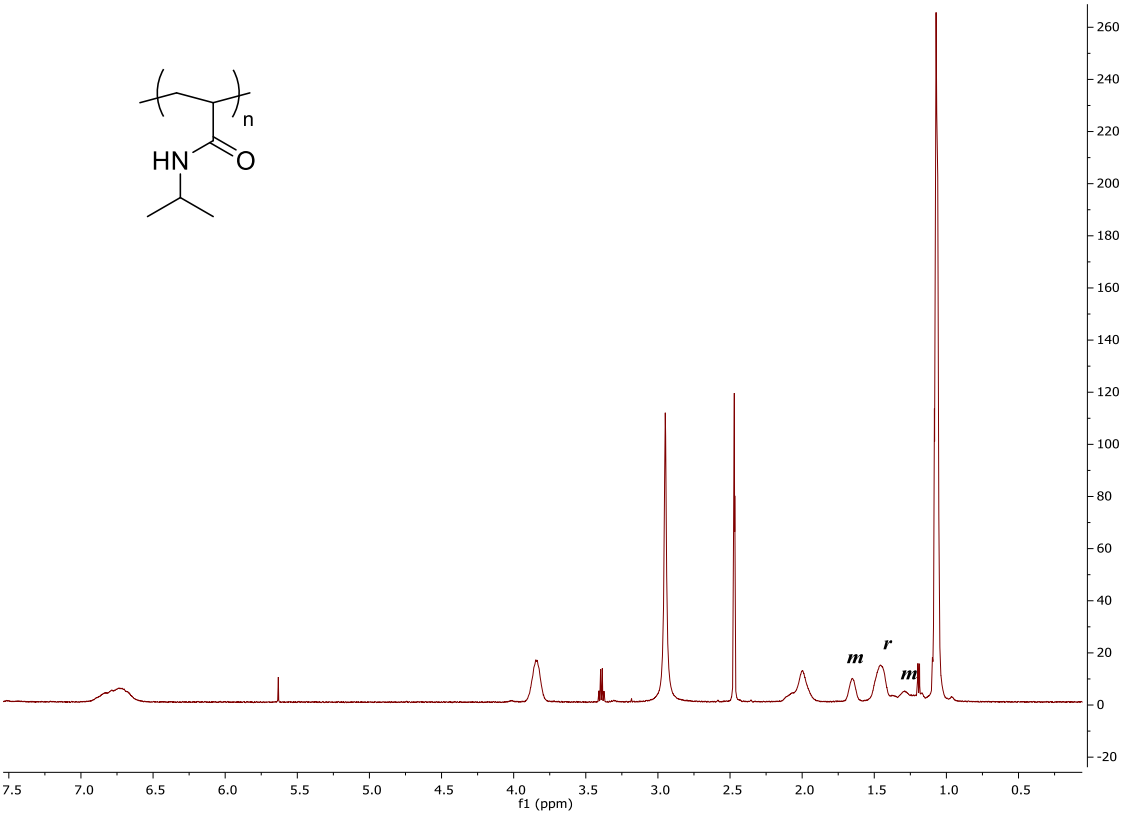

^{1}H NMR, PDEAA (DMSO – d_6, 100℃)

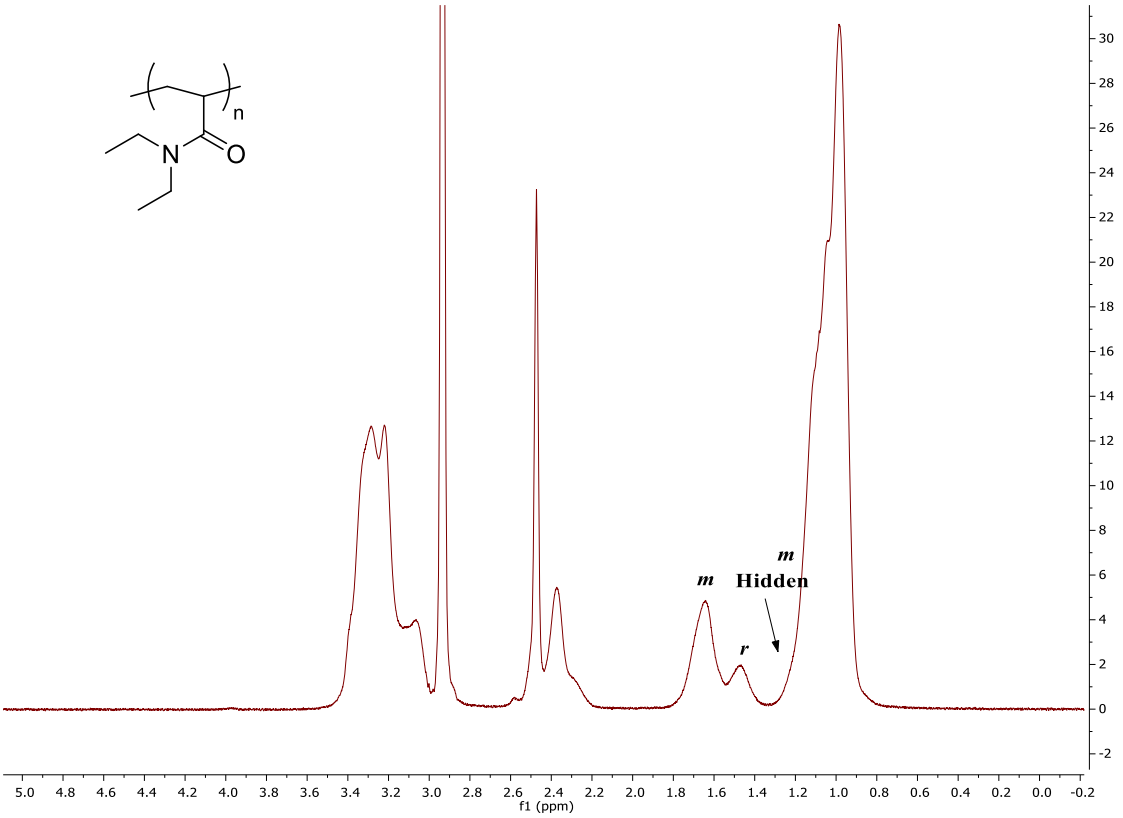

^{1}H NMR, poly (*N*-benzyl acrylamide) (DMSO – d_6, 100℃)

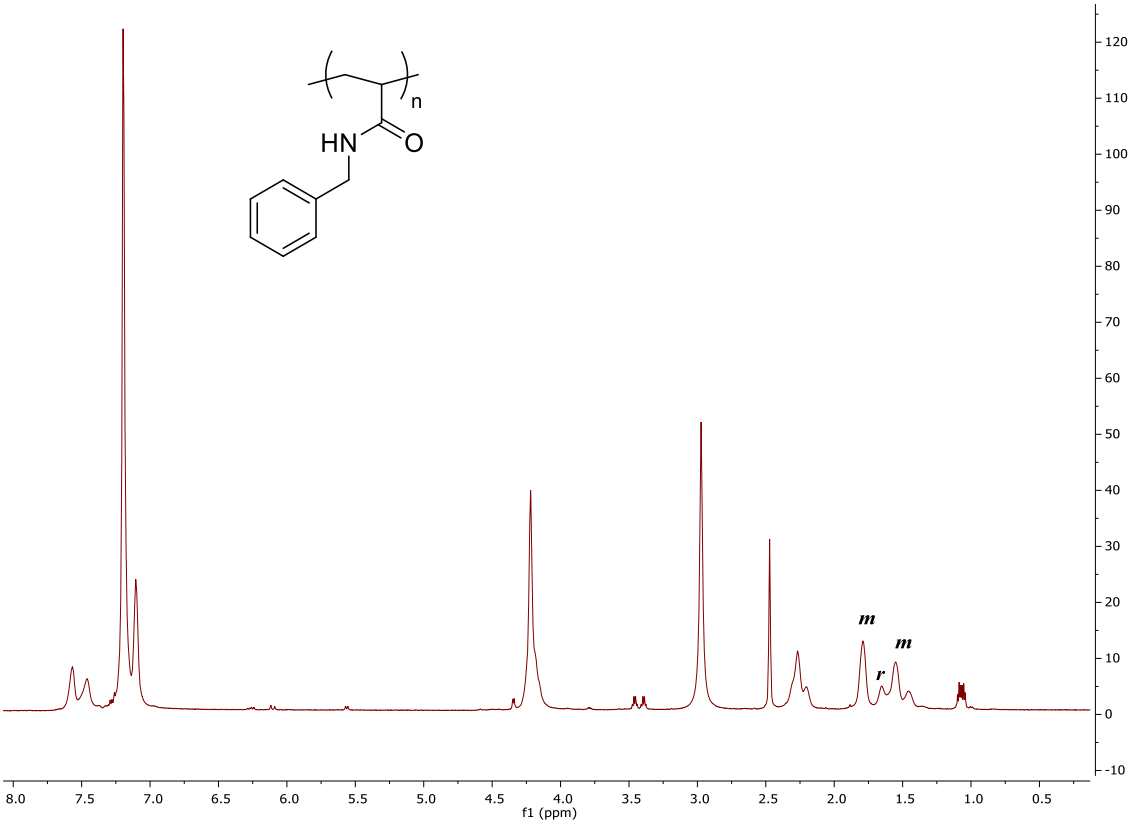

^{1}H NMR, poly (*N*-phenyl acrylamide) (DMSO – d_6, 100℃)

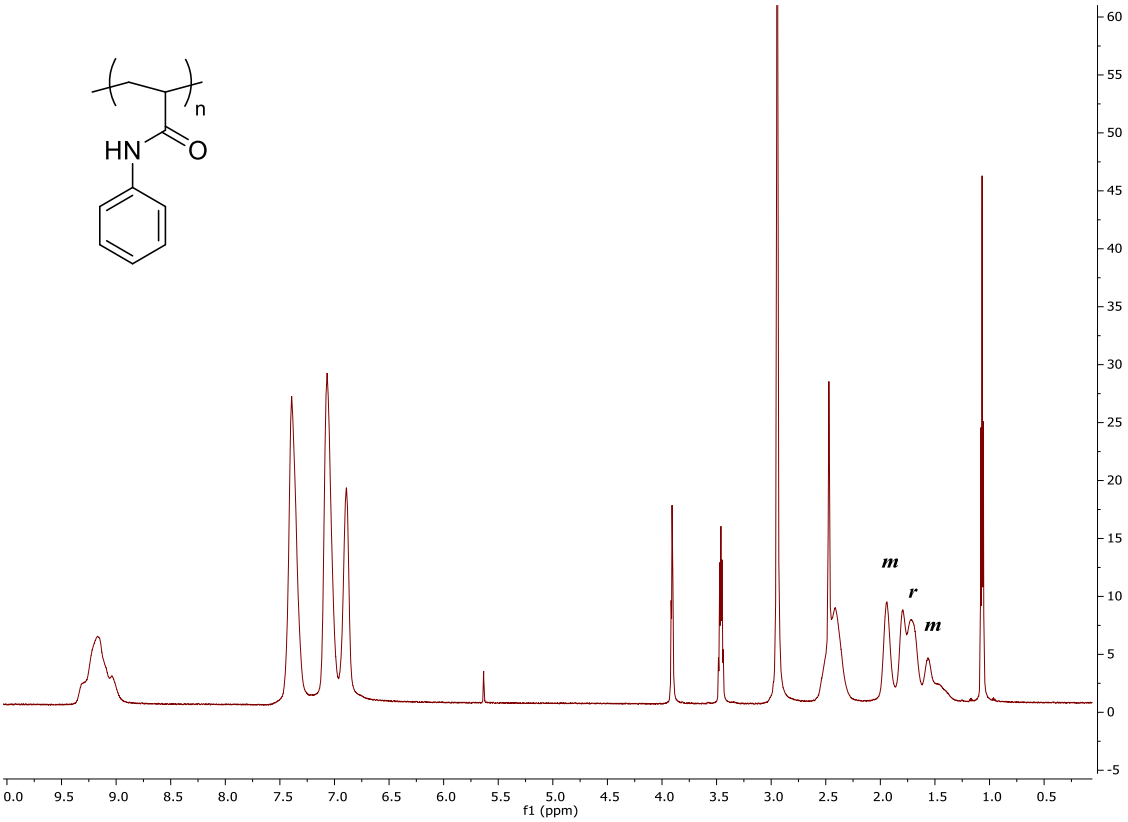

^{1}H NMR, poly (acrylamide) (DMSO – d_6, 100℃)

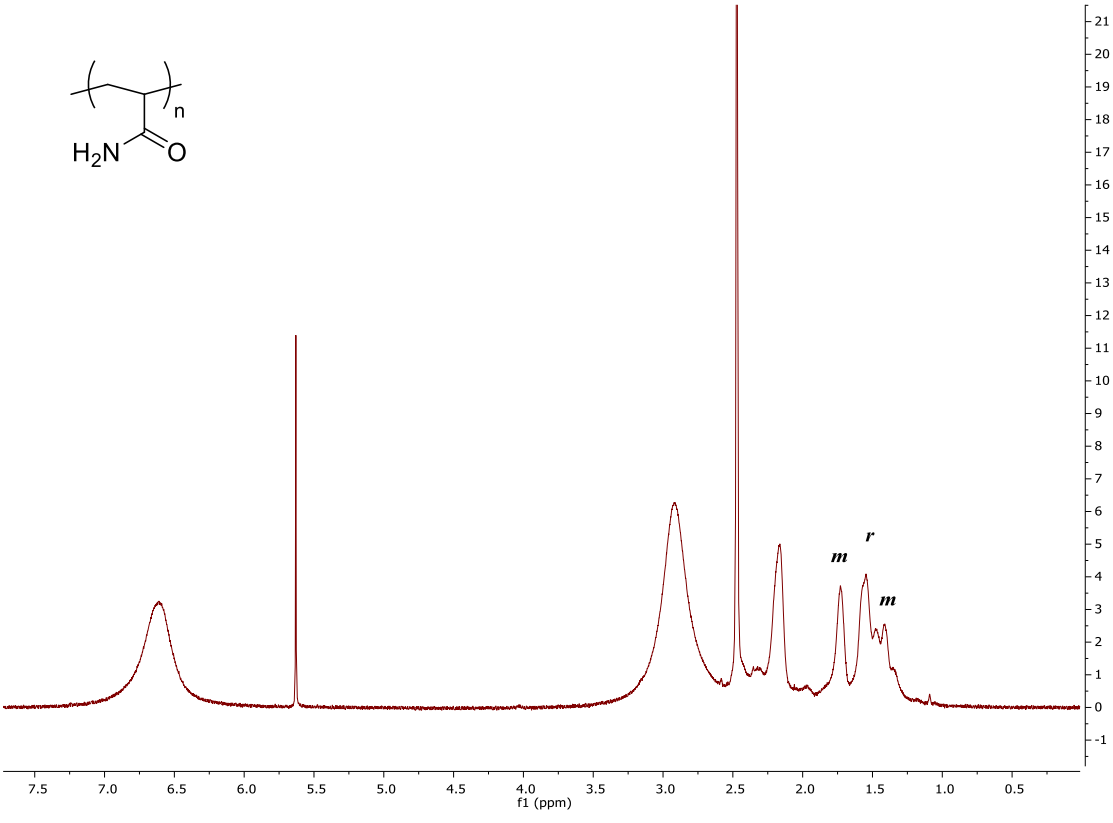

MALDI-TOF analysis data (polymerization of monomer **2.21**, **Table 2.12**)

M_n = 6877, M_w = 7191, PDI = M_w / M_n = 1.05

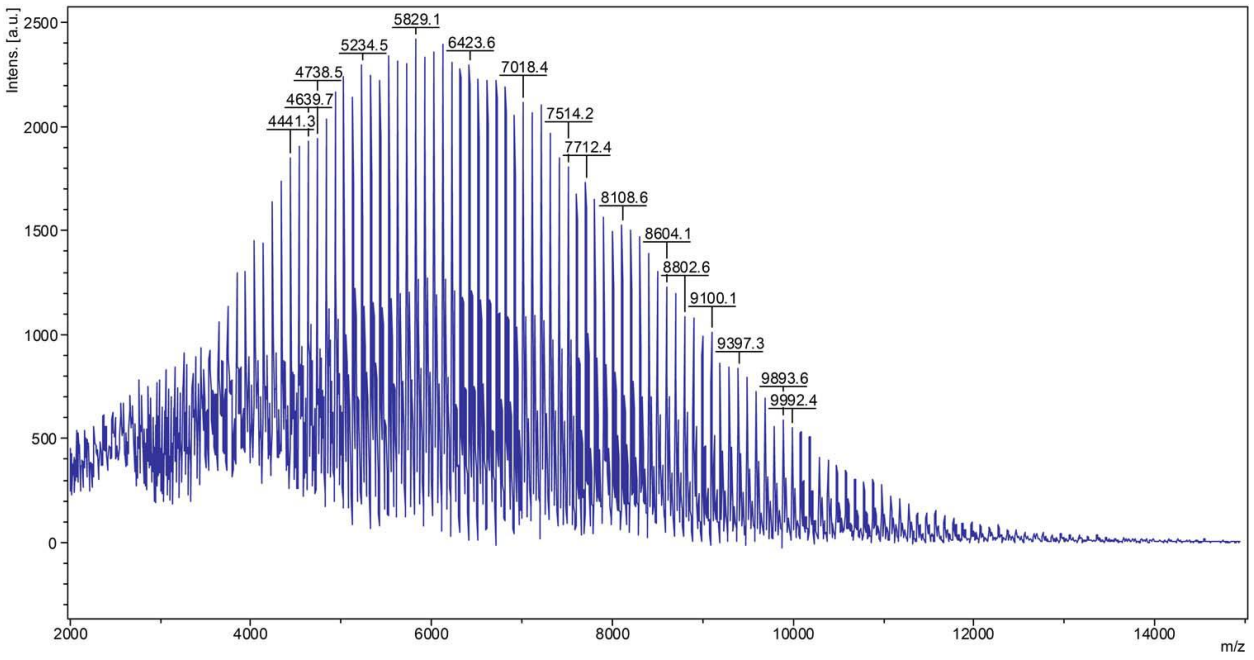

MALDI-TOF analysis data (polymerization of monomer **2.22**, **Table 2.12**)

M_n = 1606, M_w = 1691, PDI = M_w / M_n = 1.05

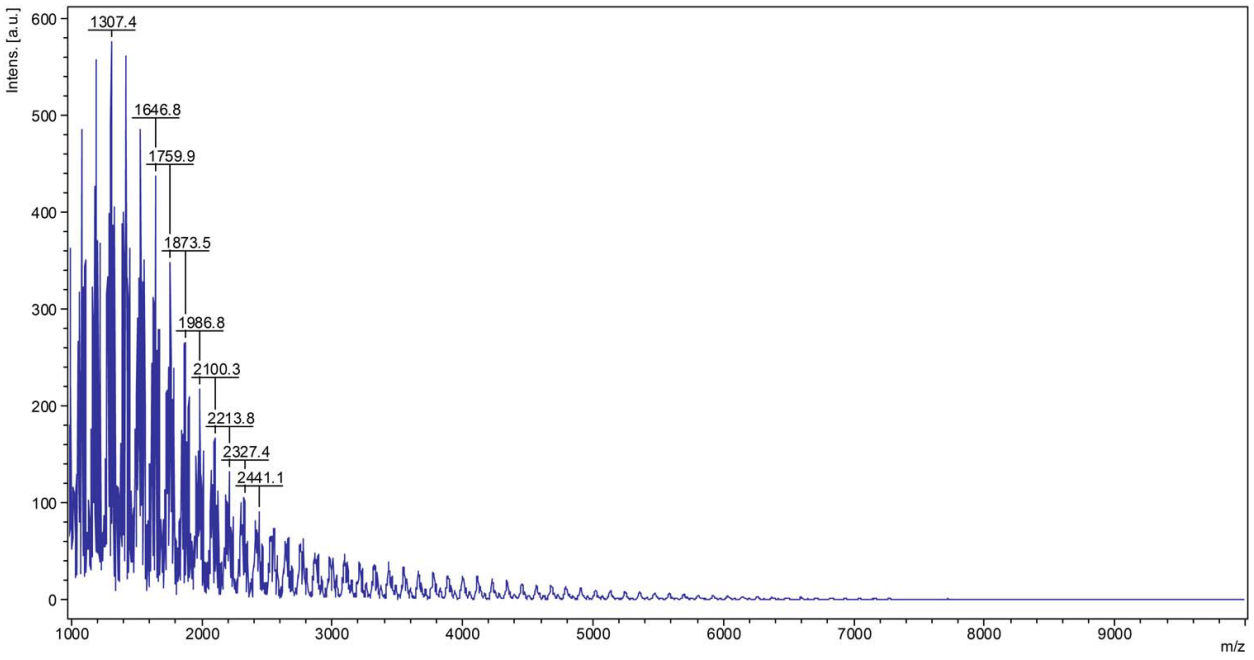

MALDI-TOF analysis data (polymerization of monomer **2.23**, **Table 2.12**)

M_n = 3882, M_w = 4208, PDI = M_w / M_n = 1.08

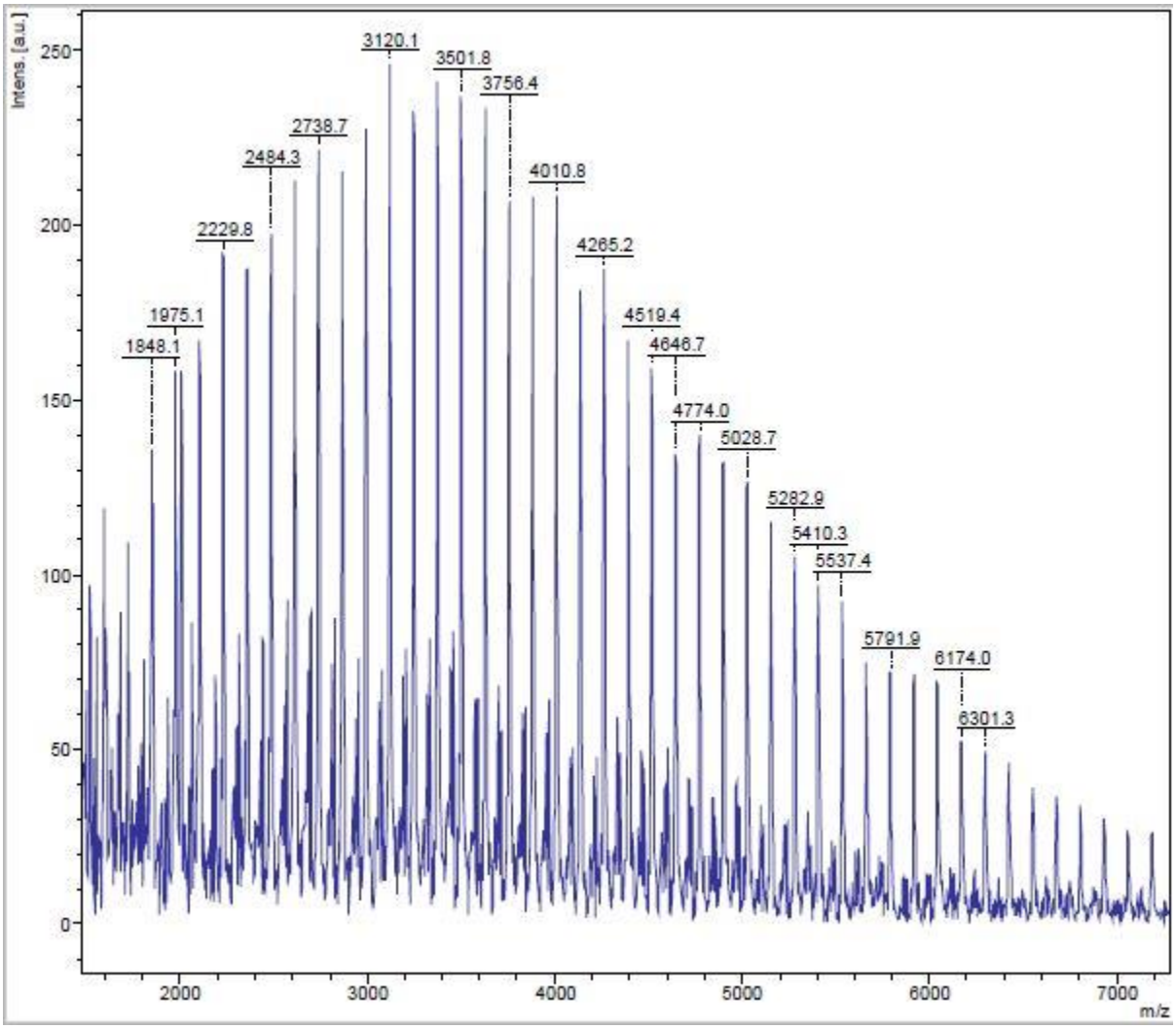

MALDI-TOF analysis data (polymerization of monomer **2.24**, **Table 2.12**)

M_n = 4414, M_w = 4689, PDI = M_w / M_n = 1.06

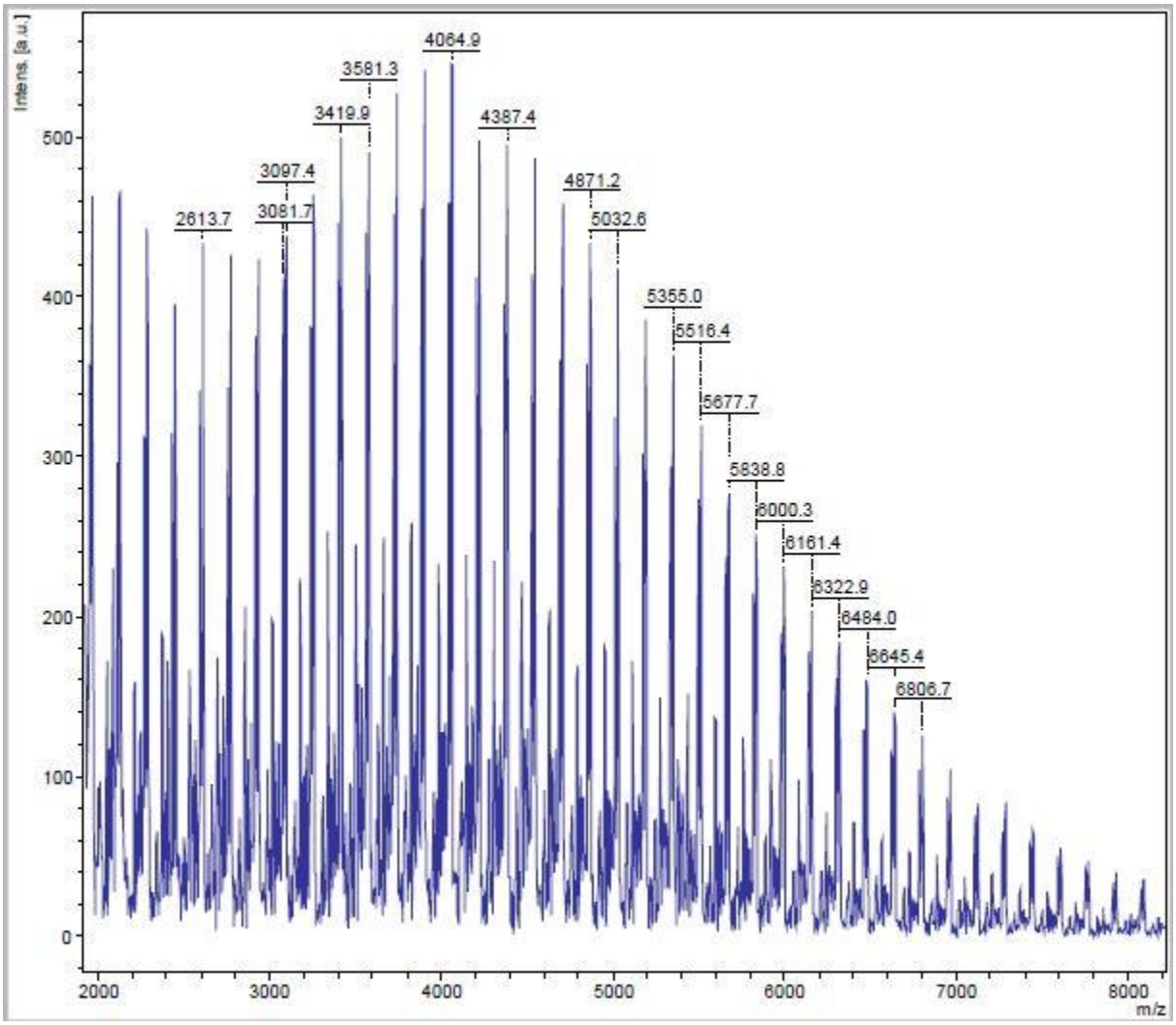

MALDI-TOF analysis data (polymerization of monomer **2.25**, **Table 2.12**)

M_n = 4381, M_w = 4714, PDI = M_w / M_n = 1.08